

A Thesis Submitted for the Degree of PhD at the University of Warwick

Permanent WRAP URL:

<http://wrap.warwick.ac.uk/108596>

Copyright and reuse:

This thesis is made available online and is protected by original copyright.

Please scroll down to view the document itself.

Please refer to the repository record for this item for information to help you to cite it.

Our policy information is available from the repository home page.

For more information, please contact the WRAP Team at: wrap@warwick.ac.uk

**SYNTHESIS AND STRUCTURAL STUDIES OF
N - AND O- DONOR COMPLEXES OF
TRANSITION AND POST-TRANSITION METAL HALIDES**

by
Mythili Ravindran

Submitted to the University of Warwick
for the degree of Doctor of Philosophy

Department of Chemistry
February 1991

THE BRITISH LIBRARY DOCUMENT SUPPLY CENTRE

BRITISH THESES N O T I C E

The quality of this reproduction is heavily dependent upon the quality of the original thesis submitted for microfilming. Every effort has been made to ensure the highest quality of reproduction possible.

If pages are missing, contact the university which granted the degree.

Some pages may have indistinct print, especially if the original pages were poorly produced or if the university sent us an inferior copy.

Previously copyrighted materials (journal articles, published texts, etc.) are not filmed.

Reproduction of this thesis, other than as permitted under the United Kingdom Copyright Designs and Patents Act 1988, or under specific agreement with the copyright holder, is prohibited.

THIS THESIS HAS BEEN MICROFILMED EXACTLY AS RECEIVED

THE BRITISH LIBRARY
DOCUMENT SUPPLY CENTRE
Boston Spa, Wetherby
West Yorkshire, LS23 7BQ
United Kingdom

To the Tamils in Sri Lanka

CONTENTS

List of tables	vi
List of figures	vii
Acknowledgements	viii
Abstract	ix
Abbreviations	x
Publications	xi

CHAPTER ONE

1.1	Introduction	1
1.1.1	Structure and bonding of trimethylamine	1
	Lewis basicity	5
	Steric requirements	8
	Reducing properties	11
1.1.2	Complexes of trimethylamine	14
1.2	Metal(II) halide-trimethylamine system	15
1.2.1	Reactions of trimethylamine with Metal dichlorides and trichlorides	15
1.2.2	The co-ordination chemistry of Mn(II)	16
1.2.3	The co-ordination chemistry of Cd(II)	18
1.2.4	The co-ordination chemistry of Cu(II)	21
1.2.4	Chlorocuprate(II) complex anions	23
1.3	Results and discussion	27
1.3.1	Reaction of trimethylamine with manganese(II) chloride	27
	The crystal structure of $(Me_3NH)[MnCl_2]$	31
	Discussion of the structure	33
1.3.2	Reaction of trimethylamine with cadmium(II) chloride	35
	The crystal structure of $(Me_3NH)[CdCl_2]$	39
1.3.3	Mode of reaction	43
1.3.4	Reaction of trimethylamine with copper(II) chloride	44
	The crystal structure of $(Me_3NCH_2Cl)_2[CuCl_4]$	47
	Discussion of the structure	50

CHAPTER TWO

2.1	Introduction	53
2.1.1	Crown ethers	57
	Names and structures of crown ethers	57
	Relative cation and ligand sizes	61
	Substitution on the macrocyclic ring	65
	Solvent effects	68
2.1.2	Macrocyclic effect	68
2.1.3	Number and type of donor atom	71
2.1.4	M^{n+} -crown interaction modes in solid complexes	72
2.2	Results and discussion	77
2.2.1	Infrared spectra	81
2.2.2	Proton nmr spectra	85
2.2.3	Crystal structures of GroupVB trichloride-crown ether complexes	86
	$AsCl_3(12-C-4)$ (I)	86
	$SbCl_3(12-C-4)$ (II)	88
	$BiCl_3(12-C-4)$ (III)	90
	$AsCl_3(15-C-5)$ (IV)	93
	$BiCl_3(15-C-5)$ (V)	95
	$SbCl_3(18-C-6).CH_3CN$ (VI)	97
	$[BiCl_3(18-C-6)]_2[Bi_2Cl_4]$ (VII)	101
2.2.4	Comparison of GroupVB trichloride-crown ether complexes	103
	M-O bond lengths and interactions	107
	Displacement of the metal atom from the mean oxygen plane	109
	C-C and C-O bond lengths	110
	Conclusions	111
2.2.5	The exceptions	112
2.2.6	Reactions of Sb(V) chloride with crown ethers	117
	Reaction with 12-C-4	120
	Reaction with 15-C-5	122
	Reaction with 18-C-6	123
	General comments	126

CHAPTER THREE

3.1	Introduction	130
3.2	Results and discussion	134

CHAPTER FOUR

4.1	Starting materials and analytical methods	139
4.2	Experimental techniques	140
4.2.1	The dry-box	140
4.2.2	Instrumentation	141
4.3	Preparation of NMe_3 complexes	142
4.3.1	NMe_3 Insoluble complexes	142
4.3.2	NMe_3 Soluble complexes	142
4.4	Experimental details for Chapter one	144
4.4.1	Trimethylamine complexes of Mn(II) chloride	144
4.4.2	Trimethylamine complexes of Cd(II) chloride	148
4.4.3	Trimethylamine complexes of Cu(II) chloride	150
4.5	Experimental details for Chapter two	151
4.5.1	Preparation of GroupVB Trichloride-crown ether complexes	152, 153
4.5.2	Preparation of Hydronium-ion(crown) antimon(V)ate complexes	157
4.6	Experimental details for Chapter three	159
4.6.1	Preparation of 2,2',6,6'-tetra(tert-butyl)diphenquinone	159
	Appendix	161
	References	187

List of tables

No.	Title	Page
	CHAPTER ONE	
1.1	Molecular dimensions of NMe_3	2
1.2	Metal halide systems reduced by trimethylamine	12
1.3	Metal complexes of trimethylamine	14
1.4	Stoichiometries and structures of selected chlorocuprates(II)	26
1.5	Molecular dimensions of $[Me_3NH][MnCl_3]$	34
1.6	Molecular dimensions of $[Me_3NH][CdCl_3]$	42
1.7	Molecular dimensions of $[Me_3NCH_2Cl]_2[CuCl_4]$	49
	CHAPTER TWO	
2.1	Trivial names of crown ethers	54-56
2.2	Properties of crown ethers	58
2.3	Cavity diameters for selected crown ethers	64
2.4	Formation constants of substituted benzo crowns with Na^+ in DMF	66
2.5	$\log k$ values for reactions in MeOH of Na^+ and K^+ with pentaglyme and 18-C-6	69
2.6	Thermodynamics of formation of metal complexes of cyclic and non-cyclic poly ethers	70
2.7	Stability constants for the formation of 1:1 complexes with the ligands $X(CH_2CH_2OCH_2CH_2OCH_2CH_2)_2Y$	72
2.8	Bond lengths and bond angles for GroupVB trichlorides	80
2.9	Crown ether complexes of GroupVB trichlorides	80
2.10	Mean M-Cl and M-O bond lengths and mean Cl-M-Cl angles in GroupVB crown ether complexes	105
2.11	Mean ring dimensions in crown ethers and their GroupVB complexes	106
2.12	Displacement of metal atoms from the mean oxygen plane	109
2.13	Reaction scheme for the formation of hydronium-ion(crown)-antimon(V)ate salts and $SbCl_5(15-C-5)$	119
	CHAPTER FOUR	
4.1	Analytical data for NMe_3 complexes of Manganese(II) chloride	146
4.2	IR data for NMe_3 complexes of Manganese(II) chloride	147
4.3	Vis-UV data for NMe_3 complexes of Manganese(II) chloride	147
4.4	Microanalytical results for NMe_3 complexes of Cd(II) chloride	149
4.5	IR data for NMe_3 complexes of Cd(II) chloride	149
4.6	Synthetic procedures for GroupVB trichloride-crown ether complexes	153
4.7	Analytical data for GroupVB trichloride-crown ether complexes	154
4.8	Spectroscopic data for GroupVB trichloride-crown ether complexes	155, 156
4.9	Microanalytical data for Hydronium-ion(crown) antimon(V)ate and $SbCl_5(15-C-5)$ complexes	158
4.10	Spectroscopic data for Hydronium-ion(crown) antimon(V)ate and $SbCl_5(15-C-5)$ complexes	159

List of figures

No.	Title	Page
CHAPTER ONE		
1.1	The structure of trimethylamine	2
1.2	Bonding model for trimethylamine	3
1.3	Simplified molecular orbital energy diagram for trimethylamine	4
1.4	Cone angle	9
1.5a	σ - bonding in metal-amine complexes	9
1.5b	σ and π bonds in metal-phosphine complexes	9
1.6	The structure of $CdX_2 \cdot P(t-Bu)_3$	19
1.7	The structure of $CdX_2 \cdot P(t-Bu)_3$	19
1.8	Structure of $Cu_2OCl_4 \cdot L_4$	22
1.9	Examples of the stereochemistry of dimeric $[Cu_2X_4]^{2-}$ species	24
1.10	$MnX_2 \cdot L_2$ in dimeric form	28
1.11	The detailed reaction scheme for $MnCl_2 \cdot NMe_3$ system	29
1.12	The crystal structure of $[Me_3NH][MnCl_4]$	31
1.13	A general reaction scheme for the formation of ionic products	36
1.14	Postulated structure of $CdCl_2 \cdot NMe_3$	37
1.15	The crystal structure of $[Me_3NH][CdCl_4]$	39
1.16	The crystal structure of $[Me_3NCH_2Cl]_2[CuCl_4]$	47
CHAPTER TWO		
2.1	Schematic diagram of $SbCl_3(15-C-5)$ complex	59
2.2	Structure of $Sn(OH_2)_2Cl_4(18-C-6) \cdot 2H_2O \cdot CHCl_3$ (schematic)	60
2.3	The selectivity of 18-C-6 for alkali and alkaline earth cations	62
2.4	Stability constants for complexes of dicyclohexano 18-C-6 with Na^+ , K^+ and Cs^+ in solvents of different dielectric constants	67
2.5	Schematic diagram to show the various types of crown anion preferences that have been observed for different M^{++}	73,75
2.6	The structure of Metal trihalide	79
2.7	Crystal structure of $SbCl_3(DMO)$	100
2.8	The crystal structure of $(18-C-6) \cdot 2MeCN$	114
2.9	Schematic diagram of $(18-C-6) \cdot 2MeCN$ to illustrate the hydrogen bonding pattern	114
2.10	Crystal structures of $BiCl_3(18-C-6)$ and $BiCl_3(18-C-6) \cdot H_2O$	116
2.11	Trigonal-bipyramidal structure of $SbCl_5$	117
2.12	Proposed structure of $[H_3O(12-C-4)]^+$ cation showing the hydrogen bonding pattern (schematic)	121
2.13	Structure of pyramidal $[H_3O(18-C-6)]^+$ (schematic)	125
2.14	The structure of $[H_3O(18-C-6)]^+$ in $[H_3O(18-C-6)][HCl_2]$	126
CHAPTER THREE		
3.1	2,6-di-(tert-butyl)phenoxide	130
3.2	Thermal activation of C-H bonds in $Ta(OAr^+)_3Me_3$	132
3.3	The crystal structure of 2,2',6,6'-tetra(tert-butyl)diphenylquinone	135
3.4	Schematic diagram for the formation of 2,2',6,6'-tetra(tert-butyl)diphenylquinone	137
CHAPTER FOUR		
4.1	Single Ampoule Reaction Vessel	143
4.2	Double Ampoule Reaction Vessel	143

ACKNOWLEDGEMENTS

My sincerest thank-you goes to Dr.G.R.Willey for his continual encouragement and assistance throughout my PhD.

The X-ray crystallographic studies carried out in collaboration with Dr.N.W.Alcock, University of Warwick and Dr.M.G.B.Drew, University of Reading and the assistance provided by the technical staff of the University of Warwick are gratefully acknowledged.

I would like to thank Dr.S.Rawle for proof reading the thesis.

Finally I thank my husband for being so patient during my last three years of research period.

ABSTRACT

Trimethylamine reacts with MCl_3 ($M = Mn, Cd, Cu$) to give mono adducts of the type $MCl_2 \cdot NMe_3$. Recrystallization of $MnCl_2 \cdot NMe_3$ (I) from the polar solvent acetonitrile yields the anionic complexes $[NMe_3H][MnCl_3]$ (II) and $[NMe_3H]_2[MnCl_4]$ (III) both from the same solution. Similarly $CdCl_2 \cdot NMe_3$ (IV) gives $[NMe_3H][CdCl_3]$ (V). Recrystallization of $CuCl_2 \cdot NMe_3$ (VI) from the chlorinated solvent CH_2Cl_2 yields the anionic complex $[Me_3NCH_2Cl]_2[CuCl_4]$ (VII). Compounds (II), (V) and (VII) were further investigated by X-ray crystal structure determinations.

The co-ordination chemistry of Group VB trichlorides with the neutral O-donor (crown ether) ligands 1,4,7,10-tetraoxacyclododecane (12-C-4), 1,4,7,10,13-pentaoxacyclopentadecane (15-C-5) and 1,4,7,10,13,16-hexaoxacyclooctadecane (18-C-6) have been investigated. 12-C-4 and 15-C-5 form neutral adducts with the pyramidal MCl_3 ($M = As, Sb, Bi$) where all oxygen atoms of the crown are co-ordinated to the metal atom in a half-sandwich structure.

For 18-C-6, $AsCl_3$ does not give complex formation, instead the crown ether forms a bis-adduct $(18-C-6)_2 \cdot 2CH_3CN$ with the solvent acetonitrile. $SbCl_3$ forms a half-sandwich adduct with 18-C-6 but with an extra molecule of CH_3CN trapped in the lattice and $BiCl_3$ forms a 2:1 complex which has the ionic formulation $[BiCl_2(18-C-6)]_2^+ [Bi_2Cl_4]^{2-}$. Here the bismuth cation is eight co-ordinate involving all six oxygen atoms of the crown and the two chlorine atoms.

The crown ethers give no simple adducts with the pentahalide $SbCl_5$. The crystals obtained from the reactions of 12-C-4 and 18-C-6 with $SbCl_5$ are the unexpected hydronium(crown) hexachloroantimon(V)ate salts, $[H_3O(12-C-4)]_2[SbCl_6]$ and $[H_3O(18-C-6)]_2[SbCl_6]$ respectively. 15-C-5 gives the neutral $Sb(III)$ adduct $SbCl_3(15-C-5)$ as the major product and the hydronium(crown) hexachloroantimon(V)ate salt as the minor product. A plausible mechanism for the formation of hydronium antimon(V)ate salts is presented and discussed.

In the preliminary study of sterically crowded aryloxy complexes of Group VB chlorides, the reaction between $SbCl_3$ and the extremely bulky 2,6-di(tertiary butyl) phenoxide has been investigated. This leads to the formation of 2,2',6,6'-tetra (tertiary butyl) diphenquinone (A) via a redox reaction. The crystal structure of this oxidation product has been determined via an X-ray study and a plausible mechanism for the formation of (A) is presented and discussed.

ABBREVIATIONS

12-C-4	12-Crown-4
15-C-5	15-Crown-5
18-C-6	18-Crown-6
18-C-5	18-Crown-5
24-C-6	24-Crown-6
30-C-10	30-Crown-10
tert-	tertiary
DB	Dibenzo
B	Benzo
R	alkyl
Me	methyl
X	halogen atom
L	ligand
THF	tetrahydrofuran
py	pyridine
M	Metal atom
Et	ethyl
Ph	phenyl
A	monocharged organic or inorganic cation
MeCN	acetonitrile
MeOH	methanol
DMF	N,N-dimethylformamide
Ar*	2,6-di(tertiarybutyl)phenyl
DMO	N,N-dimethyloxalamide
DtBuO	N,N-di(tertiarybutoxy)oxalamide
DIPO	N,N-diisopropylloxalamide
DMS	N,N-dimethylsuccinamide
DMDTO	N,N-dimethyldithiooxalamide
ir	infrared
nmr	nuclear magnetic resonance
v	stretching
δ	deformation
ρ	rocking
vs	very strong
st	strong
m	medium
w	weak
br	broad
sh	shoulder
s	sharp
λ	wave length
nm	nanometres

PUBLICATIONS

- 1) Crown Ether Complexes of Bi(III) : Synthesis and Crystal and Molecular Structures of $\text{BiCl}_3 \cdot 12\text{-Crown-6}$ and $2\text{BiCl}_3 \cdot 18\text{-Crown-6}$, N.W.Alcock, M.Ravindran and G.R.Wiley, *J.Chem.Soc., Chem.Commun.*, 1989, 1063-1065.
- 2) Synthesis and structure of Antimony(III) chloride - 1,4,7,10,13,16-hexaoxacyclooctadecane(18-crown-6)-Acetonitrile(1/1/1), N.W.Alcock, M.Ravindran, S.M.Roe and G.R.Wiley, *Inorg.Chim.Acta*, 1990, 167, 115-118.
- 3) Reactions of Trimethylamine with Mn(II) and Cd(II) Chlorides : Crystal and Molecular Structure of $[\text{Me}_3\text{NH}][\text{MnCl}_2]$, M.Ravindran, G.R.Wiley and M.G.B.Drew, *Inorg.Chim.Acta*, 1990, 175, 99-103.
- 4) Crown Ether complexes of Group VB Trihalides, N.W.Alcock, M.Ravindran and G.R.Wiley. *Acta Crystallogr.*, 1990, 46A, C-237.
- 5) Reactions of Sb(V) Chloride with Crown Ethers : Formation of Hydronium-Crown Ether Hexachloroantimon(V)ate salts, Mythili Ravindran and Gerald R Wiley, *Inorg.Chim.Acta*, 1991 (accepted for publication).
- 6) Crown Thioether Complexes of p-Block Elements : Crystal and Molecular Structures of $\text{SbCl}_3 \cdot 9\text{S}3$ (I) [$9\text{S}3 = 1,4,7\text{-trithiacyclononane}$] and $2\text{SbCl}_3 \cdot 18\text{S}6$ (II) [$18\text{S}6 = 1,4,7,10,13,16\text{-hexathiacyclooctadecane}$], N.W.Alcock, M.T.Lakin, M.Ravindran and G.R.Wiley, *J.Chem.Soc., Chem.Commun.*, 1991, 271-272.
- 7) A Study of the Copper(II) Chloride-Trimethylamine System. Crystal and Molecular Structure of Bis[trimethyl(chloromethyl)ammonium] Tetrachlorocuprate(II) $[\text{Me}_3\text{NCH}_2\text{Cl}]_2[\text{CuCl}_4]$, G.R.Wiley, M.Ravindran and M.G.B.Drew, Submitted to *J.Chem.Soc., Dalton Trans.*, 1991.

CHAPTER ONE

**Trimethylamine complexes of
Mn(II), Cu(II) and Cd(II) chlorides**

1.1 INTRODUCTION

This chapter concerns the reactions of trimethylamine with anhydrous metal(II) chlorides (MCl_2 , $M = Mn, Cu, Cd$). Characterization of products is made from full spectroscopic studies and, where possible, X-ray crystallography determination. In the introductory sections (1.1.1 and 1.1.2) the properties of trimethylamine and the reactions of trimethylamine with metal halides are discussed in some detail.

1.1.1 Structure and bonding of trimethylamine

Three different approaches to determining the structure of trimethylamine e.g., solid state crystallography [1], gas phase electron diffraction [2], microwave spectroscopy [3] show that trimethylamine is a symmetric top molecule with effective C_{3v} symmetry. In free trimethylamine the N atom is surrounded by three covalent bonding pairs and one lone pair of electrons. The VSEPR model predicts that the molecule should be pyramidal (Figure 1.1) and the C-N-C angle less than that of a regular tetrahedron. However the C-N-C angle is found to be slightly greater than tetrahedral presumably because of steric repulsion between the methyl groups (Table 1.1).

Molecular dimensions of NMe_3			
Molecular parameter	Type of Study		
	Solid state	Microwave	Electron-Diffraction
(C-N) distance (Å)	1.4535(11)	1.451	1.455(2)
(C-N-C) angle (degrees)	110.40(7)	110.9	110.6(6)

Table 1.1 Molecular dimensions of NMe_3

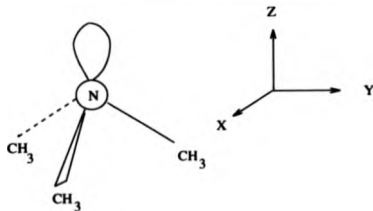


Figure 1.1 The structure of trimethylamine

A simple bonding model for trimethylamine based on valence bond theory is shown in Figure 1.2. The central sp^3 hybridized nitrogen atom overlaps with similar sp^3 hybridized carbon atoms to provide three equivalent covalent bonds together with a stereochemically active lone pair of electrons.

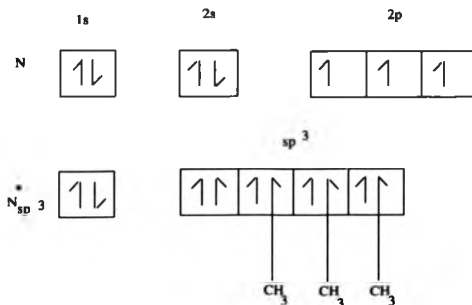
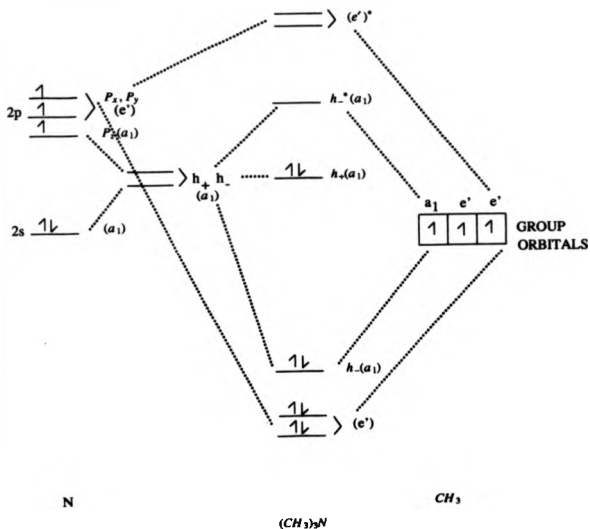


Figure 1.2 Bonding model for trimethylamine

A simplified molecular orbital energy diagram is presented in Figure 1.3 [4]. As in the valence bond approach, the central nitrogen atom and carbon atoms are sp^3 hybridized.

Figure 1.3 *Simplified molecular orbital energy diagram for trimethylamine*



Three factors particularly affect the co-ordination chemistry of trimethylamine, namely

- a) Lewis basicity
- b) steric requirements
- c) reducing properties.

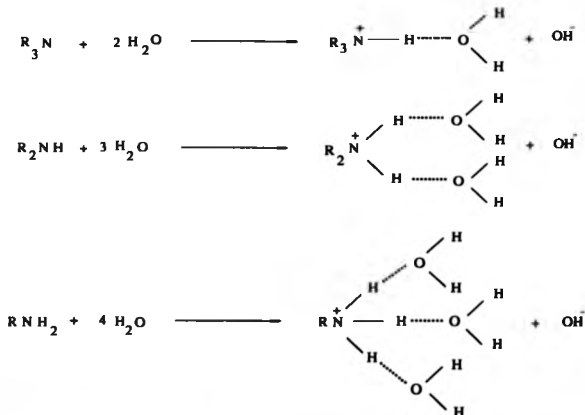
(a) Lewis basicity

Due to the presence of a nitrogen lone pair of electrons, trimethylamine is a potential Lewis base i.e., it can form donor-acceptor complexes with Lewis acids. The increased donor ability of trimethylamine in comparison to ammonia and other aliphatic amines parallels the greater inductive effects conferred by the maximum of three methyl groups. The equilibrium constant for the acid base reaction with water is,



$$K_b = \frac{[R_3NH^+][OH^-]}{[R_3N]}$$

This gives $pK_b = 4.21$ at 298K; ammonia gives $pK_b = 4.76$ at 298K consistent with the observation that trimethylamine is a stronger base. Furthermore, the increase in basicity would be expected to fall in the following order for a series of sequential methyl substitutions on ammonia $NH_3 < MeNH_2 < Me_2NH < Me_3N$. This observation is true in the gas phase where the estimated proton affinities are ($kJ\ mol^{-1}$) $NH_3(858) < MeNH_2(896) < Me_2NH(923) < Me_3N(938)$ and in aprotic solvents such as dimethyl sulphoxide. However in aqueous solution dimethylamine has the maximum basicity. This can be corroborated with solvation effects of the amines giving rise to intermolecular hydrogen bonding as shown below:



The greater solvation effects lead to an increase in the base strength since N^+ species will be more stabilized than the equivalent uncharged N species. This increase is proportional to the number of NH protons and solvation energies lie in the order



Thus the effect of introducing successive methyl groups together with solvation effects has the combined result of giving the basicity in the following order under aqueous conditions [4]:

PK_b :

$$4.74 (NH_3) < 4.28 (Me_3N) < 3.36 (MeNH_2) < 3.29 (Me_2NH).$$

The formation of $[Me_3NH] [ZnCl_2 \cdot NMe_3]$ from $ZnCl_2 \cdot 2NMe_3$ system [5], $[Me_3NH] [MnCl_2]$ and $[Me_2NH] [MnCl_4]$ from $MnCl_2 \cdot NMe_3$ [6] and $[Me_2NH] [CdCl_2]$ from $CdCl_2 \cdot NMe_3$ [6] upon recrystallization under anhydrous conditions reflect to some extent the high proton affinity of trimethylamine. In the above mentioned reactions trimethylamine acts as an internal proton scavenger. The proton source is not entirely clear. There are several possibilities, i.e., proton abstraction from the reaction solvents (benzene for the $ZnCl_2 / NMe_3$ system, acetonitrile for the $MnCl_2 / NMe_3$ and $CdCl_2 / NMe_3$ systems), proton abstraction from trimethylamine itself or proton abstraction from moisture present in the

solvents; the latter is suspected. A similar type of ionic complex is formed for the WCl_6/NMe_3 system which results in the formation of $[NMe_3H]^+ [WCl_6]^-$; here proton abstraction from trimethylamine is suggested.

(b) Steric requirements

When comparing the C-N-C bond angle of trimethylamine (110.7°) with that of ammonia (H-N-H of 107°) the steric effect of the methyl groups is seen, pushing the angle beyond that of the perfect tetrahedron, 109.28° . A parameter often used to correlate steric effects is the cone angle θ , which is defined as the angle that can enclose the Van der Waals surface of all ligand atoms about the N-M bond[8] [Figure 1.4]. The cone angle is mainly used for tertiary phosphine systems, due to the nearly constant M-P distance; e.g., for the equivalent phosphine complex PMe_3 , the cone angle is 118° .

Its application to amine adducts appears limited. This may be due to a difference in bonding schemes between N and P donors. Nitrogen is a pure σ -donor (Figure 1.5a); there are no available d-orbitals for any metal to ligand $d\pi - d\pi$ interactions as there are for trivalent phosphorous donors (Figure 1.5b).

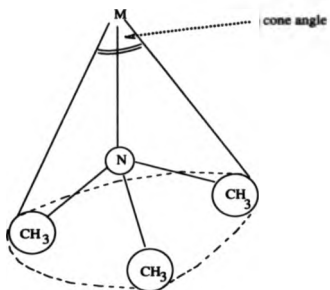


Figure 1.4 *Cone Angle*



Figure 1.5a *σ -Bonding in metal-amine complexes*

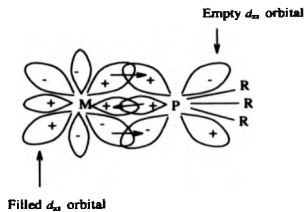


Figure 1.5b *σ and $d\pi$ - $d\pi$ bonds in metal-phosphine complexes*

The two components of the M-P interaction tend to stabilize the M-P bond length for a variety of metals usually in low oxidation states. However, the M-N bond length may vary depending on the strength of the metal ion as a Lewis acid. The variation in the M-N distance will affect the value of cone angle, which will increase as the M-N distance decreases. In general increasing the cone angle by having bulky groups tends to favour

- a) lower co-ordination numbers (co-ordinatively unsaturated)
- b) increased rates and equilibria in dissociative reactions.
- c) the formation of less sterically crowded isomers

Consider the five co-ordinate adducts of $MX_3 \cdot 2NMe_3$: in this series the known examples are M = Sc, X = Cl [9]; M = Ti, X = Cl, Br [10,11]; M = V, X = Cl, Br [12]; M = Cr, X = Cl [11,13]; M = Fe, X = Cl [5]; M = In, X = Cl [14]. Normally the co-ordination chemistries of these M(III) ions show a preference for an octahedral six-coordinate environment but association with trimethylamine always leads to a D_{3h} trigonal bipyramidal structure leaving the metal ion in a co-ordinatively unsaturated state. These five co-ordinate species are ideal for ligand exchange reactions, since the metal-ligand bonds are weak. An application of this property, allows the use of five co-ordinate trimethylamine adducts as intermediates, for example in the

formation of octahedral Cr(III) complexes which being t_2g species, are inert. The reaction of ligands such as THF, pyridine[15] with $CrCl_3 \cdot 2NMe_3$ gives $CrCl_3 \cdot 3L$ ($L = THF$ and py) in 100 percentage yields without the use of catalysts such as Zn, which would otherwise be required [16]. Other examples of the steric effects of trimethylamine occur in six co-ordinate species where there is a tendency to form *trans* geometries, e.g., $MX_4 \cdot 2NMe_3$, where $M=Zr, Sn$ [17,18], especially with such large halide ions as iodide. Inter ligand repulsions are not considered to play a major role in the case of $ZrX_4 \cdot 2NMe_3$, [17] ($X=Cl, Br$) which assigned a *cis* geometry on the basis of infrared data. The analogous hafnium complexes show a *cis* configuration for $X=Cl$ and a *trans* for $X=Br, I$ [19,20].

(c) Reducing properties

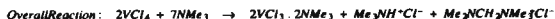
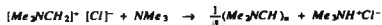
Another important feature of trimethylamine is its ability to act as a reducing agent. The reducing ability of trimethylamine has been reported for MX_4 ($M=Ti, V$ and $X=Cl, Br$) systems. Treatment of these systems with excess trimethylamine results in the formation of $MX_3 \cdot 2NMe_3$, as a major product [21-23]. For the other Group IVA metal halides e.g., zirconium and hafnium where $X=Cl, Br, I$ there is no reduction, with excess of trimethylamine

but formation of the six co-ordinate bis adducts [17,19,20]. However stoichiometric amounts of $TiCl_4$ and NMe_3 , give the adduct $TiCl_4 \cdot NMe_3$. But the corresponding VCl_4 / NMe_3 system forms either $VCl_3 \cdot NMe_3$ or $VCl_3 \cdot 2NMe_3$ or a mixture of both depending on the amount of trimethylamine [22,23]. For Ti and Cr, reduction has been observed from M(III) to M(II) as a minor product in some cases [24]. Table 1.2 lists some other systems where metal halides have been reduced with trimethylamine.

Metal halide	NMe_3 -Reduction product	Reference(s)
$MoCl_3$, Mo(III)	$MoCl_3 \cdot 2NMe_3$, Mo(II)	5
$MoCl_5$, Mo(V)	$MoCl_4 \cdot 2NMe_3$, Mo(IV)	26
$MoOCl_4$, Mo(VI)	$MoOCl_3NMe_3$, Mo(III)	5
WCl_6 , W(VI)	$[NMe_3H]_2 [WCl_6]$, W(IV)	26,7
$CuCl_2$, Cu(II)	$CuCl$, Cu(I)	25
$AuCl_3$, Au(III)	Au(I) and Au(0)	27

Table 1.2 Metal halide systems reduced by trimethylamine [28]

A possible reaction scheme for the reduction of metal(IV)chloride (and concomitant oxidation of trimethylamine) has been reported for the VCl_4 / NMe_3 system; a free radical mechanism has been proposed and the reaction scheme is shown below [22].



The evidence for this mechanism was mainly based on ir spectroscopy. The ir spectrum of the product mixture obtained from reduction of vanadium tetrachloride with a deficiency of trimethylamine showed the presence of $\nu(C=N)$ at 1696 cm^{-1} and $\nu(CH_2)$ at 3120 cm^{-1} which come from the dimethyl methylene ammonium cation ($Me_2N=CH_2^\bullet$). In an independent experiment the authors also noted, dimethyl methylene ammonium chloride undergoes

undergoes dehydrochlorination when treated with trimethylamine. This conclusion was mainly based on the formation of trimethylammoniumchloride as identified by ir spectroscopy. The authors suggested the formation of an oligomer of Me_2NCH from the deprotonation of $Me_2NCH_2^+$; which is consistent with the observation made by Yoke and Lane for the $CuCl_2 / NMe_3$ system[25]



1.1.2 Complexes of trimethylamine

Trimethylamine forms donor-acceptor complexes with many main group, transition metal, lanthanide and actinide elements. A selection of the various geometries that have been obtained is listed in Table 1.3.

Table 1.3 Metal complexes of trimethylamine

Complex(es)	Structure or Geometry	Reference(s)
TiX_3L_3 (X=Cl,Br)	trigonal bipyramid	10,11
$Ti_2Cl_6L_3$	confacial bioctahedron	29
ZrX_6L_3 (X=Cl,Br,I)	cis-octahedral (X=Cl,Br)	17
	trans-octahedral (X=Br,I)	
HfX_6L_3 (X=Cl,Br,I)	cis-octahedral (X=Cl)	19,20
	trans-octahedral (X=Br,I)	
VX_3L_3 (X=Cl,Br)	trigonal bipyramid	12
$V_2Cl_6L_3$	confacial bioctahedron	29
$Cr_2Cl_6L_3$	trigonal bipyramid	11,13
$Cr_2Cl_6L_3$	confacial bioctahedron	15
$Mo_2Cl_6L_4$	quadruply-bonded Mo_2	5
$MoOCl_4L_2$	octahedral	5
$FeCl_3L_2$	trigonal bipyramid	5
$CoCl_2L_2$	tetrahedral	30
$NiCl_2L_2$	tetrahedral	30
$ThCl_4L_3$	mono-capped octahedron	31
UCl_4L_3	trans-octahedral	32

1.2 Metal(II) halide - trimethylamine system

1.2.1 Reactions of trimethylamine with metal dichlorides and tri-chlorides

The trimethylamine chemistry of metal dihalide systems to date includes no x-ray crystal structures for neutral metal dihalo bis adducts ($MX_2 \cdot 2NMe_3$), where $M = Mn, Co, Ni, Cu, Zn$ and Cd). Except for $CoCl_2$ and $NiCl_2$ all the other metal(II) chlorides ($M = Mn, Zn, Cd$) form amine insoluble adducts. Furthermore the amine insoluble adducts are normally insoluble in many common organic solvents, which tends to complicate purification and isolation of crystalline products. Cobalt(II) chloride and nickel(II) chloride provide amine-soluble adducts, which have been characterized as tetrahedral $MX_2 \cdot 2NMe_3$ complexes on the basis of spectroscopic data [30]. The $ZnCl_2 / NMe_3$ system provides an anionic Zn(II) complex, and the structure of the complex $[Me_3NH] [ZnCl_3 \cdot NMe_3]$ has been described [5]. This complex is obtained along with other unidentified Zn(II) residues, via an attempted crystallization from benzene of the neutral adduct $ZnCl_2 \cdot 2NMe_3$ initially isolated from the $ZnCl_2 / NMe_3$ system. The anion has a tetrahedral structure. The other tetrahedral anionic $[ZnCl_3, Y]$ series include $Y=Cl$ [33], H_2O [34], THF [35],

acetone [36] and $(t-Bu)_3P$ [37], which can be viewed as precursors to $[Zn_2Cl_6]^{2-}$ following dimerization with loss of $2Y$ [35]. As an extension of the work involving $Zn(II)$, the trimethylamine derivative chemistry of $Mn(II)$, $Cu(II)$ and $Cd(II)$ is investigated here.

Reactions of trimethylamine with metal trihalides invariably provide the bis adducts, with a discrete five coordinate trigonal bipyramidal structure e.g., $M = Sc[9]$, $Ti[10,11]$, $V[12]$, $Cr[11,13]$, $Fe[5]$, $In[14]$; $X = Cl, Br$. These $MX_3 \cdot 2NMe_3$ adducts are soluble in the parent amine as well as in common organic solvents. The reason for the formation of the bis adducts is the stereochemical involvement of the ligand. This steric property of trimethylamine has been reviewed in section 1.1.1[b] (page 8).

1.2.2 The co-ordination chemistry of $Mn(II)$ d^5

The divalent state is the most important and generally the most stable oxidation state for the element. The normal co-ordination number for $Mn(II)$ is six, octahedrally co-ordinated $Mn(II)$ is normally pink in colour. Also some four co-ordinate (square planar and tetrahedral), five, six and eight co-ordinate complexes are known. But there is a lack of X-ray data to

substantiate many of the proposed structures. $[MnX_4]^{2-}$ ions are shown to be tetrahedral and normally they have a characteristic green-yellow colour.

A wide variety of adducts of anhydrous Mn(II)halides with ligands such as pyridine, acetonitrile and trialkylphosphines mostly of stoichiometry $MnX_2 \cdot L_2$ are known [8]. The simple ammine complexes of $Mn(NH_3)_6X_2$ ($X = Cl, Br, I$) are also known. Thermal dissociation of these ammine complexes give rise to the species $MnX_2 \cdot nNH_3$ where $n = 4, 2$ and 1 [38]. Aniline and pyridine and their derivatives form the species $MnX_2 \cdot 2L$ which have been shown to be octahedral with bridging halide atoms[39]. Acetonitrile also forms the adducts of the type $MnX_2 \cdot 2CH_3CN$ ($X = Cl, Br$) where the metal atom is in an octahedral environment. However larger alkyl groups such as acrylonitrile and propionitrile form 1:1 adducts of the type $MnX_2 \cdot RCN$, for which the structure is unknown[40]. A very large number of tertiary phosphines coordinate to Mn(II) salts in a number of solvents leading to the isolation of complexes of empirical formula $MnX_2 \cdot L$. However the crystal structure of $MnCl_2 \cdot 2PEt_3$ has been reported where the manganese atom is in a distorted tetrahedral environment [41]. The proposed structure for the monoadduct on the basis of ir data is certainly not a monomer, it should be at least dimeric [42] or there is the possibility for a tetrameric structure, e.g., the well known

cubane structure $\{MnX_2\}_4$ [43]. These mono phosphine adducts have the ability to co-ordinate reversibly to molecular oxygen i.e. forming highly coloured adducts [44].



1.2.3 Co-ordination chemistry of Cd(II)

The Cd(II) ion shows a variety of co-ordination numbers ranging from two to eight; within this range, six co-ordination is predominant with a variety of ligands. In many cases the stoichiometry for the six co-ordinate complexes is $CdX_2 \cdot L_2$ in which halide bridging occurs to form infinite chain structures (Figure 1.6).

Cadmium compounds with co-ordination numbers two and three are rare, although many compounds of stoichiometry $M^{+}(CdX_3)^{-}$ have been prepared. The mononuclear $(CdX_3)^{-}$ anion has not been characterized by an X-ray structure determination but as a general rule the anion $(CdX_3)^{-}$ normally shows a co-ordination number four or higher. Several salts which have been structurally characterized contain either dinuclear $[X_2CdX_2CdX_2]^{2-}$ units [45] in which cadmium is four co-ordinate or polynuclear $[-X_2CdX_2Cd-]^{2-}$ chains in which Cd is in an octahedral environment. Four and five co-ordination

generally arise from the bulkiness of large donor atoms and/or special steric requirements of the ligand [46], whereas seven and eight co-ordinate Cd(II) complexes are relatively scarce and involve only the smallest donor atoms[45].

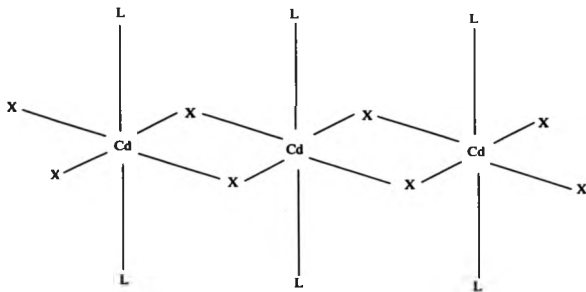


Figure 1.6 The structure of $CdX_2 \cdot L_2$

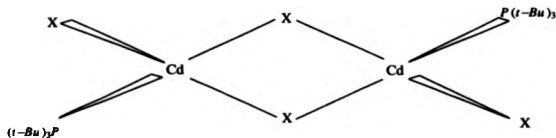


Figure 1.7 The structure of $CdX_2 \cdot P(t-Bu)_3$

The reactions of group IIB metal halides (Zn, Cd, Hg) with Lewis base ligands containing group VB donor atoms (N, P, As) have been extensively investigated. The most usual products are tetrahedral adducts of stoichiometry MX_2L_2 , (dimeric with halide bridges) or MX_2L_2 , (tetrahedral monomeric) [47-64]. However octahedral polymeric adducts are also known for the type MX_2L_2 (Figure 1.6) e.g., $CdCl_2 \cdot 2NH_3$, $HgBr_2 \cdot 2NH_3$, and $CdBr_2 \cdot 2C_2H_5N$ [48,50,58,60,63,64-67]. The 1:2 adducts are described as a distorted CsCl array of ligand and halogen atoms with Cd(II) in the six co-ordinate holes. Reactions of dialkylamines with Cd(II) halides either give 2:1 or 1:1 adducts [68]. Diethylamine or di-n-propylamine give 2:1 adducts $CdX_2 \cdot 2R_2NH$ formulated as ionic complexes of the type $[Cd_4(amine)] [CdX_4]$. With the larger bulkier amines such as di-n-butylamine, di-isobutylamine, di-n-hexylamine or dibenzylamine, CdX_2 yield 1:1 adducts, presumably because of the steric strain imposed by the presence of the larger amines.

Reactions of PR_3 with anhydrous CdX_2 in aprotic solvents give $CdX_2 \cdot 2PR_3$ (where $R = C_6H_5$, C_4H_9 , alkyl and $X = Cl, Br$) [56]. The authors suggested tetrahedral co-ordination around the cadmium atom on the basis of ir evidence. An X-ray crystal structure determination confirmed these observations for $CdCl_2 \cdot 2PPH_3$ in which the Cd atom has a pseudo tetrahedral geometry

[69]. The reaction of tri-tertiary butyl phosphine with CaX_2 ($X = Cl, Br, I$) under aprotic conditions provides complexes of 1:1 stoichiometry alone (Figure 1.7 page 19) [70]. The failure of further co-ordination in this instance is due to the large steric requirements of the ligand.

1.2.4 Co-ordination Chemistry of Cu(II) [d^9]

+2 is the most important oxidation state for copper; most Cu(I) compounds can be readily oxidized to Cu(II), but further oxidation to Cu(III) is more difficult. The d^9 configuration makes Cu(II) subject to Jahn-Teller distortion if placed in an environment of cubic symmetry. It is never observed in regular tetrahedral or octahedral environments. The majority of complexes and compounds of copper are either blue or green. Exceptions are generally caused by strong ultra-violet bands e.g., charge transfer bands tailing off into the blue end of the visible spectrum, thus causing the samples to appear red or brown. Blue or green colours are due to the presence of an absorption band in the 600-900 nm region of the UV-Vis spectrum.

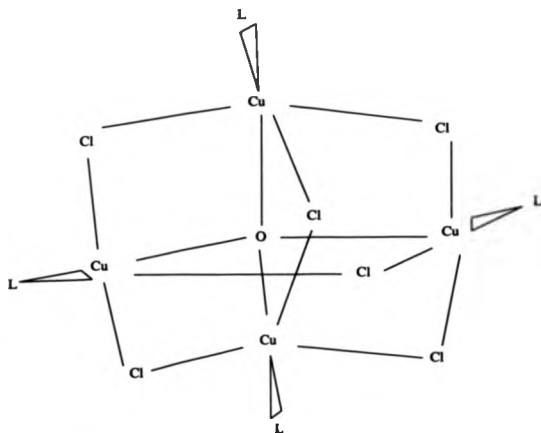


Figure 1.8 Structure of Cu_4OCl_6

Of the halides CuF_2 is colourless, CuCl_2 is yellow and CuBr_2 is almost black; the last two have structures of infinite parallel chains of square CuX_4 units sharing edges. Actually the environment around copper is that of an elongated octahedron which is completed by halide atoms of neighbouring chains. CuF_2 has a rutile structure. Cu(II) does not form compounds with iodine due to the Cu(II) being reduced to Cu(I) by iodine. The copper halides can be used to form many type of complexes with several ligands.

Ammonia forms complexes of the type $CuX_2 \cdot nNH_3$ where $n = 2, 4, 5$, and 6 and of these the hexammine complex is very unstable. $CuCl_2$ forms a bis adduct with pyridine which has a square planar arrangement of halide and pyridine around copper, with two longer and weaker Cu-Cl bonds, giving a tetragonal distorted octahedron. Bis adducts are also formed with alkylamines and aniline. But with tertiary amines according to Lane and Yoke [25] reduction of Cu(II) to Cu(I) was observed. Tertiary phosphines and arsines also reduce Cu(II) to Cu(I) [71].

Cu(II) complexes of the type $Cu_4(OCld)_4$ ($L = OPEt_3$, pyridine, ammonia) are known. The structures have a μ_4 oxygen atom at the centre of a Cu_4 tetrahedron; each Cu is bound to a ligand L, and three chlorine atoms so that Cu(II) is approximately trigonal bipyramidal. Each copper is connected to the other three coppers via three chloride bridges (Figure 1.8) [72].

1.2.5 Chlorocuprate(II) complex anions

The primary interest in the halogenocuprates(II) is due to their ability to assume very different geometries and a great variety of co-ordination numbers. The factors which give this characteristic include Jahn-Teller effect, crystal field stabilization, ligand-ligand repulsion, shape and size of

the counter ions, Van der Waals forces and hydrogen bonding interactions [73].

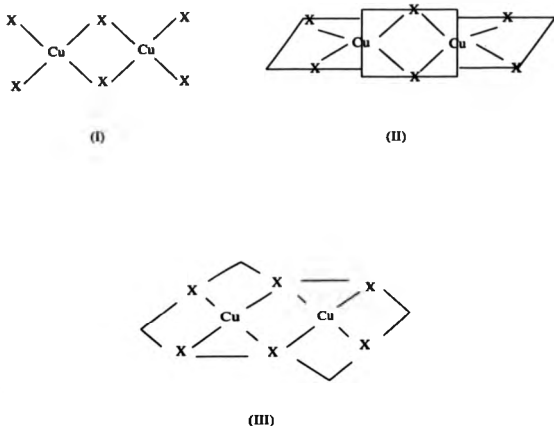


Figure 1.9 *Examples of the stereochemistry of the dimeric species: (I) planar, (II) twisted, (III) bifoldd forms*

In $[A]_2[CuCl_4]$ (where A = monocharged organic/inorganic cation) salts the stereochemistry of the anions ranges from square planar to nearly

tetrahedral. For the species $[A][CuCl_3]$, it is possible to subdivide the compounds into three general classes [74]: isolated oligomers, stacked dimers, linear chains. The stereochemistry of the dimeric species includes planar(I), twisted(II), and chair or bifolded forms(III) [Figure 1.9] [75]. The stoichiometries and structures of various chlorocuprates(II) are summarized in Table 1.4 [76].

The known trimethylammonium chlorocuprates(II) [77] are:



In our studies, reaction of excess trimethylamine with anhydrous copper(II) chloride assumes an extensive green colouration, but the final product isolated following complete removal of amine is the yellow-brown mono adduct. Attempted purification via a Soxhlet extraction with boiling dichloromethane provided a mustard-yellow semicrystalline solid. Recrystallization of the solid from dichloromethane resulted in the formation of golden yellow needles identified as the ionic salt $[Me_3N(CH_2Cl)][[CuCl_4]^{2-}]$. Here the trimethylchloromethylammonium cation must have captured the chloromethyl group from the solvent dichloromethane and the anion features Cu(II). Obviously an unknown sequence of competing reactions is occurring. (This will be discussed in detail in section 1.3).

Anion type	co-ordination geometry	example
(a) Stoichiometry $A[CuCl_3]$		
$[CuCl_3]_n$ chains	Distorted octahedral	$CuCuCl_3$
$[Cu_2Cl_4]^{2-}$ dimer	Distorted octahedral	$KCuCl_3$
$[Cu_2Cl_6]^{2-}$ dimer	Square pyramidal	$[Me_2NH_2][CuCl_3]$
(b) Stoichiometry $A_2[CuCl_4]$		
Square planar $[CuCl_4]^{2-}$	Distorted octahedral	$[NH_4]_2[CuCl_4]$
Tetrahedral $[CuCl_4]^{2-}$	Distorted tetrahedral	Cs_2CuCl_4
(c) Stoichiometry $A_3[CuCl_5]$		
$[CuCl_5]^{3-}$	Trigonal bipyramidal	$Co(NH_3)_6CuCl_5$
$[CuCl_4]^{2-} + Cl^-$	Distorted octahedral	$[dienH_3][CuCl_5]$
$[CuCl_4]^{2-} + Cl^-$	Distorted tetrahedral	Cs_3CuCl_5

Table 1.4 *Stoichiometries and structures
of selected chlorocuprates(II)*

1.3 Results and discussion

The present study is mainly concerned with Mn(II), Cd(II), and Cu(II) chloride systems. Separate discussion of each one now follows:

1.3.1 Reaction of trimethylamine with manganese(II) chloride

Reaction of trimethylamine with anhydrous manganese(II) chloride provides the mono adduct $MnCl_2 \cdot NMe_3$, which is assumed, by comparison with the tertiary phosphine analogues $MnX_2 \cdot L$ (where X = halogen NCS; L = tertiary phosphine) to have a polymeric or at least dimeric structure in the solid state (Figure 1.10) [78]. Analytical and spectroscopic data appear in Tables 4.1 and 4.2 respectively (pages 146 and 147).

The ir spectrum shows strong characteristic bands due to the presence of co-ordinated trimethylamine. One interesting facet of the tertiary phosphine complexes of Mn(II) is their general ability to reversibly co-ordinate dioxygen and other small molecules such as NO, CO, etc. under quite mild conditions[79], e.g., $MnCl_2 \cdot PMe_3$, which is the direct trimethylamine counterpart, reacts with oxygen irreversibly to produce the oxidized Mn(III) complex $MnCl_2 \cdot 2PMe_3$ along with other products[80]. However our compound $MnCl_2 \cdot NMe_3$, shows no reaction with dioxygen under various conditions.

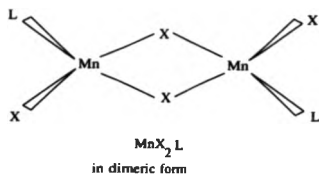


Figure 1.10

Attempted recrystallization of the mono adduct from a variety of common organic solvents failed to give crystals of suitable quality for an X-ray structure determination. However an interesting result has been obtained by Soxhlet extraction, in boiling acetonitrile which resulted in the formation of a deep green solution together with an insoluble grey residue which was left behind in the extraction thimble. Gradual removal of solvent from the saturated green solution provided a crop of pink crystals which were carefully removed. Complete removal of solvent from the remaining mother liquor provided a green solid. Subsequent recrystallizations from MeCN of these two separate products provided

- i) pink cylindrical rods of $(\text{Me}_3\text{NH})_2(\text{MnCl}_4)$ (II),
- ii) light green needles of $(\text{Me}_3\text{NH})_2(\text{MnCl}_4) \cdot 2\text{H}_2\text{O}$ (III) (Figure 1.11).

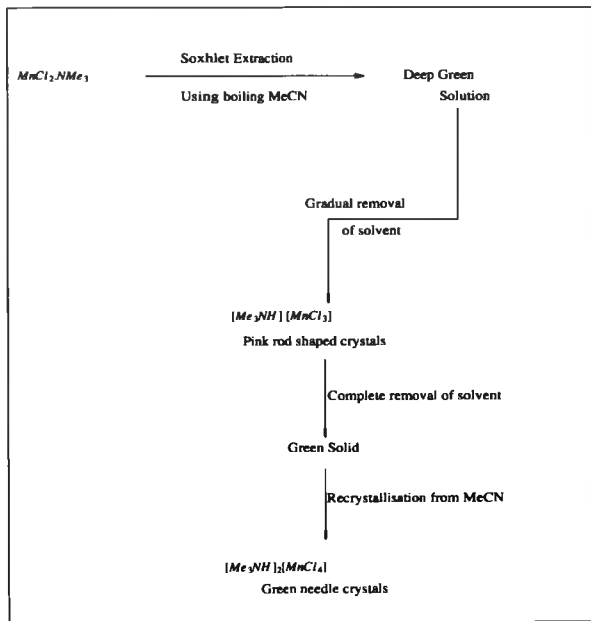


Figure 1.11 The detailed reaction scheme for $MnCl_2/NMe_3$ system

An attempted crystallization of $MnCl_2 \cdot NMe_3$ via Soxhlet extraction with boiling MeCN provides a green solution from which two products, both chloro-anions were isolated. IR data shows the presence of $[Me_3NH]^+$, where

there is a strong peak for ν_{NH^+} at 2786 cm^{-1} for $[Me_3NH][MnCl_3]$ (pink); at 2735 cm^{-1} for $[Me_3NH]_2[MnCl_4]$ (green). The Vis-UV spectra (Table 4.3, Page 147) show the presence of octahedral Mn(II) species in solution. The compound $[Me_3NH][MnCl_3]$ (II) has been fully characterized via an X-ray crystal structure determination (Figure 1.12).

Unfortunately the green crystals of $[Me_3NH]_2[MnCl_4]$ are not suitable for an X-ray crystal structure determination. However powder diffraction data suggest that the environment around Mn(II) in $[MnCl_4]^{2-}$ is also octahedral. Previous structure determinations of $[MnCl_3]^-$ [81] and $[MnCl_4]^{2-}$ [82] have been noted but with different cations to the $[Me_3NH]^+$ in our studies. In addition to the present species, other chloro anions of Mn(II) include $MnCl_4^-$ and $Mn_2Cl_7^-$ [83], $MnCl_6^-$ [84], and $Mn_2Cl_7^-$ [79] but there is no direct analogue of the tetrahedral zinc(II) species $[ZnCl_3]^-$.

The Crystal Structure of $(Me_3NH)[MnCl_3]$ (II)

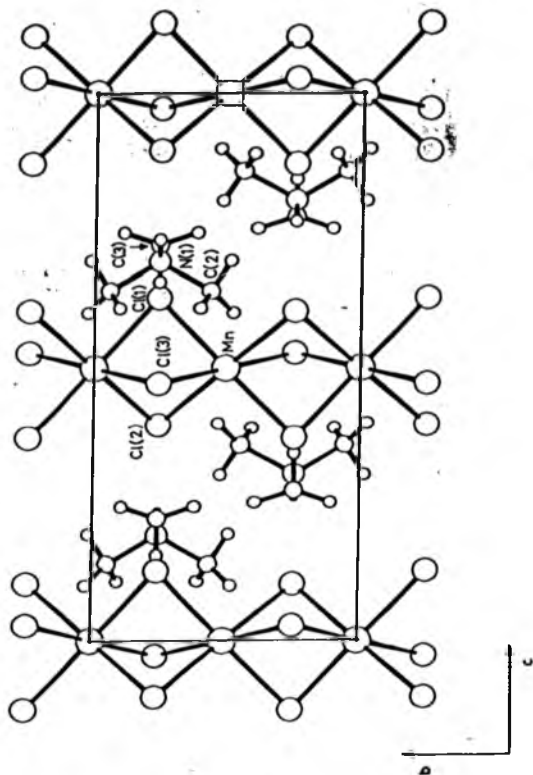


Figure 1.12

Crystal data for $(Me_3NH)[MnCl_3]$.

Formula	$MnCl_3NC_3H_{10}$
M_r	221.4
Crystal class	orthorhombic
space group	Pcnn
systematic absences	hk0, $h + k = 2n + 1$, 0kl, $k = 2n + 1$.
Crystal size	$0.25 \times 0.20 \times 0.15$ mm
a	8.938(7) Å
b	6.474(8) Å
c	14.396(14) Å
V	833.0 Å ³ ,
F(000)	444
D_x	1.76 g cm ⁻³ ,
Z	4
$\lambda(Mo-K\alpha)$	0.7107 Å
$\mu(Mo-K\alpha)$	25.17 cm ⁻¹
Scan rate	0.0333 s ⁻¹
2 θ maximum	50°
Final R value	0.077 ($R_w = 0.079$)

Discussion of the structure

Molecular Dimensions are given in Table 1.5. The structure of $[\text{Me}_3\text{NH}][\text{MnCl}_3]$ (Figure 1.12) is similar to that observed for $[\text{Me}_3\text{NH}][\text{CdCl}_3]$ [85] in that it contains $[\text{Me}_3\text{NH}]^+$ cations and one-dimensional $[\text{MnCl}_3]^-$ polymeric chains in comparable unit cells. However, for our Mn salt, it proved possible to refine the cation as ordered rather than disordered around the crystallographic mirror planes.

The Mn - Cl bond lengths in the $[\text{MnCl}_3]^-$ anion (Table 1.5) can be compared to the unique value of 2.560(2) Å found in similar chains in $[\text{NMe}_4][\text{MnCl}_3]$ [81]. However, of the three unique bonds in the anion, Mn - Cl(1) at 2.573(2) Å is significantly longer than the other two [Mn - Cl(2) 2.539(2), Mn - Cl(3) 2.525(2) Å]. It seems likely that this elongation is due to the formation of the N(1) - H ... Cl(1) hydrogen bond (N ... Cl 3.28(2), H ... Cl 2.46 Å). Similar variations in the M - Cl distances are observed in the $[\text{CdCl}_3]^-$ anion [85].

Anionic polymer chain

Mn(1) - Cl(1) 2.573(2)

Mn(1) - Cl(2) 2.539(2)

Mn(1) - Cl(3) 2.525(2)

Cl(1) - Mn(1) - Cl(2) 83.83(8)

Cl(1) - Mn(1) - Cl(3) 83.71(7)

Cl(2) - Mn(1) - Cl(3) 84.12(8)

Mn(1) - Cl(1) - Mn(1*) 77.93(8)

Mn(1) - Cl(2) - Mn(1*) 79.21(8)

Mn(1) - Cl(3) - Mn(1*) 79.74(8)

Cation

N(1) - C(2) 1.521(14)

N(1) - C(3) 1.447(17)

C(2) - N(1) - C(2*) 110.2(11)

C(2) - N(1) - C(3) 112.7(7)

* symmetry element x, .5-y, z

Table 1.5 Molecular Dimensions (Distances Å, Angles degrees)

1.3.2 Reaction of trimethylamine with cadmium(II) chloride

Preliminary studies of this system were carried out by Rajesh Karia [28]. Direct treatment of anhydrous $CdCl_2$ with an excess of trimethylamine over a period of several days gives the white amine-insoluble mono adduct $CdCl_2 \cdot NMe_3$ (IV). An attempted crystallization of $CdCl_2 \cdot NMe_3$ by Soxhlet extraction with polar solvents such as MeCN, MeOH yields crystals of $[Me_3NH][CdCl_3]$ (V) and an insoluble light brown Cd(II) containing residue which is left behind in the extraction thimble

Rather than the 1:2 adduct (as formed by Zn the other Group IIB representative) Cd forms the 1:1 complex with neat amine. Typically $CdCl_2 \cdot L$ (where X = halogen, L = substituted phosphine) complexes are dimeric with tetrahedral metal ions linked by halogen bridges e.g., X = Cl, Br; L = $(t-Bu)_3P$ [70], X = I; L = $(Et)_3P$ [86] and the same structure is assumed for $CdCl_2 \cdot NMe_3$. Summarizing the Zn(II) system : Noth et al [87] have postulated $ZnCl_2 \cdot 2NMe_3$ to be a neutral tetrahedral species as would be expected for a Zn four co-ordinate complex. The work in our laboratory showed that recrystallization of $ZnCl_2 \cdot 2NMe_3$ from benzene readily undergoes rearrangement to give the ionic complex $[Me_3NH][ZnCl_3 \cdot NMe_3]$ [5]. An X-ray crystal structure determination showed the expected tetrahedral geometry around

the Zn atom. The rearrangement gives a sterically stable anionic species. A general reaction scheme for adduct formation and rearrangement is shown in Figure 1.13 below :

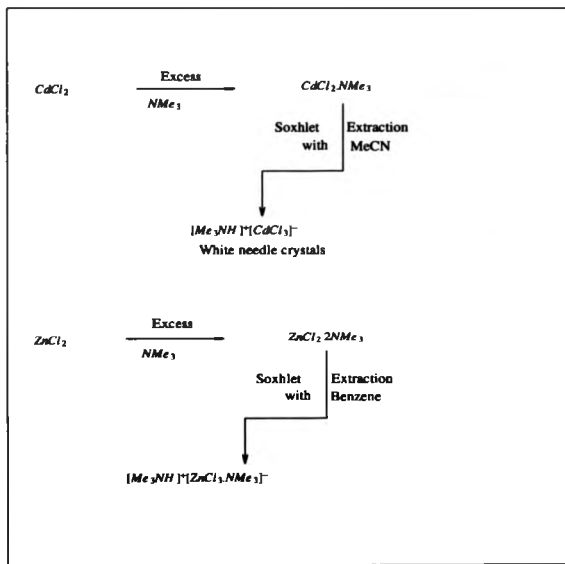


Figure 1.13 A general reaction scheme for the formation of ionic products.

Cadmium normally prefers an octahedral six co-ordinate environment, for example $CdX_2 \cdot R_3NH$ (where $X = Cl, Br$) which are normally polymeric with halogen bridging. In all cases ν_{Cd-Cl} bridging is determined at lower frequency compared with ν_{Cd-Cl} terminal [70,88,89]. Our complex $CdCl_2 \cdot NMe_3$ shows two bands below $400cm^{-1}$ which are assigned as ν_{Cd-Cl} terminal at $244 cm^{-1}$ and ν_{Cd-Cl} bridging at $210 cm^{-1}$, comparable with $[CdCl_2 (t-Bu)_3P]_2$ ν_{Cd-Cl} at $285 cm^{-1}$ and $208 cm^{-1}$ respectively [70]. Therefore we can postulate the following structure (Figure 1.14) for our $CdCl_2 \cdot NMe_3$ similar to that of $CdCl_2 (t-Bu)_3P$.

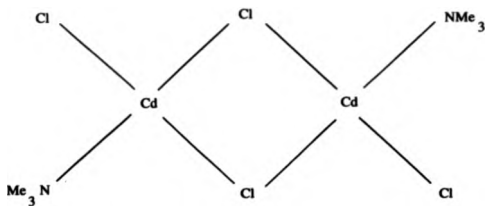


Figure 1.14 Postulated structure of $CdCl_2 \cdot NMe_3$

The formation of a bridged structure might be the reason for its poor solubility in many of the common organic solvents. Attempted recrystallization from polar solvents such as MeCN by Soxhlet extraction leads to the formation of $[Me_3NH] [CdCl_3]$ as white needle crystals and an insoluble light

brown residue containing Cd(II). The ir spectrum of $[Me_3NH][CdCl_3]$ contains a characteristic ν_{NH} band at 2778 cm^{-1} . The proton nmr spectrum shows two peaks at room temperature a sharp singlet at $\delta_{CH} = 2.78\text{ ppm}$ and a much broader signal at $\delta_{NH} = 11.75\text{ ppm}$. Both signals show a perceptible downfield shift ($\delta_{CH}=2.84$, $\delta_{NH}=12.20$) on cooling from 298K to 230K. In the present studies in a separate experiment Soxhlet extraction of $CdCl_2 \cdot NMe_3$ by boiling MeOH also results in the formation of $[Me_3NH][CdCl_3]$. The formation of ionic products from the rearrangement of neutral adducts in the presence of anhydrous solvents is open to question. Chapuis and Zuniga have reported the X-ray crystal structures of three phases of $[Me_3NH][CdCl_3]$ (174K, 295K, 415K) [85]. The basic structure is made up of one dimensional chains of face-fused $CdCl_4$ octahedra with disordered trimethylammonium cations located in the free space between the chains. Additionally the organic cation is involved in a strong hydrogen bond $N - H \cdots Cl$ with a chlorine atom. The X-ray crystal structure of our product, carried out as an independent study, is similar to those at 174 and 295K; all three structures have equivalent dimensions for the polymeric $CdCl_3$ anion.

The Crystal Structure of $[Me_3NH]_2 [CdCl_3]_2 (V)$

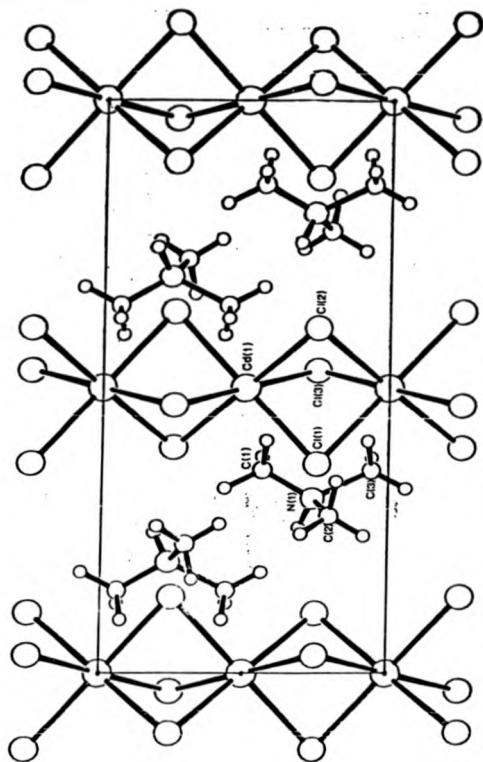


Figure 1.15

Crystal data

Formula	$\text{CdCl}_2\text{NC}_3\text{H}_{10}$
M	278.9
Crystal class	orthorhombic
a	8.855(7) Å
b	6.689(6) Å
c	14.308(10) Å
V	1280.0 Å ³
Z	4
D_c	2.18 g cm ⁻³
λ	0.7107 Å
μ	34.0 cm ⁻¹
Space group	Pcnn (No 62)
Systematic absences	hk0, h+k=2n+1, 0kl, k+l=2n+1
Scan rate	0.033° s ⁻¹
Number of data measured	990
Number of data used in refinement	548
Final R	0.073 ($R_w = 0.075$)

The cation in (V) was disordered around the mirror plane. Molecular dimensions are given in Table 1.6. The structure consists of polymeric chains of $(CdCl_3)^-$ anions together with disordered $(Me_3NH)^+$ cations. The unit cell is shown in Figure 1.15 together with the atom numbering scheme. The angles subtended by pairs of chlorine atoms on the same mirror plane at the cadmium atom are all considerably less than 90° being $83.54(12)$, $83.86(11)$ and $83.86(11)$ (degrees). The three Cd - Cl distances are somewhat different with Cd(1) - Cl(1) at $2.650(3)$ considerably greater than Cd(1) - Cl(2) and Cd(1) - Cl(3) ($2.616(3)$ and $2.609(3)$ Å respectively).

This long Cd(1) - Cl(1) bond is due to the presence of a hydrogen bond between Cl(1) and N - H. Dimensions are N...Cl 3.26 , H...Cl 2.40 Å and N-H...Cl 150° . The trimethylammonium cation is disordered.

Anionic polymer chain

Cd(1) - Cl(1)	2.650(3)
Cd(1) - Cl(2)	2.616(3)
Cd(1) - Cl(3)	2.609(3)
Cl(1) - Cd(1) - Cl(2)	83.54(12)
Cl(1) - Cd(1) - Cl(3)	83.86(11)
Cl(2) - Cd(1) - Cl(3)	83.86(11)
Cd(1) - Cl(1) - Cd(1*)	78.25(13)
Cd(1) - Cl(2) - Cd(1*)	79.47(13)
Cd(1) - Cl(3) - Cd(1*)	79.73(12)

Cation

N(1) - C(2)	1.56(10)
N(1) - C(3)	1.53(4)
N(1) - C(2*)	1.40(9)
C(3) - N(1) - C(2*)	123.7(49)
C(2) - N(1) - C(2*)	116.5(22)
C(2) - N(1) - C(3)	96.1(52)

* Symmetry element X, .5 - Y, Z

Table 1.6 Molecular Dimensions (Distances Å, Angles Degrees)

1.3.3 Mode of reaction

How the $MCl_2 \cdot NMe_3$ (where $M = Zn, Mn, Cd$) complexes rearrange in MeCN to give the corresponding anions is open to question. Studies by Goel et al [37, 70] of the $M(H)halide-(t-Bu)_3P$ systems (where $M = Co, Ni, Zn, Cd$) lend emphasis to the importance of the choice of solvent e.g., with 1-butanol, anionic complexes $[(t-Bu)_3PH] [MX_2P(t-Bu)_3]$ are isolated following phosphine protonation by the solvent; in aprotic solvents the neutral $MX_2 \cdot P(t-Bu)_3$ adducts are formed.

Unlike the formation of $[Me_4N] [CdCl_3]$ and $[NH_4] [CdCl_3]$ which simply involve the reaction of the relevant ammonium chloride salt with cadmium(II) chloride under aqueous conditions, our product $[Me_3NH] [CdCl_3]$ was obtained from $CdCl_2 \cdot NMe_3$ with MeCN or MeOH. In our studies under anhydrous conditions and without the presence of a readily available source of chloride the reaction of $CdCl_2 \cdot NMe_3$ at some stage must involve molecular rearrangement with the reaction medium to give a mixture of products.

In the present study, proton abstraction from $(MeCN, benzene, Me_3N)$ solvents is rather unlikely. A more likely possibility is the inclusion of moisture in the participating solvents. We believe traces of water in the solvent play a crucial role in initiating limited solvolysis of $M - Cl$ bonds to give

molecular rearrangement with incipient halide transfer and loss of coordinated trimethylamine. The latter provides the trimethylammonium cation following proton capture; the formation of insoluble residues, most likely $[M(II) (oxo) (hydroxo) (chloro)] (?)$ species, is seen to preserve the overall balance of metal : halogen.

1.3.4 Reaction of trimethylamine with copper(II) chloride

Direct addition of anhydrous $CuCl_2$ and an excess of trimethylamine in a sealed double ampoule vessel provides a yellow-brown solid which, by virtue of limited solubility in the parent amine, was extracted in situ (following filtration and back distillation of trimethylamine) to give a bright yellow solid.

Previously Lane and Yoke [25] have shown that direct treatment of anhydrous $CuCl_2$ with trimethylamine at $0^\circ C$ gives the stable yellow-brown mono adduct $CuCl_2 \cdot NMe_3$ (analytical values based on $CuCl_2 \cdot 1.081NMe_3$). The initial blue-green product is presumed as the bis adduct $CuCl_2 \cdot 2NMe_3$; this changes to the yellow-brown mono adduct once all the trimethylamine has been removed. In their studies oxidation of trimethylamine by $CuCl_2$ has been observed above $75^\circ C$, resulting in a dark red tarry product. Dimethyl

methylene ammonium cation is obtained as the oxidation product of trimethylamine, but the nature of the Cu(I) reduction product is not clear.

In our studies further purification of the yellow solid via a Soxhlet extraction with boiling benzene provided a bright yellow solid with a sharp melting point 154-155° C. Micro-analytical data corresponds with the mono adduct $\text{CuCl}_2 \cdot 1.1\text{NMe}_3$ - identical with that of Lane and Yoke. The ir spectrum shows all the bands of co-ordinated trimethylamine (1265 cm^{-1} , 999 cm^{-1} , 830 cm^{-1} and 564 cm^{-1}) and the far ir has two bands below 400 cm^{-1} at 250 cm^{-1} and 204 cm^{-1} assigned to Cu-Cl stretching modes. The electronic spectrum has a "d-d" band at $11,494\text{ cm}^{-1}$ with a broad shoulder at $13,089\text{ cm}^{-1}$.

Several attempts to get this mono adduct in a crystalline form (via recrystallization from benzene, acetonitrile and other non-chlorinated solvents) to undertake an X-ray structure determination were unsuccessful. However the use of a chlorinated solvent CH_2Cl_2 provided golden yellow cubic crystals suitable for X-ray structural studies. The yellow crystalline product is characterized as $[(\text{CH}_3)_3\text{NCH}_2\text{Cl}]_2 [\text{CuCl}_4]$ which melts with decomposition at 220-222° c. The ir spectrum contains bands at 1150(br,w), 970(m), 804(m), and 720(st) cm^{-1} . The strong bands at 1265, 1000, 830 and 565 cm^{-1} characteristic of co-ordinated trimethylamine are no longer present. The far

ir has a broad asymmetric band at 271 cm^{-1} with evidence of a shoulder on the higher energy side at 290 cm^{-1} , characteristic of $\nu_{\text{Cu-Cl}}$ of the tetrachlorocuprate(II) anion. (The literature values for the ν_3 (Cu-Cl stretching) for $[(Et)_4N]_2[CuCl_4]$ are at 289(sh), 268(st) and $247(\text{m})\text{ cm}^{-1}$ [90]; 267 cm^{-1} [91]; $267(\text{st})$ and $248(\text{sh})\text{ cm}^{-1}$ [92]). The electronic spectrum has a single broad band in the near ir region at $\lambda_{\text{max}}\ 9360\text{ cm}^{-1}$. Decomposition of the mono adduct with the formation of the novel trimethylchloromethylammonium cation and tetrachloro cuprate(II) anion clearly must involve some sort of rearrangement with the solvent molecule CH_2Cl_2 . Dichloromethane can provide the CH_2Cl^+ which rapidly combines with trimethylamine to give the quaternary ammonium cation. The accompanying Cl^- must be utilized in the formation of the chlorocuprate(II) anions.

The anion obtained from dichloromethane is the tetrachlorocuprate(II) anion not the trichlorocuprate(II) anion. It is not clear why the tetrachlorocuprate anion is formed in preference to the trichlorocuprate anion; perhaps the lattice energy considerations are heavily in favour of the former.

The crystal structure of $[Me_3NCH_2Cl]_2[CuCl_4]$ (VII)

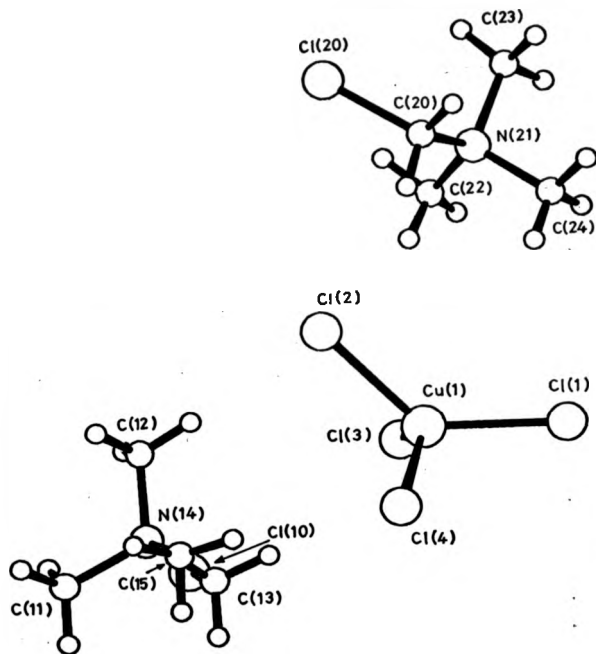


Figure 1.16

Crystal data

Formula	$\text{CuCl}_6\text{C}_6\text{H}_{12}\text{N}_2$
M	422.42
Crystal class	monoclinic
a	15.273(15) Å
b	17.493(18) Å
c	11.722(13) Å
β	75.8(1)°
V	1837.0 (Å) ³
F(000)	860
d_m	1.53 g cm ⁻³
d_c	1.53 g cm ⁻³
Z	4
μ (Mo-K α)	20.8 cm ⁻¹
Space group	$P2_1/n$
Crystal size	0.3 × 0.4 × 0.2 mm
Final R	0.062 ($R_w = 0.064$)

Table 1.7 Molecular Dimensions (Distances-Å, Angles-Degrees)

Dimensions in the Anion

Cu(1)-Cl(1)	2.245(4)
Cu(1)-Cl(2)	2.253(3)
Cu(1)-Cl(3)	2.232(3)
Cu(1)-Cl(4)	2.243(3)
Cl(1)-Cu(1)-Cl(2)	132.52(15)
Cl(1)-Cu(1)-Cl(3)	99.71(13)
Cl(2)-Cu(1)-Cl(3)	97.98(14)
Cl(1)-Cu(1)-Cl(4)	99.94(14)
Cl(2)-Cu(1)-Cl(4)	98.21(14)
Cl(3)-Cu(1)-Cl(4)	134.44(16)

Dimensions in the cations

Cl(10)-C(13)	1.728(13)
C(11)-N(14)	1.478(20)
C(12)-N(14)	1.447(15)
C(13)-N(14)	1.498(16)
C(15)-N(14)	1.575(15)
Cl(20)-C(20)	1.771(13)
C(20)-N(21)	1.467(14)
N(21)-C(22)	1.470(16)
N(21)-C(23)	1.524(15)
N(21)-C(24)	1.496(18)
Cl(10)-C(13)-N(14)	109.9(8)
C(11)-N(14)-C(12)	114.9(11)
C(11)-N(14)-C(13)	109.0(10)
C(12)-N(14)-C(13)	114.4(9)
C(11)-N(14)-C(15)	107.6(10)
C(12)-N(14)-C(15)	107.3(11)
C(13)-N(14)-C(15)	102.6(10)
Cl(20)-C(20)-N(21)	112.0(7)
C(20)-N(21)-C(22)	113.1(11)
C(20)-N(21)-C(23)	112.1(9)
C(22)-N(21)-C(23)	109.7(10)
C(20)-N(21)-C(24)	104.4(8)
C(22)-N(21)-C(24)	109.8(11)
C(23)-N(21)-C(24)	107.6(11)

Discussion of the structure

The structure which is shown in the Figure 1.16 together with the atom numbering scheme consists of two independent $(Me_3NCH_2Cl)_2$ cations and one $[CuCl_4]^{2-}$ anion. Bond lengths and bond angles are given in Table 1.7. The conformation of the cation is as expected. In the anion there is a significant deviation from both of the two ideal geometries, square planar and tetrahedral, in that the angles around the metal atom are 98.0(1), 98.2(1), 99.7(1) and 99.9(1), 132.5(1) and 134.4(1)°. The bond lengths are however regular at 2.232(3), 2.243(3), 2.245(4), 2.253(3) Å.

In a recent publication, Halvorson et al. [93] have analyzed over 60 crystal structure determinations containing the $[CuCl_4]^{2-}$ anion. The majority of the structures contain *trans* Cl-Cu-Cl angles between 125 and 145°. From a plot of *trans* angles against frequency, there is a maximum around 135° with a secondary maximum at 180°. Halvorson et al. [93] note that the occurrence of hydrogen bonds to the chlorine atoms in the anion tends to decrease the *trans* angle.

However there are necessarily no such contacts in the present structure and indeed the closest C-H...Cl contact is 2.73 Å. So it is perhaps appropriate that the present angles at 133, 134° are almost identical to the reported

maximum at 135° .

Halvorson et al. also correlate the value of the d-d electronic absorption with the *trans* Cl-Cu-Cl angle and obtain a straight line plot so that with an angle of 134° , the predicted energy is $9,500\text{ cm}^{-1}$. Our experimental value is 9360 cm^{-1} which is very close to the predicted value.

CHAPTER TWO

**Reactions of crown ethers
with Group VB
trichlorides (As,Sb and Bi) and antimony pentachloride**

2.1 Introduction

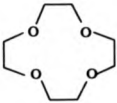
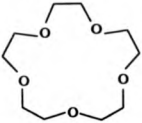
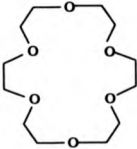
This work is mainly concerned with the general Lewis acid behaviour of the M(III) halides As, Sb, Bi (principally the chlorides) and their reactions with the crown-ethers 12-C-4, 15-C-5, 18-C-6 (Table 2.1). The reactions of Sb(V) chloride with these three crown ethers have also been studied.

Our contribution is

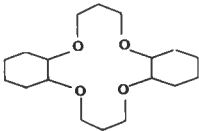
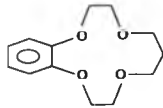
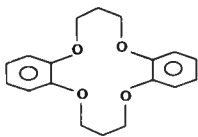
- i) to synthesize new Group VB chloro-crown ether complexes
- ii) to provide a full spectroscopic (ir, proton nmr) and X-ray structural characterization of these novel compounds,
- iii) to evaluate the co-ordination and reactivity properties of these systems, especially the stereochemical involvement of the lone pair of electrons associated with M(III) and the conformational and stereochemical aspects of the crown molecules.

The introductory sections (2.1.1-2.1.4) present a brief discussion of the properties of crown ethers.

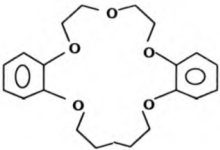
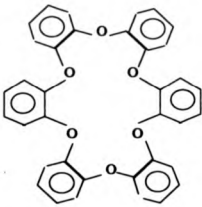
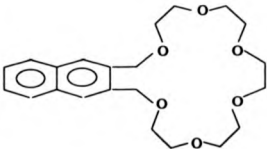
Table 2.1 *Trivial names of crown ethers*

STRUCTURE	TRIVIAL NAME
	12-Crown-4
	15-Crown-5
	18-Crown-6

[Contd.] Table 2.1

STRUCTURE	TRIVIAL NAME
	Dicyclohexano-14-Crown-4
	Benzo-13-Crown-4
	Dibenzo-14-Crown-4

[Contd.] Table 2.1

STRUCTURE	TRIVIAL NAME
	<p>Dibenzo-18-Crown-5</p>
	<p>Hexabenzocrown-6</p>
	<p>Naphtho-20-Crown-6</p>

2.1.1 Crown ethers

Cyclic polyethers (crown ethers) were the first synthetic macrocycles to be used as ligands for metal ions and they continue to be highly useful in this regard. The basic component of a crown ether is the donor ring which has the repeated units of $-OCH_2CH_2-$ (Table 2.1). A trivial nomenclature for these compounds has been devised by Pederson which is still in use [94]. The exceptional stability of macrocyclic complexes (which is approximately ten times that of open-chain analogues) is one of many reasons for the intense interest in these ligands which has been shown during recent years. The complexing ability and molecular flexibility are mainly determined by ring size and the nature of substituted moieties (these factors are discussed in detail later in this section).

Names and structures of crown ethers

Since the IUPAC names of many of these cyclic polyethers are too cumbersome for repeated use, abbreviated forms of nomenclature have been employed for their easy identification. Pederson named these cyclic polyethers as "crown" compounds, because of their ability to encapsulate or crown a metal cation. The trivial names are based on the following concepts:

- i) the number and kind of hydrocarbon rings,
- ii) the total number of atoms in the polyether ring,
- iii) the class name "crown" and
- iv) the number of oxygen atoms in the polyether ring.

A representative list of crown ethers commonly used in research studies is given in Table 2.1 (Pages 54-56). Macrocyclic polyethers can be either saturated or unsaturated; their properties are shown in Table 2.2.

Table 2.2 Properties of crown ethers

Crown ethers with aromatic side rings	Saturated crown ethers
Colourless crystalline compounds	Colourless viscous liquids or solids of low melting points
The compounds containing more than one benzo group are essentially insoluble in water and sparsely soluble in alcohols and the common organic solvents. They show good solubility in dichloromethane and chloroform.	Very much more soluble in all solvents. Most of them dissolve in petroleum ether and even display appreciable water solubility.
Absorb near 275nm in the UV-Vis region	No absorption above 220nm in the UV-Vis region

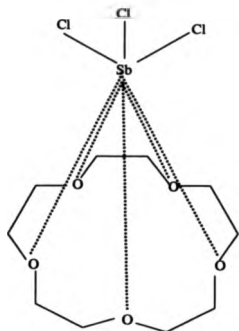


Figure 2.1 *The schematic diagram of $\text{SbCl}_5(15\text{-C-}5)$ complex*

Since Pederson's discovery [94] that crown ethers will form stable complexes with alkali metal salts, there have been many reports of complexes with different metals. However the only previous structural study of a Group VB halide-crown ether complex relates to $\text{SbCl}_5(15\text{-Crown-}5)$, in which a pyramidal SbCl_5 unit is bonded to the five oxygen atoms of the cyclic crown ether (Figure 2.1) [95]. Crown ethers can form complexes with inorganic or organic anions and cations or neutral molecules. These complexes are held together by electrostatic attractions (ion-dipole interaction). In addition to this, they can also form second sphere complexes where the crown ether

oxygen atoms are hydrogen bonded through co-ordinated water or ammonia molecules i.e., the macrocyclic polyether is not directly co-ordinated to the metal atom e.g., $\text{Sn}(\text{OH})_2\text{Cl}_4 \cdot 18\text{-C}-6 \cdot 6.2\text{H}_2\text{O} \cdot \text{CHCl}_3$ (Figure 2.2)[96]. Pederson was also the first to isolate defined crystalline complexes of crown compounds with uncharged organic molecules (thiourea, semicarbazide, etc.,) [97].

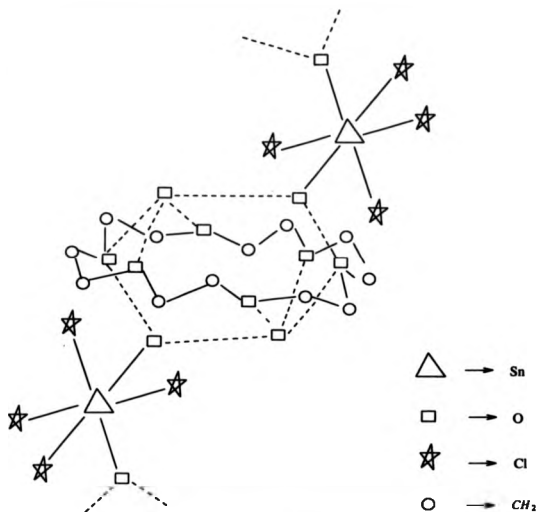


Figure 2.2 Structure of $\text{Sn}(\text{OH})_2\text{Cl}_4 \cdot (18\text{-C}-6) \cdot 6.2\text{H}_2\text{O} \cdot \text{CHCl}_3$ (schematic).

The dotted lines indicate the hydrogen bonds.

In most of the reported structures of complexes between alkali and alkaline earth metal cations and crown ethers [98, 99] the metal cation is located at the center of the hole. By way of contrast the crown ether complexes of Group VB chlorides feature "external co-ordination" with the metal atom outside the hole.

The ability of macrocyclic ligands to form stable complexes with various cations has been used to advantage in such diverse processes as isotope separation [100], the transport of ions through artificial and natural membranes [101], and the construction of ion-selective electrodes [102]. Crown ethers are also useful in organic synthesis in enhancing the nucleophilicity of anions by "freeing" them from cations in non-aqueous solvents [103]. The various parameters that determine the cation selectivity and complex stability are discussed in some detail below.

(1) Relative cation and ligand sizes

The enhancement of complex stability by a close correspondence between the ionic crystal radius of the metal ion and the radius of the cavity formed by the crown ether ring has been noted [99]. The selectivity of 18-C-6 for certain of the alkali and alkaline earth cations is shown in Figure 2.3 [104].

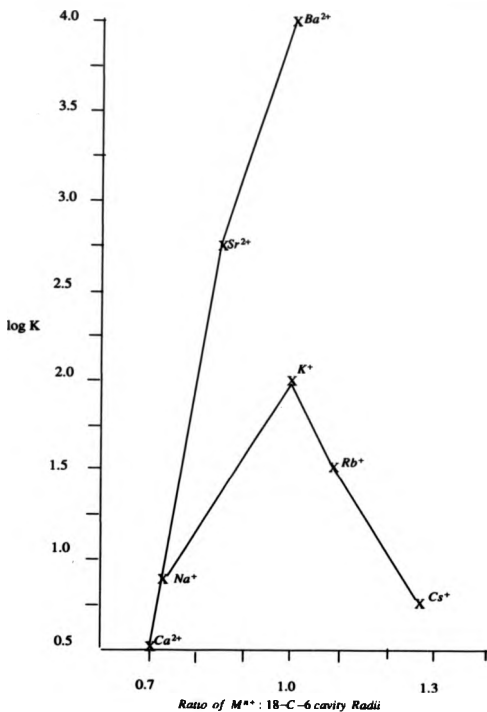


Figure 2.3 The selectivity of 18-C-6 for alkali and alkaline earth cations

The following points could be drawn from the Figure 2.3:

- I) Monovalent cations show a small change in $\log K$ with a change in the ratio of the ionic cation radius to the 18-C-6 cavity radius. Stability constants increase with charge for cations which have approximately the same ratio of M^{n+} : 18-C-6 cavity size.
- II) There are optimum stabilities for both monovalent and divalent cations. The maximum stability occurs when the ratio of the ionic cation radius to the 18-C-6 cavity radius approaches unity. The greater stability at a ratio of unity is largely due to the enthalpy term indicating a greater electrostatic bond energy for those ions that better fit the ligand cavity [106, 107]. However it is now recognized that this generalization is valid only for rigid macrocyclic ligands [108].

Cavity radii for the macrocyclic ligands were calculated originally from different types of molecular models such as Corey-Pauling-Koltun(CPK) and Fisher-Hirschfelder-Taylor(FHT). Table 2.3 shows the cavity diameters for various cyclic polyethers using different types of molecular models.

The values calculated from X-ray crystallography data show that the cavity diameter for 15-C-5 is 1.72 Å in the Na^+ (15-C-5) complex, 1.84 Å in the K^+ (15-C-5) complex and for 18-C-6 is 2.74-2.84 Å in the K^+ complex, 2.67-2.84 Å

in the Rb^+ complex and 2.73-2.85 Å in the Cs^+ complex[111]. The difference is rather large between the CPK and FHT models used, but there are some similarities between CPK models and the X-ray results.

Ligand	Diameter(Å)	Reference
All 12-C-4	1.2 (a)	[109]
All 14-C-4	1.2 (a), 1.5 (b)	[110]
All 15-C-5	1.7 (a), 2.2 (b)	[110]
All 18-C-6	2.6 (a), 3.2 (b)	[110]
All 21-C-7	3.4 (a), 4.3 (b)	[110]

(a) - According to CPK atomic models

(b) - According to FHT atomic models

Table 2.3 *Cavity diameters for selected crown ethers*

For larger macrocycles, owing to their high flexibility, the cavity diameters cannot be defined properly. Dibenzo 30-C-10 and dibenzo 60-C-20 form very stable complexes with K^+ [112]. An X-ray study of the $K(\text{dibenzo 30-C-10})(I)$ complex showed that the crown ether is wrapped around the cation K^+ to form a three dimensional cavity with all ten oxygen atoms co-ordinated

to the cation [113]. Crown ethers, whose cavity is too small to accommodate the metal ion, form sandwich type complexes e.g., benzo 15-C-5 forms particularly stable 2:1 complexes with κ^+ and κb^+ [114].

(2) Substitution on the macrocyclic ring

Cation selectivity of the ligand is changed by the addition of benzene groups to 18-C-6. In MeOH the formation constant of the Ba^{2+} complex of 18-C-6 is larger than that of the κ^+ complex by a factor of 10 [115]. Dibenzo 18-C-6 on the other hand shows the opposite preference and will bind κ^+ better than Ba^{2+} in MeOH by approximately the same amount [116]. These observations may be explained in terms of ligand bulkiness leading to the isolation of the cation from the solvent. It can also be explained in that the aromatic rings withdraw electron density from the basic oxygen donors, thus decreasing the strength of the metal-ligand interaction. Aliphatic substituents on 18-C-6 do not alter the binding properties to any measurable extent [117]. Substituted benzo derivatives of the ligand have also some effects on the binding properties. For example the dinitro derivative of dibenzo 18-C-6 has more than six times less affinity for Na^+ than has the parent compound in DMF. This is due to the electron withdrawing property of the nitro group which in turn

delocalizes the electrons from the oxygen donors. On the other hand the stability of the Na^+ complex of the corresponding amino derivative is almost identical with that of dibenzo 18-C-6. This is due to the electron donating ability of the substituent [118, 119, 120] (Table 2.4).

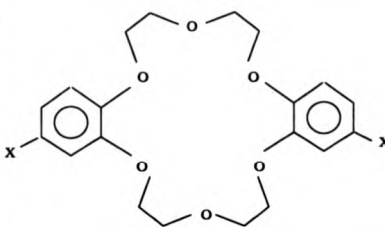
CROWN	X	log K
	H	2.69
	NH_2	2.76
	NO_2	1.99

Table 2.4 Formation constants of substituted benzo crowns with Na^+ in DMF at 30°C

Crown ethers containing oxygen atoms conjugated only with benzene rings e.g., hexa benzo 18-C-6 [121] (Table 2.1) and tri(binaphthyl)24-C-6 [122] showed no sign of complexation.

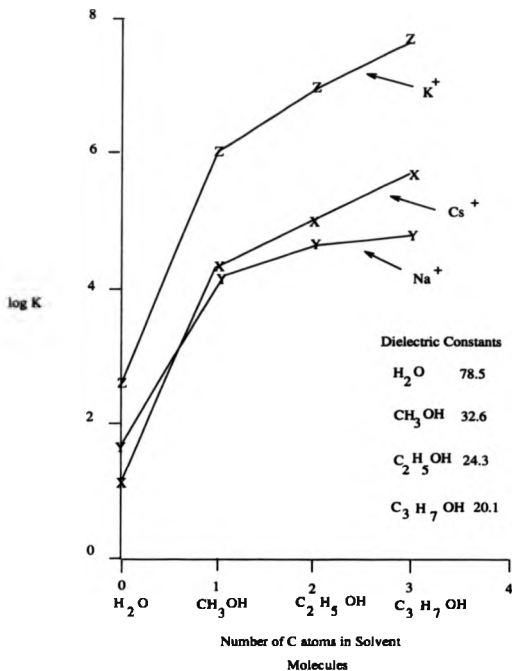


Figure 2.4 Stability constants for complexes of dicyclohexano 18-C-6 with Na^+ , K^+ and Cs^+ in solvents of different dielectric constants

(3) Solvent effects

As complexation of a cation is in competition with solvation, weaker donor solvents allow higher complex stabilities. The stability constants for the reaction of crown ethers with metal cations are 10^3 to 10^4 times larger in MeOH than in water [112]. Figure 2.4 shows the stability constants for the reactions of dicyclohexano 18-C-6 with Na^+ , K^+ , and Cs^+ in solvents of varying dielectric constants [115]. As can be seen from this figure the ligand is consistently selective for K^+ over Na^+ and Cs^+ and selectivity between Na^+ and Cs^+ reverses in going from water to alcoholic solvents.

2.1.2 Macrocyclic effect

Increased stability is observed for the complexes of cyclic ligands over those with an open chain of similar composition. This extra stability has been termed the "macrocyclic effect" by Cabbiness and Margerum [123]. They actually reported stability constants and noted the significant differences between cyclic/linear ligands and observed that the macrocyclic effect is ten times larger for cyclic tetra amine ligands than that of the multidentate amine for Cu^{2+} complexes. Crown ethers also form much more stable complexes than do their corresponding open chain analogues. A remarkable

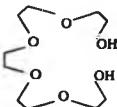
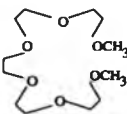
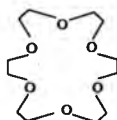
increase in the stability of Na^+ , K^+ complexes of crown ethers (18-C-6) over those of their linear counterparts (pentaglyme) in MeOH was observed by Frensdorff [112] (Table 2.5).

Polyether	Na^+	K^+
Pentaglyme(a)	1.52	2.20
18-C-6	4.32	6.10

(a) : $\text{CH}_3(\text{OCH}_2\text{CH}_2)_5\text{OCH}_3$

Table 2.5 *log K values for reaction in MeOH at 25°C
of Na^+ and K^+ with pentaglyme and 18-C-6*

Despite agreement on the existence of a macrocyclic effect, controversy has arisen over its specific thermodynamic origin. While it is well established that the chelate effect is of entropic origin, no agreement has been reached whether the macrocyclic effect is due to more favourable enthalpy or entropy terms in the cyclic ligand reactions. Kodama and Kimura[124] have concluded that the macrocyclic effect is entirely due to the favourable entropy contribution from comparing the stabilities of $[\text{Pb}(\text{18-C-6})]^{2+}$ to those of $[\text{Pb}(\text{tetraglyme})_2]^{2+}$.

Ligand	Cation	log K	ΔH k Cal/mol	T ΔS k Cal/mol
	K^+	2.05	-6.37	-3.57
	Ba^{2+}	3.96	-6.71	-1.31
	Na^+	1.0(a)	-9.14(a)	-7.7(a)
	K^+	2.27	-8.16	-5.06
	Ba^{2+}	2.57	-5.64	-2.22
	Na^+	4.33	-8.11	-2.20
	K^+	6.05	-13.21	-4.96
	Ba^{2+}	7.0	-10.38	-0.83

(a) - Reference 116

Table 2.6 *Thermodynamics of formation of metal complexes of cyclic and non-cyclic polyethers at 25°C in 99%wt. MeOH [115]*

However studies of $\log K$, H , and S values for the reactions of Na^+ , K^+ and Ba^{2+} with five podands and their non-cyclic analogues in MeOH [125] showed that the effect is due to more favourable enthalpy factors. Stabilization of the potassium complex is due to the enthalpy contribution but the Ba^{2+} complex is stabilized by both enthalpy and entropy although the enthalpy term predominates (Table 2.6).

2.1.3 Number and type of donor atom

The stabilities of macrocyclic complexes are greatly affected by the type and number of ring donor atoms. Frensdorff [112] noted that the substitution of N or S for O in 18-C-6 has a great effect (see Table 2.7) in producing macrocycles which have less affinity for alkali and alkaline earth metal ions [126]. However the effect of such substitution upon the complexation of Ag^+ was the opposite. This may be due to the soft metal system providing some contribution to the covalent character of the metal-donor bond. So far only a little quantitative work has been carried out to investigate the effect of varying the number of ring donor atoms without changing the size of the parent ring. Cram et al. [127] reported that 18-C-5 was a much poorer host for tert-butylammonium ion than 18-C-6. In the reactions of the related thia

crown ethers (oxygen atoms replaced by sulphur atoms), an increase in stability with the increase of the number of S atoms in the ring was observed for Ag^+ and Hg^{2+} [128].

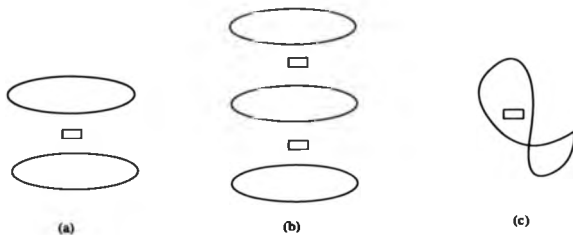
X	Y	K^+ in MeOH	Ag^+ in H_2O
O	O	6.10	1.60
NH	O	3.90	3.30
NH	NH	2.04	7.80
S	S	1.15	4.34

Table 2.7 Stability constants ($\log K$) for the formation of 1:1 complexes with the ligands $X(CH_2CH_2OCH_2CH_2OCH_2CH_2)_nY$ (from reference [112])

2.1.4 M^{n+} -crown interaction modes in solid complexes

Figure 2.5 schematically displays the various types of crown anion preferences that have been observed for different M^{n+} [129].

[A] Charge Separated Encapsulates :



[B] Cation-Cavity Compatible anion-separated Encapsulates :

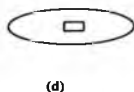


Figure 2.5 (a)-(d) (a) 1:2 sandwich encapsulate; (b) 2:3 club sandwich encapsulate; (c) 1:1 wrap-around encapsulate; (d) 1:1 cation-cavity compatible anion separated encapsulate.

[A] Charge-separated encapsulates : In these complexes the cation is exclusively co-ordinated to the crown oxygens and there is no interaction between the cation and anion.

Figure 2.5(a) shows a 1:2 sandwich encapsulate formed by two small-cavity crown molecules. Examples include : $[Na(12-C-4)_2][Cl].5H_2O$ [130], $[Na(12-C-4)_2][OH].8H_2O$ [131] and $[Na(12-C-4)_2][ClO_4]$ [132].

Figure 2.5(b) shows a 2:3 club sandwich encapsulate formed by three molecules of crowns and two cations. Examples include : $[CsNCS]_2[DB 18-C-6]_3$ [111] and $[CsNCS]_2[B 18-C-6]_3$ [111].

Finally Figure 2.5(c) shows a 1:1 wrap-around encapsulate formed by a large cavity-crown, as exemplified by $[K(DB 30-C-10)][NCS]$ [133] and $[Rb(DB 30-C-10)][NCS].H_2O$ [134].

[B] Cation-cavity compatible anion-separated encapsulates : These encapsulates as depicted in Figure 2.5(d) are normally 1:1 planar or roughly planar and there is no interaction between the cation and the anion. The cation may or may not be co-ordinated by one or more solvent molecules. Examples include : $[K(18-C-6)][NCS]$ [135] and $[Na(B 15-C-5)(H_2O)] [I]$ [136].

[C] Anion-Paired Encapsulates :

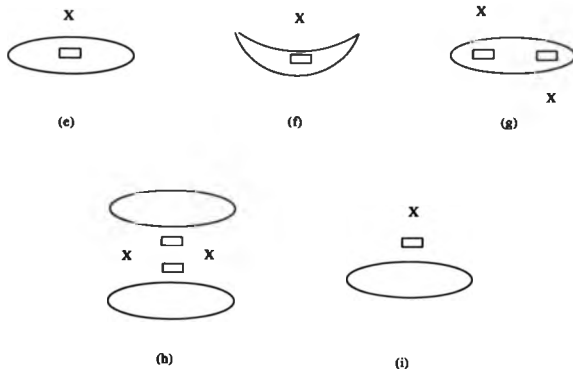


Figure 2.5 (contd.) (e)-(i) (e) 1:1 anion-paired cation-cavity compatible encapsulate; (f) 1:1 anion-paired encapsulate wherein cavity size exceeds cation size; (g) bimetallic 2:1 anion paired encapsulate; (h) 2:2 dimeric anion-paired encapsulate; (i) 1:1 anion-paired encapsulate wherein cation size exceeds cavity size.

[C] Anion-paired encapsulates : As the name suggests, this type of encapsulate incorporates direct involvement of corresponding anion(s).

Figure 2.5(e) shows a 1:1 complex of a cation-cavity compatible encapsulate such as $Li(12-C-4)(NCS)$ [137], $Na(DB 18-C-5)(NCS)$ [138] and

K(DB 18-C-6) (*U*) · thiourea [139].

The related partial wrap-around encapsulate of a cation of 1:1 complex is illustrated in Figure 2.5(f). Examples include *Ba*(DB 24-C-8) (*CIO*)₂ [140] and *Na*(DB 24-C-8) (*NCS*) · *H*₂*O* [141].

Figure 2.5(g) shows a bimetallic 2:1 complex of two smaller cations with a rather large cavity crown. Here the two cations prevent the folding of the crown and accept the anions from the axial sides. (*NaNCS*)₂ (DB 30-C-10) [142] and (*NaI*)₂ (DB 30-C-10) [141] are examples of this type of complex.

Figure 2.5(h) shows a 2:2 dimeric anion-paired encapsulate e.g., [*Rb*(*NCS*) (18-C-6)]₂ [143] and [*CS*(*NCS*) (18-C-6)]₂ [144].

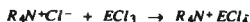
Finally, Figure 2.5(i) shows a 1:1 complex of a cation with a crown of cavity size much smaller than that of the cation (these are called half-sandwich complexes). These type of complexes are rather new, examples include : *Rb* (B 15-C-5) (*pic*) [145] and *Cs* (B 15-C-5) (*pic*) (*pic* = 2,4,6-trinitrophenolate or picrate). Neutral complexes of Group VB trichlorides have this half sandwich structure.

2.2 Results and Discussion

The only previous structural study of a Group VB halide-crown ether complex relates to $SbCl_5(15-C-5)$ [95] in which a pyramidal $SbCl_5$ unit is bonded to the five oxygen atoms of the crown ether in a half-sandwich structure; this was reported in 1987. In the present case complexes of the Group VB tri-chlorides (As, Sb, and Bi) with crown ethers 12-C-4, 15-C-5 and 18-C-6 have been synthesized and characterized by spectroscopic studies and X-ray crystal structure determinations.

Of the crown ethers studied, 12-C-4 has the smallest hole size (diameter 1.2 Å) and 18-C-6 the largest (diameter 2.6 Å). As a general observation 12-C-4 adopts c_2 symmetry in complex formation as distinct from the c_2 symmetry of the free ligand. e.g., in $Li(12-C-4)(NCS)$ [137], $[Na(12-C-4)_2][OH] \cdot 2H_2O$ [131], $[Na(12-C-4)_2][Cl] \cdot 5H_2O$ [130]. There are a few exceptions e.g., $CuCl_2(12-C-4)$ [146] where the crown adopts c_2 symmetry. The 18-C-6 adopts D_{3h} conformation in most of the complexes in contrast to the c_2 symmetry of the free ligand. Examples are $CdCl_2(18-C-6)$ [147], $HgCl_2(18-C-6)$ [147], $K(18-C-6)(NCS)$ [135] and $[SnCl(18-C-6)][SnCl_3]$ [148].

The metal trihalides used in our studies $AsCl_3$, $SbCl_3$ and $BiCl_3$ show many similarities and a few subtle variations in their properties and structures. An excellent summary of these can be found in reference [169]. The important chemical characteristic of these trihalides ECl_3 ($E = As, Sb, Bi$) is their ability to behave both as a donor (where the lone pair on E(III) can be donated to acceptor molecules) and an acceptor (because of the presence of empty d orbitals of fairly low energy). The trihalides have marked acceptor properties particularly towards the halide ions and amines. Numerous complexes have been isolated with a wide variety of compositions. e.g., direct reaction of the trihalide with the appropriate halide-ion donor provides EX_4 ;



The common structure of these trihalides is triangular pyramidal with atom E at the apex of the pyramid (Figure 2.6). Bonding is primarily between the p electrons of E and the p electrons of the halogen atoms. The remaining lone pair of electrons on E exert steric control over the shape of the molecule, as to be expected from VSEPR considerations e.g., X-E-X angles are less than the tetrahedral angle of 109° .

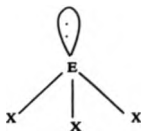


Figure 2.6 The structure of metal trihalide

Bond lengths and bond angles for the trichlorides of arsenic, antimony and bismuth are listed in Table 2.8. $AsCl_3$ is a clear, colourless liquid that may be readily distilled; antimony trichloride and bismuth trichloride are solids that sublime in vacuo. These trihalides are all moisture sensitive and are best kept under strictly anhydrous conditions.

Preparation of the complexes follows direct equimolar addition of the appropriate crown ether to a chilled solution of the metal trichloride. Acetonitrile is the solvent of choice for these complexes and these adducts were purified by washing with n-hexane and pumping in vacuo. All these reactions were carried out under strictly anhydrous conditions. All the complexes are listed in Table 2.9. Microanalytical data and spectroscopic data are listed in Tables 4.7 and 4.8 respectively. Complexes (I)-(VII) were fully characterized via X-ray crystal structure determinations.

Table 2.8 Bond lengths and bond angles for Group VB trichlorides

Compound (Ref.)	M-X (Å)	X-M-X angle(deg.)
$AsCl_3$ (155)	2.162, 2.169, 2.171(2); mean 2.167	97.3, 97.5, 98.3(1)
$SbCl_3$ (156)	2.340, 2.368; mean 2.359	90.98, 95.70(5)
$BiCl_3$ (157)	2.468(4), 2.513, 2.517(7); mean 2.496	84.45, 93.2, 94.9(3)

Table 2.9 Crown ether complexes of Group VB trichlorides

Ligand	$AsCl_3$	$SbCl_3$	$BiCl_3$
12-C-4	$AsCl_3(12-C-4)$ (I)	$SbCl_3(12-C-4)$ (II)	$BiCl_3(12-C-4)$ (III)
15-C-5	$AsCl_3(15-C-5)$ (IV)	$SbCl_3(15-C-5)$ (VIII)	$BiCl_3(15-C-5)$ (V)
18-C-6	18-C-6.2MeCN (IX)	$SbCl_3(18-C-6).MeCN$ (VI)	$[BiCl_3(18-C-6)]^+ [Bi_2Cl_8]^{2-}$ (VII), $BiCl_3(18-C-6)$ (X), $BiCl_3(18-C-6).H_2O$ (XI)

2.2.1 Infrared spectra

Bands observed in the region $4000\text{--}200\text{ cm}^{-1}$ for each complex are listed in Table 4.8 (Pages 154-156).

- [A] There are only slight changes for 12-C-4 on complex formation. e.g., asymmetric C-O-C stretching frequencies at 1136(s), 1094(s), 1022(s) and the symmetric C-O-C stretch at 913(s) for this ligand have been changed only slightly on complex formation.
- [B] In the case of 15-C-5, the ligand vibrational modes experience substantial shifts and splittings upon complexation, especially in the region of C-O-C asymmetric stretching vibration. For $\text{AuCl}_3(15\text{-C-5})$, the bands at 1118(vs,br), 1087(st), 1037(w) have been changed to 1143(st), 1129(st), 1120(st), 1103(vs), 1090(st), 1069(st), 1055(w), 1033(st); the symmetric C-O-C stretching band at 941(st) is shifted to lower frequency 935(st). For $\text{BiCl}_3(15\text{-C-5})$, bands are observed at 1124(st), 1116(st), 1084(st), 1068(st), 1049(st), 1036(st) and 1020(st) cm^{-1} respectively.
- [C] In the case of 18-C-6 there are three strong bands for the uncomplexed ligand in the region $1200\text{--}700\text{ cm}^{-1}$.
- i) the band at 1110 cm^{-1} , assigned to asymmetric C-O-C stretching,

- ii) the band at 992 cm^{-1} , assigned to CH_2 rocking motion and
- iii) the band at 863 cm^{-1} is due to the C-C stretching.

As a typical example the spectrum of the $\text{SbCl}_5(18\text{-C-6}) \cdot \text{MeCN}$ (VI) complex shows clearly the effect of metal complexation in the $1200\text{-}700\text{ cm}^{-1}$ region. Of the three strong bands in this region the 1110 cm^{-1} band (ν_{asym} C-O-C) is shifted to 1100 cm^{-1} in the complex, the 992 cm^{-1} band (CH_2 rocking) is shifted to 954 cm^{-1} in the complex, and the band at 863 cm^{-1} ($\nu_{\text{C-C}}$ stretching) is shifted to 839 cm^{-1} in the complex. Bands (CH_2 rocking) at 954 cm^{-1} and (C-C stretch) at 839 cm^{-1} are indicative of approximate D_{3h} symmetry [150] of the crown ring. The bands at 2290 cm^{-1} and 2243 cm^{-1} belong to the C-N stretching frequencies of the acetonitrile in the complex and since there is no change from that of free acetonitrile the acetonitrile clearly does not take part in any co-ordination with SbCl_5 , but rather is simply trapped as lattice solvate.

For the ionic product compound (VII) the spectrum does not have the characteristic peaks for the D_{3h} symmetry of the ring (as high lighted in the X-ray crystal structure there is severe distortion in the crown conformation).

For the neutral adduct $(18\text{-C-6}) \cdot 2\text{CH}_3\text{CN}$ (IX), the CH_2 rocking and the C-C stretch bands of the crown ligand are shifted from $992(\text{m})$ and $863(\text{m})$ to $958(\text{vs})$ and $841(\text{vs})\text{ cm}^{-1}$ respectively. These characteristic bands at 958 cm^{-1}

and 841 cm^{-1} indicate the approximate D_{3d} symmetry of the crown 18-C-6 [150]. In addition to the ligand peaks there are two additional bands at $2298(\text{w})$ and $2250(\text{s})$ assigned to $\nu_{(\text{C-N})}$ of the bound MeCN.

[D] The far ir has strong bands for complexes (I)-(VII), characteristic of $\nu(\text{metal-chloride})$ stretching modes in the region $400\text{--}200\text{ cm}^{-1}$.

The far ir of $\text{AsCl}_3(\text{crownether})$ adducts have characteristic $\nu(\text{As-Cl})$ peaks in the region $320\text{--}387\text{ cm}^{-1}$. The pure AsCl_3 [151] itself has bands at 412 cm^{-1} and 387 cm^{-1} whilst AsCl_3 in $n\text{Bu}_2\text{O}$ [152] has bands at $385\text{ cm}^{-1}(\text{vs})$, $410\text{ cm}^{-1}(\text{st})$ which in fact is very similar to the free AsCl_3 . In the present complexes, $\text{AsCl}_3(12\text{-C-4})$ displays two $\nu(\text{As-Cl})$ bands at $367\text{ cm}^{-1}(\text{st})$ and $327\text{ cm}^{-1}(\text{vs})$, whilst $\text{AsCl}_3(15\text{-C-5})$ has bands at $380\text{ cm}^{-1}(\text{st})$ and $335\text{ cm}^{-1}(\text{vs})$ respectively.

Uncomplexed SbCl_3 has two Sb-Cl stretching bands in the far ir, at $350\text{ cm}^{-1}(\text{w})$, and $330\text{--}310\text{ cm}^{-1}(\text{st,br})$. The far ir of $\text{SbCl}_3(\text{crownether})$ adducts have more than two such bands characteristic of $\nu_{(\text{Sb-Cl})}$ in the region of $345\text{--}250\text{ cm}^{-1}$. In comparison to the neutral adducts of SbCl_3 with disubstituted oxalamides, malonamides and succinamides [153], the $\nu_{(\text{Sb-Cl})}$ of crown ether adducts show a slight shift to lower energy;

i) $\text{SbCl}_3(\text{DMO})$ $\nu_{(\text{Sb-Cl})}$ $327(\text{s})$, $296(\text{st,br})\text{ cm}^{-1}$

ii) $SbCl_3(DtBuO)$ $\nu_{(Sb-Cl)}$ 370(m), 315(st,br) cm^{-1}

iii) $SbCl_3(DIPO)$ $\nu_{(Sb-Cl)}$ 385(m,br), 350(m,br), 320(st,br) cm^{-1}

iv) $SbCl_3(DMS)$ $\nu_{(Sb-Cl)}$ 340(st,br), 240(st,br) cm^{-1} .

which can be taken as some indication of the (relative) stronger binding crown > organoamide.

The Sb-Cl stretching frequencies of crown ether adducts increase in the following order

$SbCl_3(12-C-4)$ [322(st), 290(vs), 268(w)] < $SbCl_3(18-C-6)$ [345(st), 300(vs), 250(w)].

In the case of $BiCl_3(crownether)$ neutral adducts few bands are observed in the region 245-280 cm^{-1} which is comparable with the Bi-Cl stretching frequency of $BiCl_3(DMDTO)_{1.5}$ [154] (290 cm^{-1} , 245 cm^{-1}). The ionic complex (VII) has peaks at higher frequencies 354 cm^{-1} (w), 285 cm^{-1} (w,sh) and 265 cm^{-1} (st). As a general point whereas some information about stereochemistry can be inferred from the location and number of $\nu_{(M-Cl)}$ bands in the 500-200 cm^{-1} region for co-ordination compounds in general, this is not the case here e.g., participation of all or some of the oxygen atoms of the crown in metal bonding causes problems in the strict definition of co-ordination number.

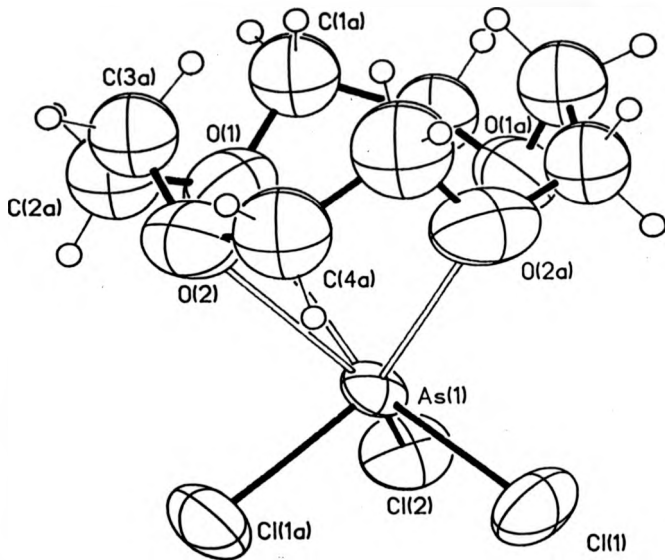
2.2.2 Proton nmr

The ^1H nmr spectra of compounds (I)-(VII) have a common feature e.g., one sharp singlet for the crown ethers which exhibits no conspicuous change in chemical shift on complex formation. This is in agreement with the crystal structure findings, which revealed that the M-O interactions in these complexes were very weak. As with the ir data there is not much information to be gained from the proton nmr data apart from confirmation of the presence of the crown ether in the complex. Therefore to investigate the conformational and stereochemical aspects of the crown molecules and the coordination number of the metal atom, especially the stereochemical activity of the lone pairs associated with each metal atom, the X-ray crystal structure determination of these complexes [(I)-(VII)] have been carried out.

2.2.3 Crystal structures of Group VB trichloride-crown ether complexes

The X-ray crystal structure determinations were carried out by Dr.N.W.Alcock, University of Warwick. My only involvement has been with the selection and loading of the crystals in the Lindemann tubes prior to data collection.

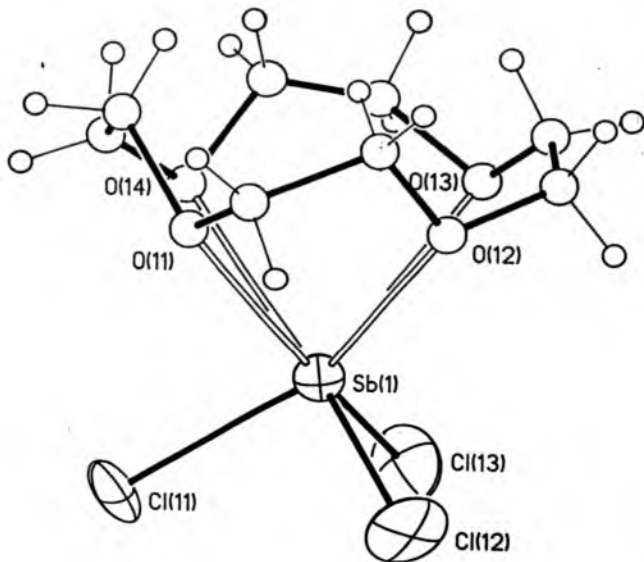
The crystal structure of $\text{AsCl}_3(12\text{-C-4})$ (I)



The As atom is bonded to three chlorine atoms 2.198-2.222 Å, Cl-As-Cl 94.9-96.5 (degrees), and the four oxygen atoms of the crown ether (2.776-2.915 Å) in a half-sandwich structure and the resulting co-ordination is seven (eight including the lone pair of electrons). The crown ether in this complex is disordered. There is a plane of symmetry containing As(1) and Cl(2) which bisects the molecule through the mid points of C(4A) - C(4AA) and C(1A) - C(1AA) and the As sits in a central location over the ring at a distance of 2.0 Å from the mean plane defined by the four oxygen atoms.

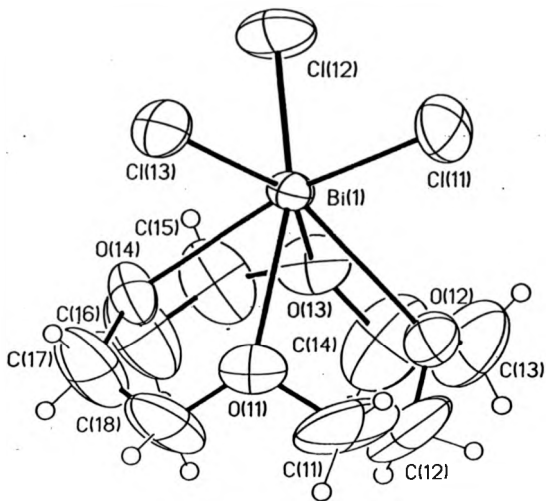
Crystal data, selected bond distances, bond angles, and torsion angles are presented in the Appendix in Tables A2.2.1, A2.2.2 A2.2.3 and A2.2.4 respectively. *Trans* O-As-O angles are virtually at right angles (90.4°). Slight elongation in the As-Cl distance is due to the influence of the ligand 12-C-4 on $AsCl_3$. The C-C and the C-O bond distances are within the expected range (mean C-C 1.497 Å and mean C-O 1.412 Å respectively). The bond angles at O atoms cover the range of 79.1-151.7° (mean 114.6°) and those at C atoms range from 98.4-122.0° (mean 109.5°). The torsion angles about C-C bonds are mostly close to $\pm 60^\circ$, those about C-O bonds are mostly close to ± 60 or 180° .

The crystal structure of $SbCl_3(12-C-4)$ (II)



The structure consists of two independent $SbCl_3(12-C-4)$ units. Each antimony atom is co-ordinated to four oxygen atoms of the crown and three chlorine atoms in a half sandwich structure. There are no close contacts indicative of any interaction between the two molecules. Crystal data, bond lengths, bond angles and torsion angles are listed in the Appendix (Tables A2.2.9, A2.2.10 A2.2.11 and A2.2.12 respectively). Within the $SbCl_3$ unit the Sb-Cl bonds (2.322–2.519 Å) show little variation and, in fact are very similar to those in the free halide (2.36 Å). *Trans* Cl-Sb-Cl angles are $91.5-93.5^\circ$ for molecule A and $90.5-95.6^\circ$ for molecule B. The antimony atom is located 1.96 Å above the O_4 mean plane for molecule A and 2.00 Å above the O_4 mean plane for molecule B. The C-C bond distances are relatively short (mean value of 1.312 Å for molecule A and 1.40 Å for molecule B). The C-O bond distances are also relatively shorter for molecule B (mean value of 1.365 Å). In both molecules the crown ethers are severely distorted, the torsion angles about C-C bonds are clearly away from the *gauche* conformation and are in the following order $-61.3, -26.3, -30.6, -37.4^\circ$ for molecule A and $-30.5, 20.9, -19.7, -8.4^\circ$ for molecule B. These large variations in bond lengths, bond angles and torsion angles are viewed as a direct offshoot of the highly disordered nature of the 12-C-4 ring in the complex.

The crystal structure of $\text{BiCl}_3(12\text{-C-4})$ (III)



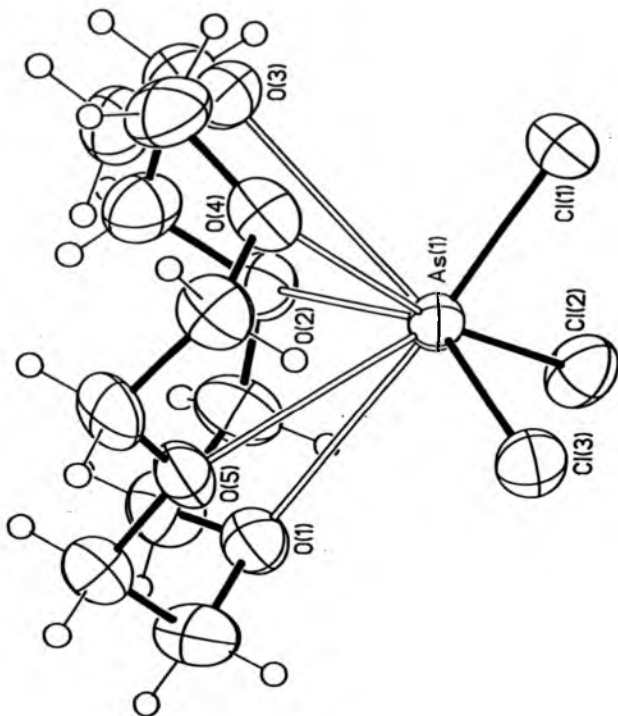
In $\text{BiCl}_3(12\text{-C-4})$ (as in its As and Sb congeners), the bismuth atom is coordinated to the four oxygens of the crown and three chlorine atoms to give a half-sandwich structure. The conformation of the ring approximates to C_4 symmetry with the four oxygens precisely coplanar; the maximum deviation from the mean plane through O(11)-O(12)-O(13)-O(14) is $\pm 0.001 \text{ \AA}$. The Bi-O bond distances 2.652(8)-2.742(9) \AA show no substantial variation though they are significantly longer than the "expected" covalent distance (sum of covalent radii approximately 2.25 \AA). The trans O-Bi-O angles and the Cl-Bi-Cl angles are all close to 90° leaving no substantial hole for lone pair occupancy. Thus the co-ordination geometry about bismuth would seem to argue for the absence of a stereochemically active lone pair, although, the BiCl_3 unit has very similar dimensions to those of the parent halide molecule (which is normally considered to be pseudo tetrahedral with an active lone pair (Table 2.2.8)) [157].

It seems reasonable to conclude that if such a lone pair is present in $\text{BiCl}_3(12\text{-C-4})$ complex, its spatial requirements are considerably less than would have been expected. It may be that this results from the compression exerted by the small and somewhat inflexible 12-C-4 ring transmitted by the interaction of Bi with the lone pairs of the constituent oxygen atoms. Slight

elongation in the Bi-Cl distance in the complex is due to the influence of the ligand 12-C-4 on BiCl_3 (average Bi-Cl distance in the complex is 2.519 Å, and in the BiCl_3 itself is 2.496 Å). As observed in previous 12-C-4 complexes the individual C-C bonds 1.364(35)-1.438(27); mean 1.402 Å appear to be abnormally short whereas C-O bonds vary between 1.374(22)-1.446(20) Å; mean 1.413 Å. Bond angles at carbon cover the range 113.9(19)-116.9(19)°; mean 115.3° and those at oxygen lie within the range 110.6(13)-113.9(13)°; mean 111.9°. The Bi atom is located at a distance of 1.84 Å above the mean plane defined by the four oxygen atoms.

Crystal data, bond lengths and angles, and torsion angles are listed in the Appendix (Tables A2.2.16, A2.2.17 and A2.2.18 respectively).

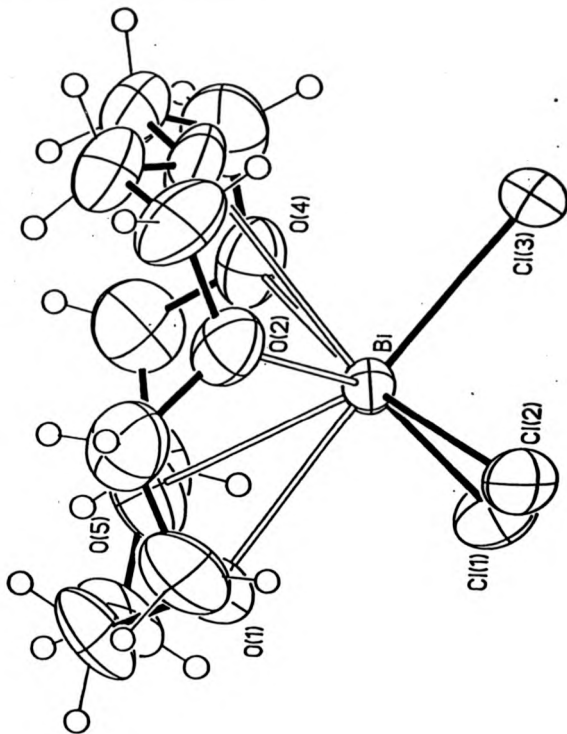
The crystal structure of $\text{AsCl}_3(15\text{-C-5})$ (IV)



The AsCl_3 forms a 1:1 complex with 15-C-5. In this complex, the As atom is eight co-ordinate (nine including the lone pair of electrons) being bonded to the five macrocyclic oxygen atoms and three chlorine atoms. The As atom lies 1.85 Å above the least-squares plane of the ether O atoms. The observed mean As-O distance is 3.039 Å (2.944-3.156 Å).

Crystal data, selected bond lengths, bond angles and torsion angles are given in the Appendix (Tables A2.2.5, A2.2.6 A2.2.7 and A2.2.8 respectively). All bond lengths and bond angles are within the expected ranges with the exception of a relatively short aliphatic C-C (mean value of 1.495 Å) bonds. The torsion angles about C-C bonds are close to $\pm 60^\circ$, those about C-O bonds are mostly close to $\pm 60^\circ$ or 180° but one C(6)-O(4) angle is 110° . Bond angles at O atoms range from 113.3 – 115.3° (mean 113.9°), those at C atoms from 106.8 – 115.1° (mean 111.0°). Since the structure of the parent macrocycle is not known as yet, it is difficult to point out any conformational changes (if any) that take place during complexation.

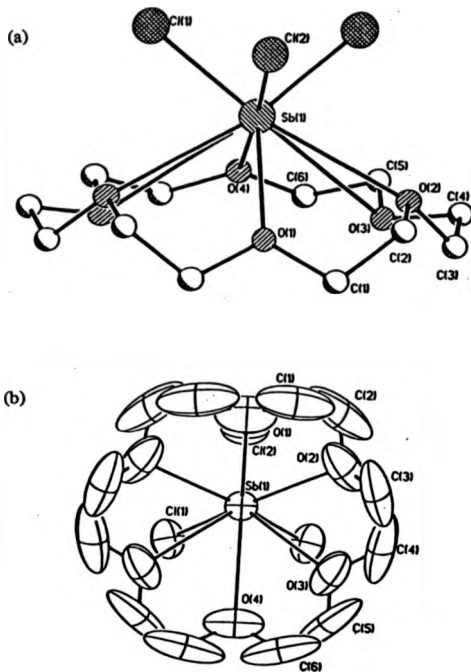
The crystal structure of $\text{BiCl}_3(15\text{-C-5})$ (V)



The structure of this adduct shows the five oxygen atoms of the crown are co-ordinated to the BiCl_3 in a half sandwich arrangement. The resulting co-ordination number of the bismuth atom is eight (nine including the lone pair of electrons). The BiCl_3 unit has very similar dimensions to those of the parent halide molecule with the Bi-Cl (2.53 Å) bond distances slightly elongated than those of the parent halide (mean 2.496 Å).

Crystal data, bond lengths and bond angles, and torsion angles are listed in the Appendix (Tables A2.2.19, A2.2.20 and A2.2.21 respectively). Torsion angles about C-C bonds are all close to $\pm 60^\circ$ whilst those about C-O are mostly close to $\pm 60^\circ$ or 180° . The bismuth atom sits over the ring at a distance of 1.61 Å from the mean plane defined by the five oxygen atoms. The C-C bond distances are within the range of 1.451–1.536 Å (mean value of 1.478 Å) and the C-O bond distances vary between 1.397–1.483 Å with the mean value of 1.425 Å. The bond angles at C cover the range of 105.3 – 114.4° (mean 109.4°); those at O cover the range of 110.6 – 117.0° (mean 112.3°).

The crystal structure of $SbCl_3(1R-C-6)MeCN$ (VI)



(a) Structure of the $SbCl_3(1R-C-6)$ molecule showing the atom numbering scheme used. (b) A perspective view of the complex with thermal ellipsoids shown at 50% probability. Hydrogen atoms are omitted for clarity.

Crystal data, selected bond distances and angles, and torsion angles are given in the Appendix (Tables A2.2.13, A2.2.14 and A2.2.15 respectively). The central Sb atom is bonded to three chlorine atoms and all six oxygen atoms of the 18-C-6 cyclic ether to give the characteristic half sandwich structure. Within the $SbCl_3$ unit the Sb-Cl bonds (2.361(3) - 2.391(2) Å) show little variation and the Cl - Sb - Cl bond angles are right angles (90.0(1), 90.3(1)). The influence of the ligand is expressed by the lengthened Sb - Cl bonds and decreased Cl - Sb - Cl angles (-0.021 Å, and -3.14°) relative to the solid state structure of antimony (III) chloride.

A plane of symmetry containing Sb(1), Cl(2), O(4) and O(1) bisects the molecule. The Sb atom is clearly displaced from a central position over the ring and lies closer to the trio of oxygen atoms O(1) O(2) O(2A); this preference is reflected in the non-uniform Sb-O bond distances which fall into two distinct sets, i.e., those linking O(1) O(2) O(2A), 2.989(10)-3.025(11) Å and those linking O(4) O(3) O(3A), 3.290(12)-3.401(10) Å. When compared with the sum of the covalent radii (2.2 Å) and, in turn, $SbCl_3$ 15-C-5 (Sb-O 2.787(5)-2.997(4) Å, mean 2.902 Å) these Sb-O distances are conspicuously long and suggest extremely weak binding of the crown ether ligands to Sb(III).

As shown by bond angle parameters the ring adopts the "crown" conformation (D_{3h}) - a situation common to many 18-C-6 complexes wherein angles about C-C bonds are close to $\pm 65^\circ$ whilst those about C-O bonds approach $\pm 180^\circ$ and the six oxygen atoms lie alternatively 0.29-0.31 Å above and below their mean plane. The Sb atom is located 1.65 Å above this mean plane. As observed in previous 18-C-6 complexes the individual C-C bonds 1.391(21)-1.473(22) Å appear to be abnormally short whereas, apart from C(3)-O(2), 1.351(17) Å, C-O bonds 1.397(17)-1.441(18) Å are much as expected [135,143,144,158, 159]. The estimated value of the 18-C-6 hole size for a D_{3h} conformation is 2.85 Å (diameter)[148] as compared with the observed Sb - O (mean) 3.183 Å - and the $SbCl_3$ unit assumes a position on one side of the ring. With the smaller crown complex $SbCl_3(15-C-5)$, the Sb sits essentially in a central location equidistant from all five oxygen atoms [95]. As shown by the ellipsoids of thermal motion the large amplitude of vibration and the high degree of anisotropy displayed by the carbon and oxygen atoms (C>O) indicate significant internal motions in the ring at room temperature. Bond angles at carbon cover the range of 108.5(1.0)-114.6(1.3)°, mean 110.8°, and those at oxygen lie within the range 110.5(1.2)-115.0(1.3)°, mean 112.9°. The anomalous bond length C(3)-O(2) 1.351 Å; the angle at O(2) 112.1(1.0)° and that at C(3) 111.2(1.2)° are probably due to the more disordered

nature of the crown ring.

There are only few structures reported in which an antimony is strongly bonded to three chlorine atoms and weakly to at least one oxygen atom; these examples exhibit varying co-ordination numbers and geometries. Thus in *N,N'*-dimethyloxalamide antimony trichloride[153], the mean Sb-O distance is 2.799 Å, mean Sb-Cl distance is 2.379 Å. The crystal structure of the complex *SbCl₃(DMO)* is shown in Figure 2.7 (Reproduced from J.Chem.Soc., Dalton Trans., 1987, 263).

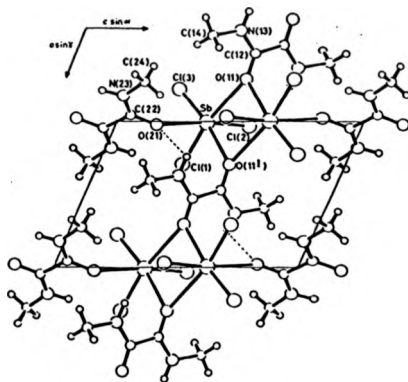
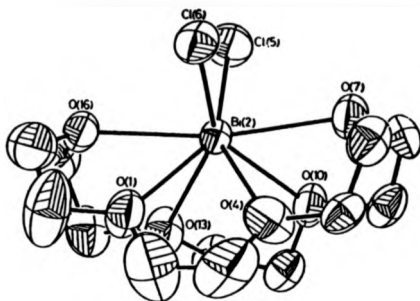
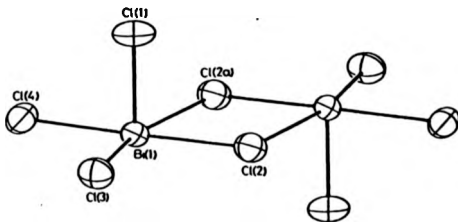


Figure 2.7 The crystal structure of *SbCl₃(DMO)*

The crystal structure of $[BACl_2(18-C-6)]_2^+ [B_2Cl_4]^{2-}$ (VII)



$[BACl_2(18-C-6)]^+$ cation



$[B_2Cl_4]^{2-}$ anion

The 2:1 adduct (VII) contains two $[BiCl_2, 18-C-6]^+$ cations and a $[Bi_2Cl_4]^{2-}$ anion. In each cation the $BiCl_2$ unit is co-ordinated to all six of the oxygen atoms and the resulting eight-co-ordinate geometry approximates to a bicapped trigonal prism. Crystallographic data, bond lengths, bond angles, and torsion angles are listed in the Appendix (Tables A2.2.22, A2.2.23, A2.2.24 and A2.2.25 respectively).

Compared with other three neutral $BiCl_3(\text{Crown ether})$ adducts the Bi-O distances in $[BiCl_2, 18-C-6]^+$ are perceptibly shorter but, surprisingly, in view of the mono-charged $BiCl_2^+$ unit present, the Bi-Cl distances (mean $2.50(1) \text{ \AA}$) are essentially the same. The third potential capping position of the prism points outwards through the center of the crown ether ring and the large O-Bi-O angles across this position (mean 108°) strongly suggest a stereochemically active lone pair pointing in this direction. The "wrap-around" encapsulation [129] of the $BiCl_2^+$ unit results in severe distortion of the crown-6 ring (O-C-C-O torsional angles $-9.3, -50.2, 55.6, -55.9, -47.6, 43.4^\circ$) away from the idealized D_{3h} point symmetry. In the absence of any long range cation-anion interactions it is unlikely that the $[Bi_2Cl_4]^{2-}$ counter-anion plays any part in the ring puckering.

The centrosymmetric $\text{Bi}_2\text{Cl}_8^{2-}$ anion shows the same geometry as previously observed in $[\text{Bi}_2\text{Cl}_{14}]$ [160], with two square-based pyramids sharing a basal edge. The lone pairs are clearly fully active giving a pseudo-octahedral geometry around each bismuth centre. Surprisingly, two of the terminal Bi-Cl distances in $[\text{Bi}_2\text{Cl}_8]^{2-}$ [2.500(6), 2.506(6) Å] are identical to those in the cation, being substantially shorter than that linking the third terminal chlorine atom [2.701(6) Å]. As expected the Bi-Cl bonds in the rather unsymmetrical bridge [2.787(6) and 2.966(6) Å] are significantly longer [161].

2.2.4 Comparison of Group VB-Crown ether Complexes

Mean dimensions relating to metal trichloride parameters are given in Table 2.10 (Page 105) and those relating to the crown ether ring parameters are given in Table 2.11 (Page 106).

In all the present complexes the metal halide is situated outside the macrocyclic cavity. The fact that the metal atom (As, Sb, Bi) is found "above" and not "inside" the central cavity can be explained by both the presence of three chlorine atoms on the metal atom and the preferred specific interactions of the (stereochemically active) lone pair of electrons of

the metal with the lone pairs of the oxygen atoms of the ring.

Normally, lone pair steric activity, or inactivity, is deduced from geometrical information about a given atomic site, i.e., irregular co-ordinations are usually considered to stem largely from stereochemically active lone pairs. These are identified with apparent empty volumes within co-ordination polyhedra. The argument by Nicholson et al. [95] for lone pair involvement in the case of $SbCl_3(15-C-5)$ ($Sb-Cl$ 2.405(1)–2.433(1) Å, $Cl-Sb-Cl$ 88.67(5)–93.25(5)°) that the presence of a $SbCl_3$ pyramidal structure in both the parent molecule and the 15-C-5 complex is synonymous with retention of a stereochemically active lone pair following complexation, is equally applicable to the systems under consideration here. Since only small structural changes occur on complexing with 15-C-5 Nicholson et al. concluded that the lone pair on antimony must point towards the centre of the crown ring.

The parameters of the MCl_3 unit do not appear to change much on co-ordination, which again indicates the weak interaction of the crown ring with the metal halide. In all our complexes the lone pairs are clearly fully active which is indicated by a clear space without any steric stress (exception $BICl_3(12-C-4)$).

Complex	M-Cl	Cl-M-Cl	M-O
<i>AsCl₃</i> (12-C-4)	2.206	95.4	2.78-2.92
<i>AsCl₃</i> (15-C-5)	2.210	94.9	2.95-3.15
<i>SbCl₃</i> (12-C-4)	2.410	93.0	2.71-2.96
<i>SbCl₃</i> (15-C-5)	2.416	90.8	2.79-3.00
<i>SbCl₃</i> (18-C-6) <i>MeCN</i>	2.38	90.2	2.99-3.40
<i>BiCl₃</i> (12-C-4)	2.52	92.9	2.65-2.74
<i>BiCl₃</i> (15-C-5)	2.53	90.0	2.78-2.92
<i>BiCl₃</i> (18-C-6)	2.50	88.1	2.84-3.16
[<i>BiCl₃</i> (18-C-6)] ⁺	2.50	91.0	2.49-2.66

Table 2.10 Mean M-Cl and M-O bond lengths (\AA) and mean Cl-M-Cl bond angles (deg.) in Group VB-crown ether complexes

Complex	mean C-C	mean C-O	mean C-C-O	mean C-O-C
12-C-4	1.5035	1.428	110.75	113.6
AuCl ₃ (12-C-4)	1.497	1.412	109.5	114.6
SbCl ₃ (12-C-4)	1.312(A), 1.40(B)	1.426(A), 1.365(B)	118.7(A), 123.0(B)	113.7(A), 115.9(B)
BaCl ₂ (12-C-4)	1.402	1.413	115.48	111.98
AuCl ₃ (15-C-5)	1.495	1.412	111.05	113.94
SbCl ₃ (15-C-5)	1.529	1.457	108.1	116.5
BaCl ₂ (15-C-5)	1.478	1.425	109.4	112.3
18-C-6	1.507	1.411	109.8 (106.4 to 114.6)	113.5 (113.3 to 114.0)
SbCl ₃ (18-C-6).MeCN	1.426	1.403	110.8	112.9
[BiCl ₂ (18-C-6)] ⁺	1.434	1.416	112.2	117.7

A = Molecule A; B = Molecule B

Table 2.11 Mean ring dimensions in crown ethers and their

GroupVB Complexes

Now the discussion in the variations of the following parameters follows :

- i) M-O bond lengths and interactions,
- ii) displacement of the metal atom from the mean plane defined by the crown oxygen atoms,
- iii) C-C and C-O bond lengths.

(i) M-O bond lengths and interactions

- a) The change with the size of the metal atom

The average As-O distance for $AsCl_3(12-C-4)$ is 2.846 Å which is shorter than the mean value of 3.039 Å ($AsCl_3(15-C-5)$). These As-O bond distances are long and suggest extremely weak binding of crown ether ligands to As(III) in the relative order $12-C-4 > 15-C-5$.

The mean dimension of Sb-O distance for $SbCl_3(12-C-4)$ is 2.797 Å (2.710-2.914 Å) for molecule A and 2.868 Å (2.814-2.958 Å) for molecule B. When compared with the mean dimensions of Sb-O distance of $SbCl_3(15-C-5)$, 2.903 Å (2.79-3.00 Å) and $SbCl_3(18-C-6)$, 3.176 Å (2.99-3.40 Å) the Sb-O(12-C-4) distance is shorter and the weak binding of crown ether ligands to Sb(III) occur in the relative order $12-C-4 > 15-C-5 > 18-C-6$.

The mean Bi-O distances of $\text{BiCl}_3(12\text{-C-4})$, $\text{BiCl}_3(15\text{-C-5})$ and $\text{BiCl}_3(18\text{-C-6})$ are 2.702 Å (2.65-2.74 Å), 2.83 Å (2.78-2.92 Å) and 2.986 Å (2.84-3.16 Å) respectively. Again these Bi-O interactions are weak and are in the relative order of 12-C-4 > 15-C-5 > 18-C-6. But in the $(\text{BiCl}_3(18\text{-C-6}))^+$ cation the mean Bi-O distance is 2.606 Å (2.49-2.66 Å) where the interaction is much stronger than with the neutral trihalide.

Therefore we can come to the following conclusion. In the case of $\text{BiCl}_3(18\text{-C-6})$ system the cation BiCl_3^+ interacts much more strongly than the neutral BiCl_3 . Here the interaction between the metal atom and crown ether increases with the charge on the metal atom.

M-O(crown) interaction: Neutral < cationic

b) The change with the number of the oxygen atoms in the crown ring.

We can see from the Table 2.10 that the M-O interaction is more for the smaller crown ring i.e., the M-O interaction decreases with the increase in the number of oxygen atoms for a particular metal atom.

M-O(crown) interaction: M-(18-C-6) < M-(15-C-5) < M-(12-C-4)

(ii) Displacement of the metal atom from the mean oxygen atom plane

The displacements of the metal atom from the mean plane for the GroupVB crown ether complexes are given in Table 2.12 below ;

Complex	displacement of the metal from the mean oxygen plane (Å)
<i>AsCl₃</i> (12-C-4)	2.00
<i>AsCl₃</i> (15-C-5)	1.85
<i>SbCl₃</i> (12-C-4)	1.96[A], 2.00[B]
<i>SbCl₃</i> (18-C-6).MeCN	1.65
<i>BiCl₃</i> (12-C-4)	1.84
<i>BiCl₃</i> (15-C-5)	1.61

Table 2.12 Displacement of metal atoms from the mean oxygen plane

It is clear from the Table 2.12 that the displacement of the metal atom decreases as the size of the metal atom increases, i.e.,

*Displacement of the metal atom from the mean oxygen plane
of the crown ring : $As-O_4 > Sb-O_4 > Bi-O_4$*

And also the displacement decreases with the increase in the number of donor oxygen atoms i.e.,

*Displacement of the metal atom from the mean oxygen plane
of the crown ring : $M-O_4 > M-O_3 > M-O_2$*

(iii) C-C and C-O bond lengths

When compared with other 12-C-4 complexes $SbCl_3$ and $BiCl_3$ complexes show C-C distances which are extremely short (Table 2.11), e.g., mean C-C for $[Lu(12-C-4)][NCS]$ is 1.5125 Å, for $[Na(12-C-4)_2][Cl].5H_2O$ is 1.497 Å and for $[Na(12-C-4)_2][OH].8H_2O$ is 1.485 Å. But the mean C-O distances are within the expected range. Since the crown rings are severely distorted it is very difficult to point out the conformation of the cyclomer for $SbCl_3(12-C-4)$. But for $BiCl_3(12-C-4)$ the conformation of the ring approximates to C_4 symmetry similar to $[Na(12-C-4)_2][OH].5H_2O$, $[Na(12-C-4)_2][Cl].8H_2O$ and $[Lu(12-C-4)][NCS]$.

The torsional angles for $\text{BiCl}_3(12\text{-C-4})$ also display C_4 symmetry.

For GroupVB-15-C-5 complexes mean C-C and C-O distances lie within the expected range. The point symmetry is very close to C_4 for $\text{AsCl}_3(15\text{-C-5})$ and $\text{SbCl}_3(15\text{-C-5})$.

(iv) Conclusions

- a) Metal-oxygen interactions are weak however these interactions are stronger for smaller rings, $\text{M-O}(12\text{-C-4}) > \text{M-O}(15\text{-C-5}) > \text{M-O}(18\text{-C-6})$.
- b) M-Cl bond lengths are slightly longer than in free halides for neutral arsenic, antimony and bismuth (except $\text{BiCl}_3(18\text{-C-6})$) crown ether complexes.
- c) Interaction of 18-C-6 with the cation BiCl_2^+ (Bi-O distances vary between 2.49-2.66 Å) is much stronger than with trihalide BiCl_3 (Bi-O distances vary between 2.84-3.16 Å).
- d) There is a space for lone pair of electrons without any steric stress in most of the the GroupVB-Crown ether complexes with the exception of $\text{BiCl}_3(12\text{-C-4})$.
- e) M-O bond lengths are very much longer than M-Cl bond lengths in the crown ether complexes i.e., bond strength of $\text{M-O} \ll \text{M-Cl}$ in the complexes.

2.2.5 The Exceptions

The two systems that behave differently in MeCN solvent medium, (i.e., not giving the expected half-sandwich complex) are $AsCl_3/18-C-6$ and $BaCl_2/18-C-6$.

(i) $AsCl_3/18-C-6$ system

The only evidence for adduct formation is the ir spectrum of the crude product originally isolated, which has the characteristic peaks for 18-C-6 and $AsCl_3$. Recrystallization from acetonitrile failed to give an adduct instead we isolated the crown-solvate adduct $(18-C-6)_2CH_3CN$ [162]. Formation of this acetonitrile-crown ether adduct has been used to purify 18-C-6 and it was first reported by Gokel et al [163]. The structure of the 1:2 host-guest adduct (Figure 2.8) is formed as a result of the $-C-H...O$ hydrogen bonding. Unfortunately for us the synthesis and crystal structure of this complex appeared in the literature (162) six months before we obtained our crystals.

Our observations on the reaction of 18-C-6 with $AsCl_3$ in MeCN support the conclusion [164] that this polyether acts as a weaker Lewis base than 15-C-5 and 12-C-4. $AsCl_3$ is noted as a weak Lewis acid and it would seem reasonable that the interactions between the $As...O(crown)$ are not strong enough to support complex formation in the case of 18-C-6.

Crown ethers, most notably 18-C-6, are capable of forming host-guest complexes with neutral polar substrates possessing a suitable hydrogen atom arrangement. The crown adopts a conformation that allows optimum host-guest interaction, thereby losing its free state C_i symmetry. In most cases this preferred symmetry is approximately D_{3h} . In 1:2 host-guest complexes the guest molecules are co-ordinated above and below the plane of the crown ether subject to certain symmetry requirements. In the product isolated (18-C-6).2MeCN the D_{3h} conformation of the crown is stabilized by forming hydrogen bonds with two acetonitrile molecules.

Uncharged molecules that form complexes with crown ethers all contain either polar O-H bonds (alcohols [165] and water [166]), polar N-H bonds (thiourea [97] and sulphonamides [167], [168]) or polar C-H bonds (acetonitrile [163], malonitrile [170], dimethyl acetylene carboxylate [171 a-c], dimethyl sulphone [171d], dimethyl sulphate [172], dimethyl carbonate [172], dimethyl oxalate [172], dimethyl fumarate [172]. It is still surprising that the weak interactions between $CH_3 \cdots O(crown)$ are favoured in the case of 18-C-6 rather than adduct formation with $AsCl_3$.

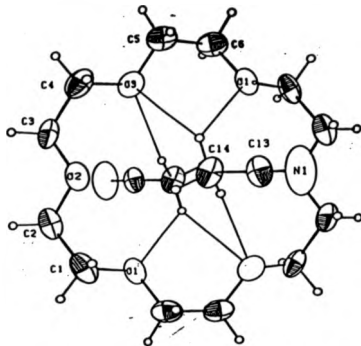


Figure 2.8 *The crystal structure of 18-C-6.2MeCN*

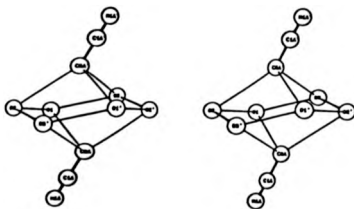


Figure 2.9 *Stereoscopic skeletal drawing of the 2:1 complex illustrating connectivity of oxygen atoms (18-C-6) and the tilting of the acetonitriles*

(ii) $\text{BiCl}_3/18\text{-C-6}$ system

The crown ether complex $(\text{BiCl}_3)_2 \cdot 18\text{-C-6}$ has the ionic formulation $[\text{BiCl}_2(18\text{-C-6})]_2^+ [\text{Bi}_2\text{Cl}_4]_2^{2-}$, in which the bismuth cation is eight co-ordinate involving all six oxygen atoms of the crown and two chlorine atoms. To our knowledge, this is the first report of the structure of a discrete $[\text{BiCl}_2]^+$ complexed ion. Whilst this work was being carried out a report appeared in the literature [173] of the neutral adducts $\text{BiCl}_3(18\text{-C-6})$ and $\text{BiCl}_3(18\text{-C-6}) \cdot \text{H}_2\text{O}$ (carried out in acetone solvent medium). These are shown in Figure 2.10, reproduced from *Inorg.Chim.Acta*, 1990, 171, 11.

According to Nicholson et al [173] the ionization energy for bismuth trichloride (4779.0 KJ/mol) is very high and this should preclude any ionic species. Nevertheless we have obtained the ionic product (VII) from direct addition using acetonitrile as solvent. The following rationale can be given for the formation of the ionic product: BiCl_3 has a relatively high tendency to ionize into $[\text{BiCl}_2]^+$ and $[\text{Cl}]^-$



Bismuth trichloride might form two different products (neutral $\text{BiCl}_3(18\text{-C-6})$ and ionic $[\text{BiCl}_2(18\text{-C-6})]^+ [\text{BiCl}_4]^-$ with the crown 18-C-6 which may co-exist in solution under equilibrium conditions (paths 1 and 2). We presume that

under our conditions the ionic product is obtained (path 2) as a crystalline product as a result of more favourable lattice energy considerations. Path 1 is evidently favoured in acetone, path 2 is in acetonitrile although the role of the solvent acetonitrile is open to question.

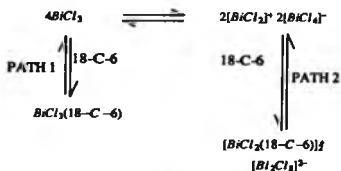
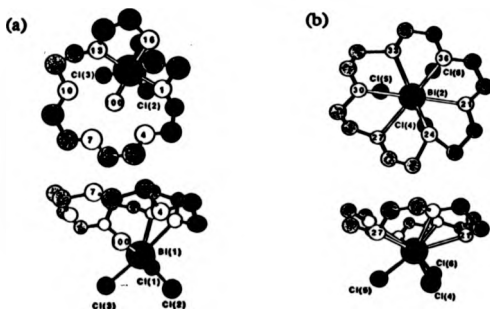


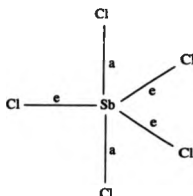
Figure 2.10 Crystal structures of (a) $\text{BiCl}_3(\text{18-C-6}) \cdot \text{H}_2\text{O}$

and (b) $\text{BiCl}_3(\text{18-C-6})$.



2.2.6 Reactions of antimony pentachloride with crown ethers

This section reports the reactions between antimony pentachloride and the three crown ethers 12-C-4, 15-C-5 and 18-C-6.



e = the distance between antimony
and the equatorial chlorine atom = 2.29 Å

a = the distance between antimony
and the apical chlorine atom = 2.34 Å

Figure 2.11 Trigonal-bipyramidal structure of $SbCl_5$

$SbCl_5$ adopts trigonal-bipyramidal geometry in the solid state. However it dimerizes in solution, with the two antimony atoms being joined by a double chloride bridge. As detected by Raman spectroscopy [174] the Sb atom in $SbCl_5$ is somewhat displaced from the equatorial plane of the trigonal bipyramid. The crystal structure of $SbCl_5$ has been solved at $-30^\circ C$, and shows a trigonal-bipyramidal structure with Sb-Cl (equatorial) 2.29 Å and Sb-Cl

(apical) 2.34 Å [105]. For comparison, values from the vapour state structures are Sb-Cl (equatorial) 2.31 Å and Sb-Cl (apical) 2.43 Å.

The two important chemical properties of $SbCl_5$ are

- i) it is a powerful oxidizing agent
- ii) it is a powerful halogen acceptor (Lewis acid).

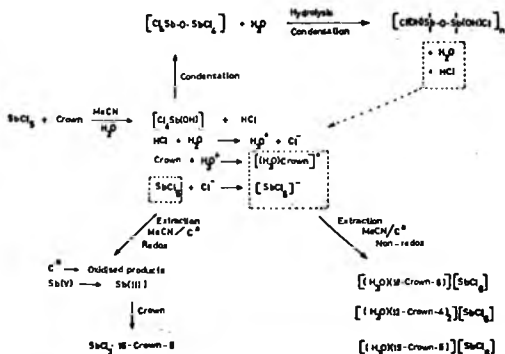


Examples of $SbCl_5$ acting as an oxidizing agent for transition metal carbonyls are well known [175,212] and equally, redox reactions involving the hexachloroantimonate $[SbCl_6]^-$ ion and organic compounds are well established [176]. Antimony pentachloride forms a very large number of adducts with electron donors, and has the ability to accept chloride ions, forming the hexachloro antimon(V)ate- $[SbCl_6]^-$ anion. The reaction system $TiCl_4/SbCl_5/MeCN$ provides $[TiCl_3(MeCN)_3]^+ [SbCl_6]^-$ [177, 178], reflecting the powerful halide acceptor properties of $SbCl_5$. The $[SbCl_6]^-$ anion has been used to stabilize organometallic transition metal cations, as in [179] $[(\pi-C_3H_3)Fe(CO)_2CHR=C=NH]^+ [SbCl_6]^-$ (R = H, Me). $SbCl_5$ abstracts a chloride from both $AsCl_3$ and PCl_3 , making it the most powerful halide acceptor of the Group VB pentachlorides [148].

Here we describe the reactions of pentavalent $SbCl_5$ and the crown ethers 12-C-4, 15-C-5 and 18-C-6 which have revealed a quite unexpected pattern of hydronium ion (H_3O^+)-crown ether antimon(V)ate salt formation.

Direct addition of the crown ethers (12-C-4, 15-C-5, 18-C-6) to antimony pentachloride in MeCN at $-20^\circ C$ under a dry nitrogen atmosphere provides characteristic yellow solutions which rapidly assume a deep red colour on warming to room temperature. The products obtained from those separate reactions following conventional work-up with a final extraction with boiling acetonitrile/activated charcoal are listed in Table 2.13.

Table 2.13 Reaction scheme for the formation of hydronium-ion (crown)-antimon(V)ate salts and $SbCl_5$ (15-C-5)



(I) Reaction with 12-C-4

Here the resulting faint yellow solution obtained from the final acetonitrile/activated charcoal extraction provided pale yellow needles of the hydronium-ion crown ether 1:2 complex $[H_3O(12-C-4)_2][SbCl_6]$ as identified by spectroscopic (Table 4.10) and analytical (Table 4.9) data.

An intense band [$\nu_{\text{as-C}}$ stretch] at 338cm^{-1} in the far ir spectrum and an intense charge transfer band $\lambda_{\text{max}} 37,091\text{cm}^{-1}$ in the UV-Vis spectrum and a clearly resolved singlet $\delta -0.12$ ppm in the ^{121}Sb nmr spectrum denote the presence of the $[SbCl_6]^-$ anion. No significant changes are observed in the ir band profile of the ligand between $1500-800\text{cm}^{-1}$. The proton nmr spectrum exhibits a sharp singlet for the crown (CH_2) protons $\delta 3.63$ (Uncomplexed ligand $\delta 3.51$) but we were unable to locate the protons of the hydronium cation. Only one example of hydronium ion encapsulation by 12-C-4 has been reported previously: addition of concentrated aqueous HPF_6 to the crown dissolved in dichloromethane affords $[H_3O(12-C-4)_2][PF_6]$ [180].

A sandwich structure is proposed for the cation where the hydronium ion is hydrogen bonded with two alternate oxygens of one crown ether molecule and one oxygen of the second molecule, as illustrated in Figure 2.12. For comparison $[Na(12-C-4)_2][OH] \cdot 8H_2O$ [131] and $[Na(12-C-4)_2][Cl] \cdot 5H_2O$ [130] each contain a $[Na(12-C-4)_2]$ cation unit in which the sodium ion is sandwiched between two crown ether rings.

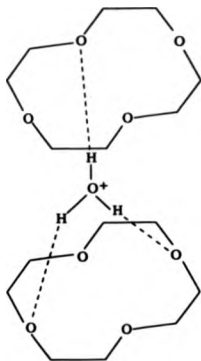


Figure 2.12 Proposed structure of $(H_3O(12-C-4))^+$ cation showing the hydrogen bonding pattern (schematic)

(II) Reaction with 15-C-5

The light yellow solution resulting from the final extraction with acetonitrile/activated charcoal yielded colourless needle crystals of the 1:1 "tervalent" adduct $SbCl_5(15-C-5)$ and a minute crop of pale yellow crystals of the assumed hydronium ion-crown ether (1:1) complex $(H_3O^+)(15-C-5) [SbCl_6]^-$. Spectroscopic and analytical data are listed in Tables 4.10 and 4.9 respectively.

The proton nmr spectrum of $SbCl_5(15-C-5)$ consists of one sharp signal for the ring protons at δ 3.77 ppm. In the ir spectrum the two strong ligand bands $\nu_{(C-O-C)}$ at 1112 cm^{-1} and 1090 cm^{-1} assume a multiplet pattern 1134, 1110, 1094-1078(doublet), 1064 cm^{-1} ; bands at $322, 280\text{ cm}^{-1}$ are assigned to ν_{Sb-Cl} vibrations.

For the hydronium ion-(15-C-5) complex an intense band $\nu_{(Sb-Cl)}$ 340 cm^{-1} in the ir spectrum, a charge transfer band λ_{max} $37,050\text{ cm}^{-1}$ in the Vis-UV spectrum and a clearly resolved singlet δ -0.13 ppm in the ^{121}Sb nmr spectrum confirm the formation of an antimonate salt which, in the absence of satisfactory microanalyses, we assume to be of 1:1 stoichiometry $(H_3O^+)(15-C-5) [SbCl_6]^-$. The proton nmr shows ring protons δ_{CH} , 3.61 ppm but we were unable to locate the cation (H_3O^+) protons. Heo and Bartsch [180] have

reported the formation of an ill-defined and difficult to handle $[(H_2O)^+-15-C-5]$ complex, which answers to neither 1:1 nor 1:2 stoichiometry, following addition of concentrated aqueous HPF_6 to a dichloromethane solution of 15-C-5.

(iii) Reaction with 18-C-6

The resulting yellow solution provided colourless chunky crystals of the hydronium-crown ether (1:1) complex $[H_3O^+(18-C-6)][SbCl_6^-]$, as identified by spectroscopic (Table 4.10) and analytical (Table 4.9) data. Typically the ir spectrum shows ligand ρ_{CH} , rocking, 970 cm^{-1} , ν_{C-C} stretching, 839 cm^{-1} , and splitting of the ν_{C-O-C} asymmetric stretching band into a doublet 1141 cm^{-1} , 1094 cm^{-1} following complexation; the dominant band in the far ir region ν_{Sb-Cl} 338 cm^{-1} is characteristic for $SbCl_4^-$ [193b]. An intense charge transfer band, λ_{max} $37,023\text{ cm}^{-1}$ in the Vis-UV spectrum and a clearly resolved singlet δ -0.10 ppm in the ^{121}Sb nmr spectrum also identifies the $[SbCl_6]^-$ [178, 181]. The proton nmr spectrum shows a singlet δ 3.67 ppm for the crown protons (δ 3.51 ppm for the free ligand) and a weak signal at δ 10.1 ppm assigned to the hydronium ion.

Izatt et al. (1972) [182] first postulated hydronium ion encapsulation by a crown ether for the complexes $[H_3O(dicyclohexyl\ 18-C-6)] [X]$ $X = ClO_4, PF_6$ on the evidence of ir spectroscopic data. Confirmation that a hydronium cation had been anchored into the crown cavity came some ten years later with the X-ray crystal structure determination by Behr et al. [183] of $[H_3O(tetracarboxylic\ 18-C-6)] [Cl]$. The list of complexes featuring hydronium ion encapsulation by 18-C-6 (and substituted derivatives) now includes:

- i) $[H_3O(18-C-6)] [Y]$ $Y = PF_6, BF_4, I, Br_3$ [180];
- ii) $[H_3O(18-C-6)]_2 [MoO_4]$ [184];
- iii) $[H_3O(dicyclohexyl\ 18-C-6)]_2 [Th(NO_3)_6]$ [185];
- iv) $[H_3O(18-C-6)] [HCl_2]$ [186] and the related HBr_2 salts [187];
- v) $[H_3O(dicyclohexyl\ 18-C-6)]_2 [UO_2Cl_4] \cdot 2Benzene$ [188];
- vi) $[H_3O(dicyclohexyl\ 18-C-6)]_2 [UCl_4]$ [188];
- vii) $[H_3O(18-C-6)]_2 [Pd_2Cl_6]$ [189];
- viii) $[H_3O(18-C-6)]_2 [MCl_4]$ $M = Zn, Mn$ [190].

In all cases the hydronium ion is located in the crown cavity by three strong O-H...O hydrogen bonds involving alternate oxygen atoms of the crown ring with the possibility of further stabilization from ion-dipole O(hydronium)...O(crown) interactions. The variations in the separation of

the hydronium ion from the mean plane of the six oxygen atoms of the ring have been discussed in relation to the geometry (pyramidal or planar) adopted by the hydronium ion. Figure 2.13 shows the hydrogen bonding pattern of the pyramidal hydronium ion with three alternate oxygens of the crown 18-C-6. The structure of the $(H_2O(18-C-6))^+$ cation in $[H_2O(18-C-6)][HCl_2]$ is shown in Figure 2.14 [186] (reproduced from the *J.Amer.Chem.Soc.*, 1987, 109, 8100) where the hydrogen atoms could not be located with certainty. For this structure a planar geometry has been suggested for the cation. However as the authors have suggested, determination of the proton positions from low-temperature data is necessary to provide conclusive proof of the geometry about the oxonium oxygen atom.

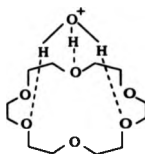
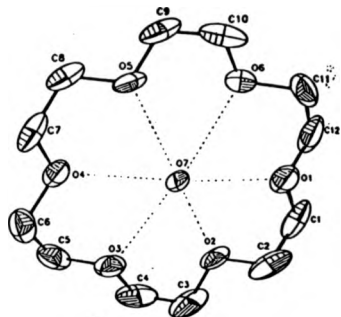


Figure 2.13 Structure of pyramidal $[H_2O(18-C-6)]^+$ (schematic)

Figure 2.14 Structure of $[H_3O(18-C-6)]^+$ in $[H_3O(18-C-6)][HCl_2]$. The hydrogen atoms of the oxonium ion could not be located.



(iv) General Comments

The main point of interest arises from the separate reaction routes observed e.g., the formation of $[SbCl_4]^-$ salts in the case of 12-C-4, 15-C-5 and 18-C-6 and accompanying redox formation of the neutral Sb(III) "half-sandwich" complex $SbCl_3 \cdot L$ in the case where $L = 15-C-5$. The yields in each case are less than 25% (based on the $SbCl_5$ used). In the absence of any concrete

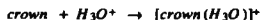
kinetic/labelling evidence to monitor the complex reactions involved, the following points are put forward as a rationale for the observed hydrolysis/reduction interactions (Table 2.13).

For hydronium ion-antimonate salt formation, limited hydrolysis of $SbCl_5$ initiated by the adventitious presence of water, most probably from the crown ether (other possibilities are from the charcoal or from the solvent MeCN) used can be viewed as the dominant reaction. Inclusion of water molecules by crown ethers has been noted [191] particularly for 18-C-6 where a well-defined hydration complex $(18-C-6) : H_2O \rightarrow 1:4-6$ has recently been described [192]. Onset of Sb-Cl hydrolysis involving either solvated $SbCl_5 \cdot MeCN$ or weakly complexed $SbCl_5(crown)_x$ species (which might be the reason for the formation of the initial yellow solutions) leads to formal $[SbCl_4(OH)]$ species and the release of HCl as the primary source of both cation $[H^+ + H_2O]$ and anion $[SbCl_5 + Cl^-]$. Condensation of formal $[SbCl_4(OH)]$ species releases yet more H_2O and formation of μ -oxo-chloro[Sb-O-Sb] oligomeric/polymeric species which, of themselves, are susceptible to Sb-Cl hydrolysis reactions with release of further H_2O and HCl etc. With a negligible amount of water present (and hence the absence of Sb-Cl hydrolysis to any recognizable extent) redox formation of Sb(III) involving $SbCl_5$

("oxidant")/activated charcoal ("reductant") now becomes the dominant reaction. Again the observation that $[H_2O(12-C-4)_2][SbCl_4]$ and $[H_2O(18-C-6)][SbCl_4]$ can be recrystallized unchanged from acetonitrile/activated charcoal solutions would seem to preclude any redox reactions involving $[SbCl_4]^-$ either directly or indirectly via regeneration of free $SbCl_5$ and chloride ion.

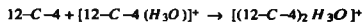
The two pathways are not mutually exclusive and, as observed in the case of $SbCl_5/15-C-5$ both can be involved to a lesser or greater degree. In our view the critical factor in these systems which determines the final outcome i.e., $[SbCl_4]^-$ versus $Sb(III)$ complex formation is the extent of water present both initially and as sustained in situ via condensation/hydrolysis reactions.

An insight of the relative complexing abilities of 12-C-4, 15-C-5 and 18-C-6 with the hydronium ion is provided by the thermochemical data ΔH (enthalpy), ΔS (entropy), obtained by Sharma and Kebabie [193a] from measurements of the ion-molecule equilibria



in the gas phase. Whereas the formation of an $[18-C-6(H_2O)]^+$ complex accommodating three strong hydrogen bonds $O-H^+ cation \cdots \cdots O_{cage}$ with three alternate ring oxygen atoms is the most favoured ($-\Delta H$ 88.5 kcal/mol, $-\Delta S$ 55.8

eu), formation of an $[15-C-5(H_2O)]^+$ complex ($-\Delta H$ 76.9 kcal/mol, $-\Delta S$ 43.2 eu) though less favourable is not clearly not excluded. For the latter two bonding arrangements have been mooted : either two strong $O-H^+ cation \cdots \cdots O_{ring}$ hydrogen bonds aided by favourable $-CH_2-O-CH_2-$ dipole orientations together with a third severely weakened hydrogen bond to a third oxygen atom of the ring or three nearly equivalent but somewhat weakened $O-H^+ cation \cdots \cdots O_{ring}$ hydrogen bonds implicit with a distorted structure. In either case only three of the five available ring oxygen atoms are directly involved in hydrogen bonding. Significantly for $[12-C-4(H_2O)]^+$ complex formation, exact values for enthalpy/entropy changes could not be obtained due to interference by the further equilibrium



The successful isolation of $[H_2O(12-C-4)_2] [SbCl_6]$ and $[H_2O(12-C-4)_2] [PF_6]$ [180] as stable complexes comes as no great surprise.

CHAPTER THREE

**Reaction of lithium 2,6-di(tert-butyl)phenoxide
with antimony pentachloride**

3.1 Introduction

This chapter describes the reaction of the bulky oxygen donor ligand 2,6-di(*tert*-butyl)phenoxide (Figure 3.1) with antimony pentachloride.

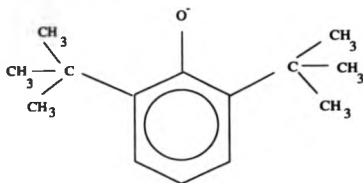


Figure 3.1 2,6-di(*tert*-butyl)phenoxide

There has been considerable interest in the effect of sterically demanding ligands on the synthesis and properties of organometallic derivatives of the main group elements. The synthesis of such complexes is an obvious method to approach abnormally low co-ordination numbers. In recent years there has also been a resurgence of interest in the application of metal alkoxides as precursors for the deposition of pure metal oxides using either sol-gel or MOCVD techniques [194] e.g., hydrolysis of heteropolymetallic alkoxides of the metals Y, Ba and Cu via the sol-gel [195, 196] process

offers a route to high purity superconducting oxides such as $YBa_2Cu_3O_{7-x}$ [197]. In the field of metal alkoxide chemistry, much use has been made of 2,6-dialkyl substituted aromatic alcohols. Titanium tetrachloride, for example, reacts with 2,6-diphenylphenol in refluxing toluene to give $[TiCl_2(OC_6H_3Ph_{2-2,6})_2]$ in 90% yield [198], while yttrium trichloride forms $Y(OR)_3(THF)_3$ with 2,6 dimethyl phenoxide in THF [199]. With simple ligands such as $OCMe_3$ and $OCHMe_2$, polymetallic complexes are formed instead of simple $Y(OR)_3$ species, but a homoleptic $Y(OR)_3$ complex has been obtained with 2,6 ditert-butyl phenoxide [200].

Relatively few complexes of Bi(III) alkoxides have been reported in the literature these include $Bi(OCMe_3)_3$ of which the structure has not yet been published and $Bi(2,6\text{-dimethyl}C_6H_3O)_3$ which has a stereochemically active lone pair i.e., monomer formation with the three ligands directed away from a fourth co-ordination site presumably occupied by a lone pair [201]. Bismuth-containing compounds are useful due to their importance as heterogeneous catalysts [202] and also useful as superconducting materials with high critical temperatures [203].

One important aspect of metal alkoxide chemistry is the ability of the alkoxide group to act as either a terminal, doubly or triply bridging group,

allowing systems with the metal in a higher co-ordination number [204]. The degree of polymerization of the metal alkoxides $(M(OR)_n)_x$ can be controlled by using the steric effect of branched chain alkoxo groups [205]. For example a monomeric $Fe(OR)_3$ species was obtained by using a tertiary alkoxo group [206].

2,6 di-tert-butyl phenoxide has been shown to sometimes undergo the mild activation of the aliphatic carbon-hydrogen bonds of the tertiary butyl groups [207, 208].

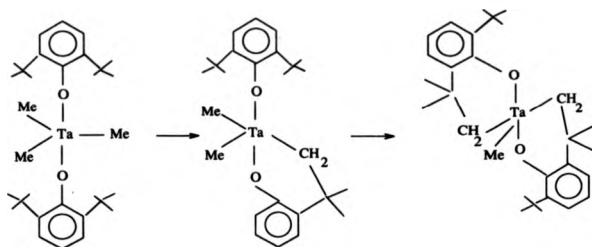


Figure 3.2 Thermal activation of C-H Bonds in $Ta(OAr^*)_3Me_3$ [211]

Since antimony pentachloride gave unexpected products with crown ethers (chapter two) we decided to investigate its reaction with bulky alkoxide ligands in terms of the degree and extend of halide replacement. The choice of ligand was 2,6-di(tert-butyl)phenoxide. The addition of parent

phenol to the metal halide was unsuccessful, generating mixtures of products difficult to purify. The method of choice we used for the introduction of the sterically crowded 2,6 di(tert-butyl) phenoxide was metathetic exchange between the metal halide and $LiOAr^+$ in hydrocarbon solvent.



The reaction of the lithium salt of 2,6-di(tertiary butyl)phenoxide with $Sb(V)$ chloride leads to the formation of 2,2',6,6'-tetra(tertiary butyl)diphenquinone via a redox reaction. Examples of $SbCl_5$ acting as an oxidizing agent for transition metal carbonyl complexes are known [175, 212]; equally redox reactions involving the hexachloro antimonate $[SbCl_6]^-$ ion and organic compounds are well established [176] wherein complex chlorides of $Sb(III)$ are produced.



The unstable $[SbCl_6]^{3-}$ usually decays to the more favourable $[SbCl_4]^-$ in tandem with Cl^- although the dinuclear anion $[Sb_2Cl_9]^{3-}$ has also been identified as a product of reaction [209].

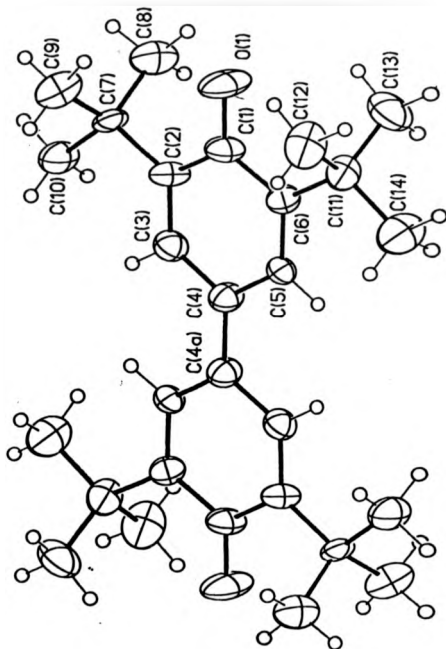
3.2 Results and discussion

The reaction between SnCl_4 and lithium 2,6 di(tertiary butyl)phenoxide (5 equivalents) gives an initial deep red solid from which 2,2',6,6'-tetra(tertiary butyl)diphenoquinone (I) was obtained as red-brown platelets following pentane extraction, chromatographic separation and finally recrystallization from pentane. The proton nmr spectrum of (I) in CDCl_3 comprises two singlets δ 1.38, 8.3 with relative intensities 9:1 readily assigned to tert-butyl and aromatic protons respectively; the ir spectrum contains an intense $\nu_{\text{C=O}}$ band at 1605 cm^{-1} ; the mass spectrum gives a parent-ion peak (M^+ , 408) consistent with the $\text{C}_{28}\text{H}_{40}\text{O}_2$ formulation. An X-ray crystal structure determination of (I) was carried out. The structure of (I) is shown in Figure 3.3. The most interesting feature comprises the significant shortening of the C(4)-C(3) (1.439 Å) and C(4)-C(5) (1.441 Å) bonds compared to C(1)-C(2) (1.479 Å) and C(1)-C(6) (1.478 Å) which adjoin the carbonyl group. The C(4)=C(4a) (1.402 Å) bond distance is relatively long when compared with C(2)=C(3) (1.346 Å) and C(5)=C(6) (1.343 Å) bonds. Bond angles and bond lengths are in good agreement with ref.[210].

Following our crystal structure determination we have discovered that (I) has been noted in the literature; anodic oxidation of M (M = Zn, Cd, Hg)

in non-aqueous solutions of 2,6-di(*tert*-butyl)phenol [210] provided compound (I).

Figure 3.3 *The crystal structure of 2,2',6,6'-tetra(*tert*-butyl) diphenoquinone*



Previously Ledwith et al [176e] have reported that 2,4,6-tri(tert-butyl)phenoxide is immediately oxidized by $SbCl_5$ in tetrahydrofuran solution to the blue phenoxy-radical. This in turn, gives the dimeric phenoxide and regeneration of the starting phenol (via hydrogen atom abstraction from solvent) on standing.

The formation of (I) (Figure 3.4) begins with initial release of chloride ion from metathetical reaction of $SbCl_5$ and the excess of $LiOAr^+$. This facilitates formation of the hexachloroantimonate ion as oxidizing agent.



Here we suggest the oxidation of 2,6-di(tertiarybutyl)phenoxide by $[SbCl_6]^-$ must lead to the formation of 2,6-di(tertiarybutyl)phenoxy radical as in step [A]. Dimerization of this radical or the reaction of this radical at a para position of another molecule of radical [step B], followed by elimination of H_2 [step C] leads to the formation of 2,2',6,6'-tetra(tertiarybutyl)biphenoxinone. Further oxidation of this biphenoxinone by $[SbCl_6]^-$ [step D] leads to the formation of (I). The reduction products in steps A and D, assumed to be complex chloro-Sb(III) anions, were not pursued.

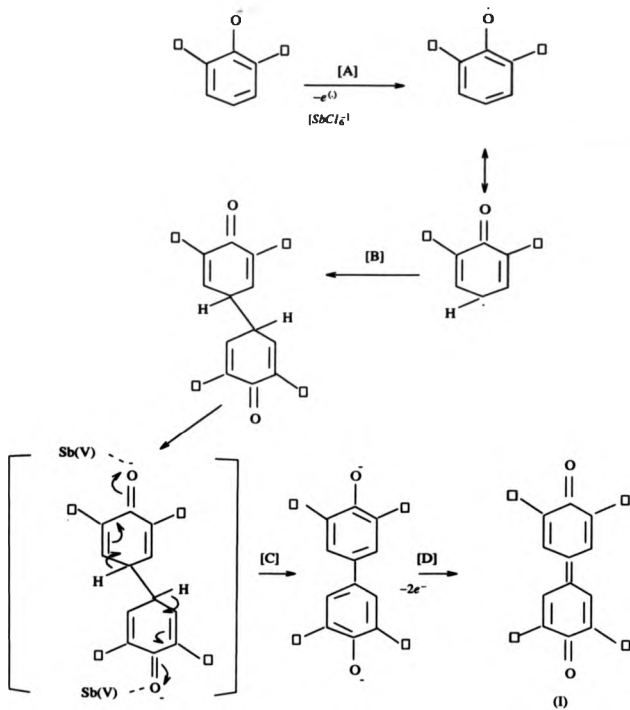


Figure 3.4 Schematic diagram for the formation of 2,2',6,6'-tetra(tert-butyl)diphenylquinone

CHAPTER FOUR

Experimental

4.0 EXPERIMENTAL

4.1 Starting materials and analytical methods

4.1.1 Starting materials

Acetonitrile, chloroform, dichloromethane and methanol were obtained from Fisons Scientific Ltd., Loughborough and refluxed over CaH_2 prior to use.

Benzene, diethylether and n-hexane were obtained from BDH Chemicals Ltd., Poole, and stored over Na wire and distilled under normal pressure of nitrogen from Na/Benzophenone.

Antimony trichloride, was obtained from BDH Chemicals Ltd., Poole, and purified by sublimation in vacuo.

Antimony pentachloride, arsenic trichloride and bismuth trichloride were used as supplied by the BDH Chemicals Ltd., Poole.

Cadmium(II) chloride, manganese(II) chloride and copper(II) chloride were used as supplied by the Aldrich Chemical Co. Ltd., Gillingham.

The crown ethers (12-C-4, 15-C-5, 18-C-6) were obtained from Aldrich Co. Ltd., Gillingham and pumped dry under vacuum prior to use.

All deuterated solvents were used as supplied by the Aldrich Chemical Co. Ltd., Gillingham.

Trimethylamine was obtained from BDH Chemicals Ltd., Poole and was stored in vacuo over P_2O_5 and NaOH pellets.

4.1.2 Analysis

Microanalyses (carbon, hydrogen, nitrogen and chlorine) were determined professionally by Medac Ltd., Brunel University, Uxbridge.

4.2 Experimental techniques

The majority of compounds described in this thesis are air and moisture sensitive and therefore necessitated handling under an inert atmosphere (N_2) in the dry-box and/or with conventional Schlenk systems or in high vacuum.

4.2.1 The Dry Box

The loading of reaction vessels, and the preparation of samples for spectroscopic analyses were carried out in a steel glove-box. The box was constantly flushed with dry nitrogen and the internal atmosphere of the box was

monitored by P_2O_5 in open dishes. Entrance to the box was achieved via an 'air lock' entry port, which was flushed with an independent supply of dry nitrogen.

4.2.2 Instrumentation

Infrared spectra were recorded ($4000-200\text{ cm}^{-1}$) on a perkin-Elmer 580B instrument as nujol mulls between CsI plates.

Proton nmr spectra were recorded on a Perkin-Elmer R34 (220MHz) spectrometer. Tetramethylsilane was used as the internal standard for organic deuterated ($CDCl_3$, CD_3CN) nmr solvents.

^{121}Sb nmr spectra were obtained (95.72 MHz) on a Bruker WH400 spectrometer.

Vis-UV spectra were made with a Shimadzu UV35 spectrophotometer using MeCN or benzene solutions sealed in quartz cells with a light path of 1 cm.

4.3 Preparation of NMe_3 Complexes

4.3.1 NMe_3 -insoluble complexes

The amine insoluble adducts were prepared in a resealable single ampoule vessel (Figure 4.1). The vessel was evacuated on the vacuum line and flushed with nitrogen. The solid reactant was then introduced in the dry box and the ampoule reconnected to the vacuum line. Dry NMe_3 was condensed on to the solid at 77K and the vessel was sealed in vacuo. Reaction occurs upon the reactants warming to room temperature. Typically reactions are allowed to complete over a period of two weeks with regular shaking. Excess amine is removed into a separate single ampoule containing P_2O_5 on the vacuum line. The adduct is freed from residual amine by pumping on the vacuum line overnight.

4.3.2 NMe_3 -soluble complexes

These reactions were carried out in a double ampoule system (Figure 4.2). The system was connected to the vacuum line, evacuated, flushed with dry nitrogen and then transferred to the dry box. The solid material was introduced into bulb B in the dry box, the vessel reconnected to the vacuum line

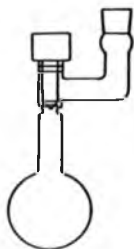


Figure 4.1 *Single ampoule reaction vessel*

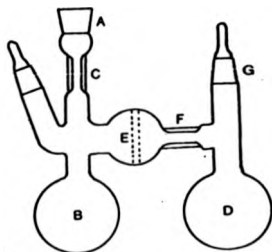


Figure 4.2 *Double ampoule reaction vessel*

and evacuated. Dry NMe_3 was condensed into bulb B at 77K and resealed at point C in vacuo. On warming to room temperature, reaction occurs. The amine-soluble product was tipped into bulb D via sinter E and the NMe_3 is back-distilled by cooling bulb B with iced water. This process was repeated until complete extraction was achieved. The product was isolated by distilling the excess amine into a single ampoule in the vacuum line and freed from residual amine by overnight pumping on the vacuum line. The final product is isolated by sealing at point F.

4.4 Experimental for Chapter one

4.4.1 Preparation of trimethylamine complexes of Mn(II) chloride

The complex was prepared by direct treatment of anhydrous manganese(II) chloride (~2g) with an excess (30cm³) of trimethylamine in a single-ampoule vessel following the procedures reported above. An insoluble precipitate was formed, the reaction taking about one week to consume all the pale pink manganese(II) chloride. Excess amine was removed on the vacuum line and the off-white product was washed with n-pentane and dried in vacuo. Microanalytical and spectroscopic data (Tables 4.1 and 4.2

respectively) show the adduct to be formulated as $MnCl_2 \cdot NMe_3$ (I).

Treatment of (I) (1.66g) by Soxhlet extraction using boiling MeCN over a period of 24 hours resulted in the formation of a deep green solution and an insoluble grey residue left behind in the extraction thimble. Gradual removal of solvent from the saturated green solution provided a crop of pink crystals which were carefully removed. Complete removal of solvent from the remaining mother liquor provided a dark green solid. Subsequent recrystallizations from MeCN of these separate products provided respectively:

- a) pink cylindrical rod crystals of $[Me_3NH][MnCl_3]$ (II) (0.74g)
- b) light green needle crystals of $[Me_3NH]_2[MnCl_4]$ (III) (0.31g)

(Tables 4.1, 4.2 and 4.3 show the relevant microanalytical and spectroscopic data). The UV-Vis spectrum of (II) is only partially resolved due to its limited solubility in MeCN.

Complex	C	H	N	Cl
<i>MnCl₂ · NMe₃</i> (I)				
Calculated	19.5	4.9	7.6	38.3
Found	19.2	4.8	7.6	38.1
<i>[Me₃NH] [MnCl₂]</i> (II)				
Calculated	16.3	4.6	6.3	48.0
Found	16.6	4.7	6.6	47.6
<i>[Me₃NH]₂[MnCl₄]</i> (III)				
Calculated	22.7	6.3	8.8	44.8
Found	22.4	6.0	8.7	44.3

Table 4.1 Analytical data (%) for (I), (II) and (III)

Table 4.2 IR data (cm⁻¹) for (I), (II) and (III)

Complex	$\nu(\text{CN})_{\text{asy}}$	$\rho(\text{CH}_3)$	$\nu(\text{CN})_{\text{sym}}$	$\delta(\text{CN})_{\text{asy}}$	$\nu(\text{N}-\text{H})^*$	$\nu_{\text{Me}-\text{Cl}}$
$\text{MnCl}_2 \cdot \text{NMe}_3$ (I)	1255	989	811	509		230, 310
$[\text{Me}_3\text{NH}][\text{MnCl}_3]$ (II) (Pink)	1260	984	816	465	2786	225
$[\text{Me}_3\text{NH}]_2[\text{MnCl}_4]$ (III)(green)	1260	975	814	470	2735	286, 265, 240

Table 4.3 Vis-UV data (nm) for (II) and (III)

Complex	$\lambda_{\text{max}} (\text{MeCN})$
$[\text{Me}_3\text{NH}][\text{MnCl}_3]$ (II)	444,430,360,307 (only partially resolved, due to limited solubility in MeCN)
$[\text{Me}_3\text{NH}]_2[\text{MnCl}_4]$ (III)	687,664(sh),630(sh), 590,446,430,357,306

4.4.2 Preparation of trimethylamine complexes of Cd(II) chloride

Direct reaction of anhydrous CdCl_2 with excess trimethylamine was carried out in a single ampoule system. A white viscous slurry was formed over a period of one week. Removal of excess amine leaves the product as a white solid which was washed with n-hexane and dried in vacuo. Infrared and microanalytical data show the adduct to be formulated as $\text{CdCl}_2 \cdot \text{NMe}_3$ (IV) (Tables 4.4 and 4.5).

Treatment of (IV) (1.34g) by Soxhlet extraction using boiling MeCN for three days provided a clear, colourless solution and an insoluble off-white residue in the extraction thimble. Storage of the saturated solution at 0°C resulted in the deposition of white needle crystals of $[\text{Me}_3\text{NH}] [\text{CdCl}_3]$ (V) (0.87g). The product was collected, washed with n-pentane and dried in vacuo. Microanalytical and spectroscopic data are listed in Tables 4.4 and 4.5 respectively.

Complex	C	H	N
<i>CdCl₂ · NMe₃</i>			
Calculated	14.9	3.7	5.8
Observed	14.4	3.7	5.2
<i>[NMe₃H] [CdCl₃]</i>			
Calculated	12.9	3.6	5.0
Observed	12.8	3.6	5.2

Table 4.4 Micro analytical data (%) for (IV) and (V)

Complex	$\nu(\text{CN})_{\text{asy}}$	$\rho(\text{CN})$	$\nu(\text{CN})_{\text{sym}}$	$\delta(\text{CN})_{\text{asy}}$	$\nu(\text{N-H})^*$	$\nu_{\text{Cd-Cl}}$
<i>CdCl₂ · NMe₃</i>	1260	1012	825	488		244, 210
<i>[NMe₃NH] [CdCl₃]</i>	1255	980	815	460	2778	

Table 4.5 Infrared data (cm^{-1}) for (IV) and (V)

4.4.3 Preparation of trimethylamine complexes of Cu(II) chloride

Addition of excess trimethylamine ($\sim 30 \text{ cm}^3$) to anhydrous Cu(II) chloride ($\sim 2 \text{ g}$) in a double ampoule system initially gave a very pale lime-green colour, which did not last, giving way to a yellow-brown colour. Due to the limited solubility of the yellow-brown solid in the parent amine, it was extracted in situ to give a yellow solid. Removal of amine after a week gave a yellow solid on the right hand side of the ampoule and a mixture of yellow and brown solid in the left hand side of the ampoule. Further purification of the yellow solid was carried out by washing it with n-hexane several times and pumping it dry. The yellow solid was then Soxhlet extracted with boiling benzene to produce a bright yellow solution. Upon pumping off solvent a bright yellow solid was formed (VI), (Melting point: $154\text{--}155^\circ\text{C}$; Analysis calculated for $\text{CuCl}_2 \cdot 1.1\text{NMe}_3$: C, 19.9%; H, 5.00%; N, 7.72%; Cl, 35.6%. Observed: C, 19.75%; H, 4.99%; N, 7.69%; Cl, 36.01%. IR spectrum (cm^{-1}): 1265, 999, 830, 564, 250. Vis-UV (cm^{-1}): 11,494, 13,089(sh).

Several attempts to get this product in a crystalline form using non-chlorinated solvents such as benzene, acetonitrile were unsuccessful. However recrystallization of the Soxhlet extracted product with charcoal using dichloromethane provided small golden-yellow cubic crystals of

$(Me_3NCH_2Cl)_2[CrCl_4]$ (VII), (Melting point: 220-222 °C; Analysis calculated: C, 22.74%; H, 5.25%; N, 6.63%; Cl, 50.34%; and observed: C, 22.65%; H, 5.30%; N, 6.56%; Cl, 49.89%. IR (cm^{-1}): 1150(br,w), 970(m), 804(m), 720(st), 290(sh) and 271. Vis-UV (cm^{-1}): 9360.

4.5 Experimental for Chapter two

4.5.1 Preparation of crown ether complexes of Group VB trichlorides

All manipulations were conducted under an inert atmosphere (dry nitrogen) using standard Schlenk techniques and a conventional "dry box" containing a tray of P_2O_5 . The complexes were prepared by direct addition of an acetonitrile solution of the appropriate crown ether (1 equivalent) to a chilled, stirred solution of the appropriate metal(III) chloride (1 equivalent) in acetonitrile. To illustrate the procedure the preparation of $BaCl_2(12-C-4)$ is described here.

Preparation of $BaCl_2(12-C-4)$ Complex (III)

An acetonitrile (50cm^3) solution of 12-C-4 (1.179 g, 1.1 ml, 6.70 mmol) was added dropwise to a stirred, chilled (0°) solution of $BaCl_2$ (2.115 g, 6.70 mmol) in acetonitrile (100cm^3). The resulting colourless solution was allowed to warm up to room temperature and stirred overnight. A white micro crystalline slurry was formed during that period. Solvent removal in vacuo provided a white semi-crystalline solid which was thoroughly washed with n-hexane and pumped dry. Recrystallization from acetonitrile provided long prismatic crystals of the product of diffraction quality (yield : 88.4%). Microanalytical and spectroscopic data are listed in Tables 4.7 and 4.8 respectively. (melting point : it does not melt below 250°C)

Other reactions between metal(III) chlorides (As, Sb, Bi) and the crown ethers were performed similarly, and are summarized in Table 4.6. The solvent used was acetonitrile unless otherwise indicated. Microanalytical values and spectroscopic data for these complexes are listed in Tables 4.7 and 4.8 respectively.

Table 4.6 Synthetic procedures for GroupVB trichloride-crown ether complexes

Reaction	Reagent in Dropping Funnel	Reagent in Schlenk tube	Product
$AsCl_3 + 12-C-4$ 1:1	12-C-4 1 ml, 1.089 g, 6.20 mmol	$AsCl_3$ 0.5 ml, 1.08 g, 5.96 mmol	$AsCl_3(12-C-4)$ (I) 1.3 g, 61.0%
$SbCl_3 + 12-C-4$ 1:1	12-C-4 1.5 ml, 1.63 g, 9.30 mmol	$SbCl_3$ 2.1 g, 9.21 mmol	$SbCl_3(12-C-4)$ (II) 2.6 g, 69.9%
$AsCl_3 + 15-C-5$ 1:1	15-C-5 1.2 ml, 1.33 g, 6.04 mmol	$AsCl_3$ 0.5 ml, 1.08 g, 5.95 mmol	$AsCl_3(15-C-5)$ (IV) 1.6 g, 67.0%
$BiCl_3 + 15-C-5$ 1:1	15-C-5 1.5 ml, 1.66 g, 7.60 mmol	$BiCl_3$ 2.38 g, 7.55 mmol	$BiCl_3(15-C-5)$ (V) 3.4 g, 84.2%
$AsCl_3 + 18-C-6$ 1:1	18-C-6 1.4 g, 5.30mmol in benzene	$AsCl_3$ 0.4 ml, 0.86 g, 4.80 mmol	$18-C-6 \cdot 2CH_3CN$ (IX) 0.6 g, 32.8%
$SbCl_3 + 18-C-6$ 1:1	18-C-6 1.6 g, 6.05 mmol in benzene	$SbCl_3$ 1.4 g, 6.14 mmol	$SbCl_3(18-C-6) \cdot CH_3CN$ 2.3 g, 71.2% (VI)
$BiCl_3 + 18-C-6$ 1:1	18-C-6 1.3 g, 4.90 mmol	$BiCl_3$ 1.55 g, 4.92 mmol	$(BiCl_3)_2(18-C-6)$ 3.95 g, 89.8% (VII) (ionic product)

Table 4.7 Analytical data for GroupVB trichloride-crown ether complexes

Complex	C	H	Cl	N
AsCl_3 (12-C-4) (I)				
Calculated	26.88	4.51	29.75	
Observed	27.01	4.54	29.85	
AsCl_3 (15-C-5) (IV)				
Calculated	29.91	5.02	26.49	
Observed	30.06	5.04	26.27	
(18-C-6). $2\text{CH}_3\text{CN}$ (IX)				
Calculated	55.49	8.73		8.08
Observed	55.57	8.77		7.69
SbCl_3 (12-C-4) (II)				
Calculated	23.76	3.99	26.31	
Observed	23.90	4.06	26.36	
SbCl_3 (15-C-5) (VIII)				
Calculated	26.79	4.49	23.72	
Observed	26.76	4.66	24.01	
SbCl_3 (18-C-6). CH_3CN (VI)				
Calculated	31.52	5.10	19.94	2.62
Observed	31.22	5.28	20.15	2.10
BiCl_3 (12-C-4) (III)				
Calculated	19.55	3.28	21.64	
Observed	19.68	3.31	21.52	
BiCl_3 (15-C-5) (V)				
Calculated	22.42	3.76	19.86	
Observed	22.50	3.82	20.14	
$[\text{BiCl}_2(18\text{-C-6})]_2^+ [\text{Bi}_2\text{Cl}_6]^{2-}$ (VII)				
Calculated	16.10	2.70	23.77	
Observed	16.13	2.81	22.58	

Table 4.8 Spectroscopic data for GroupVB trichloride-crown ether complexes

Compound	Proton nmr (δ ppm) reference - TMS	Ir(cm^{-1})	UV-Vis (nm)
12-C-4	3.65s(CDCl_3), 3.58s(CD_3CN)	2904vs, 2864vs, 1469vs, 1449st, 1363m, 1289m, 1250m, 1136vs, 1094vs, 1022st, 913vs, 844vs, 548m.	
15-C-5	3.58s(CCl_4), 3.57s(CD_3CN)	2862m,br, 1450st, 1356st 1300 m,br, 1250st, 1118vs,br, 1087st, 1037w, 980m, 941st, 854st, 517m 1320m,sh, 1308m, 1280w	
18-C-6	3.62s(CDCl_3), 3.51s(CD_3CN)	1354m, 1346m, 1298m, 1279w[214z,sh, 1261m, 1239m, 1222w, 1142sh, 1127sh, 1110vs, 1078sh, 1060w, 1042w, 992m, 902m, 889w, 863m, 832m, 570m, 538m, 465m	
$\text{AsCl}_3(12\text{-C-4})$ (I)	3.74s(CDCl_3)	1302m, 1289m, 1247m, 1235w, 1135vs, 1086vs, 1027st, 912st, 845st, 549m, 367st, 327vs	
$\text{SbCl}_3(12\text{-C-4})$ (II)	3.75 (CDCl_3)	1300m, 1287m, 1246m, 1233w, 1132vs, 1086vs, 1015st, 912st, 840st, 548m, 322st, 290vs, 268w	
$\text{BiCl}_3(12\text{-C-4})$ (III)	3.86(CD_3CN)	1300m, 1285m, 1243m, 1230w, 1130st, 1078vs, 1008st, 915st, 840st, 550m, 280st, 245vs	303
$\text{AsCl}_3(15\text{-C-5})$ (IV)	3.73s(CDCl_3)	1255m, 1245m, 1143st, 1129st, 1120st, 1103vs, 1090st, 1069st, 1055w, 1033st, 935st, 855st, 825w, 800w, 565m, 380st, 335vs	

[contd.]

[Contd.] Table 4.8

Compound	Proton nmr δ ppm reference TMS	ir(cm^{-1})	UV-Vis (nm)
$\text{SbCl}_3(15\text{-C-5})$ (VIII)	3.77(CDCl_3)	1314m, 1304m, 1248m, 1241m, 1134m, 1118st,sh, 1110st, 1094vs, 1078vs, 1064m, 1046w, 1039st, 1024st, 933st, 850st, 818w, 808w, 788w, 722w, 322st, 280vs	
$\text{BiCl}_3(15\text{-C-5})$ (V)	3.83(CD_3CN)	1300m, 1258m, 1243m, 1124st, 1116st, 1084st, 1068st, 1049st, 1036st, 1020st, 945st, 928m, 908w, 858st, 820m, 280m, 245vs	287
$(18\text{-C-6}) \cdot 2\text{CH}_3\text{CN}$ (IX)	3.73s, 2.04s(CDCl_3)	2298w, 2250st, 1286m, 1253m, 1238sh, 1138sh, 1108vs, 1060w, 1058w, 958vs, 920w, 866w, 841vs, 522m, 386w	
$\text{SbCl}_3(18\text{-C-6}) \cdot \text{CH}_3\text{CN}$ (VI)	3.76, 1.99(CDCl_3)	2298w, 2254st, 1300m, 1254m, 1134m,sh, 1100vs,br, 1044m, 954vs, 869m, 839vs, 814w, 345st, 300vs, 250w	
$[\text{BiCl}_2(18\text{-C-6})]_2 [\text{Bi}_2\text{Cl}_8]^{2-}$ (VII)	3.83(CD_3CN)	1309m, 1257m, 1245m, 1142w,sh, 1132w,sh, 1105w,sh, 1072vs, 1057vs, 1047vs, 1022m,sh, 1000w,sh, 937st, 900m, 852m, 815m, 354w, 285w,sh, 265st.	312, 284

s:sharp, st:strong, vs:very strong, sh:shoulder, m:medium, w:weak.

4.5.2 Preparation of Hydronium-ion-antimon(V)ate Complexes

(a) Preparation of $[H_2O(18-C-6)][SbCl_6]$

18-C-6 (2.93g, 11.1 mmol) in acetonitrile (20 cm³) was added dropwise to a cooled (-20°C), stirred solution of $SbCl_5$ (3.32g, 11.1 mmol) in acetonitrile (50 cm³) under a dry nitrogen atmosphere. The yellow solution initially formed changed to a deep red colour on warming to room temperature. This solution was stirred for 24 hours. Removal of solvent provided a brown-red tacky solid which was thoroughly washed with hexane (6x20 cm³). Repeated extraction of this material using boiling acetonitrile and activated charcoal finally gave a light yellow solution from which colourless chunky crystals of $[H_2O(18-C-6)][SbCl_6]$ were obtained (1.33g, 19.4% based on $SbCl_5$). Micro analytical and spectroscopic data are listed in Tables 4.9 and 4.10 respectively.

(b) Preparation of $[H_2O(12-C-4)_2][SbCl_6]$

Following the procedure as in (a) above, the reaction of 12-C-4 (2.18g, 12.4 mmol) and $SbCl_5$ (3.68g, 12.3 mmol) in acetonitrile provided colourless needle crystals of $[H_2O(12-C-4)_2][SbCl_6]$ (1.96g, 22.6% based on $SbCl_5$).

Microanalytical and spectroscopic data are listed in Tables 4.9 and 4.10 respectively.

(c) Preparation of $SbCl_3(15-C-5)$ and $[H_3O(15-C-5)][SbCl_6]$

Following the procedure as in (a) above, the reaction of 15-C-5 (1.66g, 7.6 mmol) and $SbCl_3$ (2.26g, 7.5 mmol) in acetonitrile provided a matte of colourless crystals in which small numbers of pale yellow cubic crystals are interspersed. Physical separation by careful manipulation under a microscope provided $SbCl_3(15-C-5)$ (0.45g, 13.3% based on $SbCl_3$) and $[H_3O(15-C-5)][SbCl_6]$ (0.04g, 1.1% based on $SbCl_3$). Microanalytical and spectroscopic data are listed in Tables 4.9 and 4.10 respectively.

Table 4.9 Microanalytical data for hydronium-ion(crown) antimon(V)ate and $SbCl_3(15-C-5)$ complexes

Compound	C	H	Cl
$[H_3O(18-C-6)][SbCl_6]$			
Calculated	23.33	4.40	34.43
Observed	23.43	4.37	34.4
$[H_3O(12-C-4)_2][SbCl_6]$			
Calculated	27.22	4.99	30.13
Observed	27.28	4.85	30.33
$SbCl_3(15-C-5)$			
Calculated	26.79	4.49	23.72
Observed	26.76	4.66	24.01

Table 4.10 Spectroscopic data for hydronium-ion(crown) antimonate and $SbCl_5(15-C-5)$ complexes

Compound	Ir cm^{-1}	proton nmr(ppm)	λ_{max} cm^{-1}
$[H_3O(18-C-6)][SbCl_6]$	1286, 1250, 1141, 1094, 1077, 970, 946, 839, 723, 338, 266	3.67	37,023
$[H_3O(12-C-4)_2][SbCl_6]$	1298, 1287, 1242, 1132, 1090, 1020, 914, 845, 716, 550, 338, 260	3.63	37,091
$SbCl_5(15-C-5)$	1314, 1304, 1241, 1134, 1110, 1094, 1078, 1064, 1046, 1039, 1024, 932, 850, 818, 808, 788, 722, 580, 560, 542, 506, 322, 280	3.77	
$[H_3O(15-C-5)][SbCl_6]$	1305, 1291, 1252, 1135, 1095, 1073, 1022, 958, 919, 340	3.61	37,050

4.6 Experimental for Chapter three

4.6.1 Preparation of 2,2',6,6'-tetra(tert-butyl)diphenoquinone.

A solution of $SbCl_5$ (3.5g, 11.5 mmol) in acetonitrile was added dropwise to a chilled (-10°) suspension of $LiOAr'$ ($Ar' = 2,6$ -di(tert-butyl)phenoxyde) (12.2g, 57.7 mmol) in hexane (formed in situ by direct treatment of $Ar'OH$

and *n*-BuLi). The resulting yellow mixture was allowed to warm to room temperature and then stirred for 24 hours to afford a deep red solution. Removal of solvents in vacuo left a dark red residue. Extraction with pentane gave an insoluble residue (not further investigated) and a clear red solution which was evaporated to dryness to give a red solid. Chromatographic separation of this solid on alumina with hexane as eluant followed by recrystallization from pentane (-40° C) gave red-brown platelets of 2,2',6,6'-tetra-*tert*-butyldiphenylquinone (I) (yield: 2.3g, 9.8%). Melting point 239-240° C. Analysis Found: C, 82.2; H, 9.9; $C_{28}H_{40}O_2$ requires: C, 82.3; H, 9.9 %). 1H nmr (220MHz; Solvent $CDCl_3$; Standard Me_4Si , ppm), δ : 1.38 (36H, s, CMe_3) and 8.3 (4H, s, ring-H). IR (cm^{-1}), ν_{max} (nujol mull): 1637(m), 1605(vs), 1565(m) cm^{-1} . Vis-UV, λ_{max} (hexane): 400, 419 nm. Mass spectrum, M/Z (electron impact), 408 (M^+ , 100%).

APPENDIX

Table A2.2.1 *Crystal data for* $\text{AsCl}_3(12-C-4)$

Formula	$\text{C}_8\text{H}_{18}\text{O}_8\text{AsCl}_3$
M_r	357.5
Crystal class	Orthorhombic
Spacegroup	Pnma
$a(\text{\AA})$	7.864(4)
$b(\text{\AA})$	11.876(5)
$c(\text{\AA})$	14.936(8)
$V(\text{\AA}^3)$	1395(1)
Z	4
Systematic absences	$(0,k,l), l = 2n + 1$ $(h,k,0), h + k = 2n + 1$
$D_c (\text{g cm}^{-3})$	1.70
Crystal size (mm)	$0.8 \times 0.4 \times 0.8$
$\mu(\text{Mo-K}\alpha) (\text{mm}^{-1})$	3.0
T (K)	298
Transmission range	0.43-0.21
Final R	0.070

Table A2.2.2 Bond lengths (Å) for $\text{AsCl}_5(12\text{-C-4})$

As(1)-Cl(1)	2.198	As(1)-Cl(1A)	2.198
As(1)-Cl(2)	2.222	As(1)-O(1)	2.776
As(1)-O(2)	2.915	O(1)-C(1A)	1.378
O(1)-C(1B)	1.467	O(1)-C(2A)	1.439
O(1)-C(2B)	1.376	O(2)-C(3A)	1.327
O(2)-C(3B)	1.403	O(2)-C(4A)	1.525
O(2)-C(4B)	1.382	C(1A)-C(1BB)	1.511
C(1B)-C(1AA)	1.511	C(2A)-C(3A)	1.492
C(2B)-C(3B)	1.491	C(4A)-C(4BB)	1.489
		C(4B)-C(4AA)	1.489

Table A2.2.3 Bond angles (deg.) for $\text{AsCl}_2\text{C}_2\text{H}_2$

Cl(1)-As(1)-Cl(1A)	96.5	Cl(1)-As(1)-Cl(2)	94.9
Cl(1A)-As(1)-Cl(2)	94.9	O(1)-As(1)-O(1A)	62.1
O(1)-As(1)-O(2)	59.2	O(1)-As(1)-O(2A)	90.4
O(2)-As(1)-O(2A)	60.3	C(2A)-O(1)-C(1A)	114.8
C(2A)-O(1)-C(1B)	145.4	C(2B)-O(1)-C(1A)	79.1
C(2B)-O(1)-C(1B)	110.1	C(3A)-O(2)-C(4A)	119.4
C(3A)-O(2)-C(4B)	82.1	C(3B)-O(2)-C(4A)	151.7
C(3B)-O(2)-C(4B)	114.5	O(1)-C(1A)-C(1BB)	104.4
O(1)-C(1B)-C(1AA)	115.9	C(4AA)-C(4B)-O(2)	99.1
C(4BB)-C(4A)-O(2)	116.6	O(2)-C(3A)-C(2A)	98.4
O(2)-C(3B)-C(2B)	122.0	C(3A)-C(2A)-O(1)	119.4
C(3B)-C(2B)-O(1)	100.4		

Table A2.2 4 *Torsion angles (deg.) for AsCl₃(12-C-4)*

C(2A)-O(1)-C(1A)-C(1BB)	157.1
C(2B)-O(1)-C(1A)-C(1BB)	157.4
C(2A)-O(1)-C(1B)-C(1AA)	84.3
C(2B)-O(1)-C(1B)-C(1AA)	77.6
O(1A)-C(1AA)-C(1B)-O(1)	64.1
O(1)-C(1A)-C(1BB)-O(1A)	-64.1
C(1A)-O(1)-C(2A)-C(3A)	-67.2
C(1B)-O(1)-C(2A)-C(3A)	-78.4
C(1A)-O(1)-C(2B)-C(3B)	-150.9
C(1B)-O(1)-C(2B)-C(3B)	-157.8
C(4B)-O(2)-C(3A)-C(2A)	155.9
O(1)-C(2A)-C(3A)-O(2)	-70.5
C(4A)-O(2)-C(3B)-C(2B)	79.3
C(4B)-O(2)-C(3B)-C(2B)	75.0
O(1)-C(2B)-C(3B)-O(2)	62.4
C(3A)-O(2)-C(4A)-C(4BB)	-60.4
C(3B)-O(2)-C(4A)-C(4BB)	-66.0
C(3A)-O(2)-C(4B)-C(4AA)	-156.5
C(3B)-O(2)-C(4B)-C(4AA)	-159.1
O(2A)-C(4AA)-C(4B)-O(2)	76.7
O(2)-C(4A)-C(4BB)-O(2A)	-76.7
C(2AA)-O(1A)-C(1AA)-C(1B)	-157.1
C(2BA)-O(1A)-C(1AA)-C(1B)	-157.4
C(2AA)-O(1A)-C(1BB)-C(1A)	-84.3
C(2BA)-O(1A)-C(1BB)-C(1A)	-77.6

Table A2.2.5 *Crystal data for* $\text{AsCl}_3(15\text{-C-5})$

Formula	$\text{C}_{10}\text{H}_{20}\text{O}_5\text{AsCl}_3$
M_r	401.551
Crystal Class	Orthorhombic
Space Group	$P2_12_12_1$
a (Å)	7.731(3)
b (Å)	12.815(4)
c (Å)	16.011(6)
V (Å ³)	1586
Z	4
Systematic absences	$h00, h \neq 2n; 0k0, k \neq 2n; 00l, l \neq 2n$
D_c (gcm ⁻³)	1.68
Crystal size (mm)	0.11×0.29×0.67
μ (Mo-K α) (mm ⁻¹)	2.66
Transmission range	0.45-0.70
T (K)	298
Final R	0.031

Table A2.2.6 *Bond lengths (Å) for AsCl₃(15-C-5)*

As(1) - Cl(1)	2.209	O(3) - C(4)	1.406
As(1) - Cl(2)	2.218	O(3) - C(5)	1.390
As(1) - Cl(3)	2.202	O(4) - C(6)	1.426
As(1) - O(1)	3.008	O(4) - C(7)	1.410
As(1) - O(2)	3.043	O(5) - C(8)	1.409
As(1) - O(3)	3.046	O(5) - C(9)	1.427
As(1) - O(4)	2.944	C(1) - C(2)	1.501
As(1) - O(5)	3.156	C(3) - C(4)	1.501
O(1) - C(1)	1.404	C(5) - C(6)	1.482
O(1) - C(10)	1.424	C(7) - C(8)	1.490
O(2) - C(2)	1.412	C(9) - C(10)	1.499
O(2) - C(3)	1.408		

Table A2.2.7 Bond angles (deg.) for $\text{AsCl}_4(15\text{-C-5})$

Cl(1) - As(1) - Cl(2)	93.6
Cl(1) - As(1) - Cl(3)	96.5
Cl(2) - As(1) - Cl(3)	94.4
C(10) - O(1) - C(1)	113.4
C(2) - O(2) - C(3)	113.4
C(4) - O(3) - C(5)	113.5
C(6) - O(4) - C(7)	115.3
C(8) - O(5) - C(9)	114.1
O(1) - C(1) - C(2)	109.5
C(1) - C(2) - O(2)	113.4
O(2) - C(3) - C(4)	107.9
C(3) - C(4) - O(3)	115.1
O(3) - C(5) - C(6)	110.5
C(5) - C(6) - O(4)	113.5
O(4) - C(7) - C(8)	113.3
C(7) - C(8) - O(5)	107.0
O(5) - C(9) - C(10)	106.8
C(9) - C(10) - O(1)	113.5

Table A2.2.8 *Torsion angles (deg.) for AsCl₅(15-C-5)*

C(10) - O(1) - C(1) - C(2)	178.1
C(3) - O(2) - C(2) - C(1)	-79.1
O(1) - C(1) - C(2) - O(2)	-65.2
C(2) - O(2) - C(3) - C(4)	177.8
C(5) - O(3) - C(4) - C(3)	-74.8
O(2) - C(3) - C(4) - O(3)	-61.8
C(4) - O(3) - C(5) - C(6)	-168.6
C(7) - O(4) - C(6) - C(5)	-110.0
O(3) - C(5) - C(6) - O(4)	-67.3
C(6) - O(4) - C(7) - C(8)	73.3
C(9) - O(5) - C(8) - C(7)	-178.6
O(4) - C(7) - C(8) - O(5)	60.6
C(8) - O(5) - C(9) - C(10)	-176.7
C(1) - O(1) - C(10) - C(9)	-81.3
O(5) - C(9) - C(10) - O(1)	-60.9

Table A2.2.9 *Crystal data for SbCl₃(12-C-4)*

Formula	$C_{16}H_{16}O_4SbCl_3$
M_r	404.325
Crystal Class	Monoclinic
Space Group	Pa
a (Å)	14.988(9)
b (Å)	7.938(3)
c (Å)	12.022(9)
β (deg.)	90.49(5)
V (Å ³)	1430
Z	4
Systematic absences	h0l, h \neq 2n
D_c (g cm ⁻³)	1.88
Crystal size (mm)	0.15 \times 0.48 \times 0.24
μ (Mo-K α) (mm ⁻¹)	2.50
Transmission range	0.69-0.84
Final R	0.058

Table A2.2.10 Bond lengths (Å) for $\text{SbCl}_5(12-C-4)$

Molecule A

Sb(1)-Cl(11)	2.519	O(12)-C(13)	1.462
Sb(1)-Cl(12)	2.407	O(13)-C(14)	1.325
Sb(1)-Cl(13)	2.389	O(13)-C(15)	1.491
Sb(1)-O(11)	2.710	O(14)-C(16)	1.454
Sb(1)-O(12)	2.854	O(14)-C(17)	1.363
Sb(1)-O(13)	2.914	C(11)-C(12)	1.505
Sb(1)-O(14)	2.712	C(13)-C(14)	1.163
O(11)-C(11)	1.490	C(15)-C(16)	1.262
O(11)-C(18)	1.486	C(17)-C(18)	1.316
O(12)-C(12)	1.337		

Molecule B

Sb(2)-Cl(21)	2.322	O(22)-C(23)	1.248
Sb(2)-Cl(22)	2.369	O(23)-C(24)	1.391
Sb(2)-Cl(23)	2.432	O(23)-C(25)	1.239
Sb(2)-O(21)	2.814	O(24)-C(26)	1.490
Sb(2)-O(22)	2.958	O(24)-C(27)	1.310
Sb(2)-O(23)	2.852	C(21)-C(22)	1.277
Sb(2)-O(24)	2.848	C(23)-C(24)	1.319
O(21)-C(21)	1.534	C(25)-C(26)	1.520
O(21)-C(28)	1.287	C(27)-C(28)	1.482
O(22)-C(22)	1.423		

Table A2.2.11 Bond angles (deg.) for $\text{SbCl}_3(12\text{-C-4})$

Molecule A

Cl(12)-Sb(1)-Cl(11)	91.5
Cl(13)-Sb(1)-Cl(11)	92.7
Cl(13)-Sb(1)-Cl(12)	93.5
O(11)-C(11)-C(12)	106.0
C(11)-C(12)-O(12)	108.4
C(12)-O(12)-C(13)	113.1
O(12)-C(13)-C(14)	123.4
C(13)-C(14)-O(13)	127.9
C(14)-O(13)-C(15)	129.1
O(13)-C(15)-C(16)	123.3
C(15)-C(16)-O(14)	122.2
C(16)-O(14)-C(17)	99.3
O(14)-C(17)-C(18)	130.3
C(17)-C(18)-O(11)	107.8
C(18)-O(11)-C(11)	113.2

Molecule B

Cl(22)-Sb(2)-Cl(21)	94.2
Cl(23)-Sb(2)-Cl(21)	90.5
Cl(23)-Sb(2)-Cl(22)	95.6
O(21)-C(21)-C(22)	119.6
C(21)-C(22)-O(22)	132.4
C(22)-O(22)-C(23)	114.6
O(22)-C(23)-C(24)	118.0
C(23)-C(24)-O(23)	137.4
C(24)-O(23)-C(25)	109.0
O(23)-C(25)-C(26)	123.6
C(25)-C(26)-O(24)	115.3
C(26)-O(24)-C(27)	104.8
O(24)-C(27)-C(28)	120.1
C(27)-C(28)-O(21)	117.5
C(28)-O(21)-C(21)	135.1

Table A2.2.12 *Torsion angles (deg.) for SbCl₅(12-C-4)*

Molecule A

C(18)-O(11)-C(11)-C(12)	84.1
C(13)-O(12)-C(12)-C(11)	163.2
O(11)-C(11)-C(12)-O(12)	-61.3
C(12)-O(12)-C(13)-C(14)	-88.7
C(15)-O(13)-C(14)-C(13)	127.7
O(12)-C(13)-C(14)-O(13)	-26.3
C(14)-O(13)-C(15)-C(16)	-110.2
C(17)-O(14)-C(16)-C(15)	136.2
O(13)-C(15)-C(16)-O(14)	-30.6
C(16)-O(14)-C(17)-C(18)	-89.2
C(11)-O(11)-C(18)-C(17)	158.6
O(14)-C(17)-C(18)-O(11)	-37.4

Molecule B

C(28)-O(21)-C(21)-C(22)	-120.1
C(23)-O(22)-C(22)-C(21)	120.4
O(21)-C(21)-C(22)-O(22)	-30.5
C(22)-O(22)-C(23)-C(24)	-124.2
C(25)-O(23)-C(24)-C(23)	109.9
O(22)-C(23)-C(24)-O(23)	20.9
C(24)-O(23)-C(25)-C(26)	-111.9
C(27)-O(24)-C(26)-C(25)	146.5
O(23)-C(25)-C(26)-O(24)	-19.7
C(26)-O(24)-C(27)-C(28)	-99.3
C(21)-O(21)-C(28)-C(27)	146.5
O(24)-C(27)-C(28)-O(21)	-8.4

Table A2.2.13 Crystallographic Data for $\text{SbCl}_3(18\text{-C-6})\cdot\text{MeCN}$

Formula	$\text{C}_{10}\text{H}_{27}\text{O}_6\text{NSbCl}_3$
M_r	533.6
Crystal Class	Orthorhombic
Space group	$Pnma$
hkl ranges	$h = 0 \rightarrow 24, k = 0 \rightarrow 17, l = 0 \rightarrow 10.$
a (Å)	19.473(6)
b (Å)	13.946(5)
c (Å)	8.032(3)
V (Å ³)	2181.1(1.1)
Z	4
Systematic Absences	$0kl, k+l = 2n+1; hk0, h = 2n+1$
D_c (g cm ⁻³)	1.63
Crystal Size (mm)	0.2×0.25×0.5
μ (Mo-K α)	16.7 cm ⁻¹
T (K)	293
Final R	0.0503 ($R_w = 0.0475$)

Table A2.2.14 *Selected bond distances (Å) and bond angles*

(deg.) for $\text{SbCl}_4(1\text{B}-\text{C}-6)\cdot\text{MeCN}$

Bond lengths

Sb(1) - Cl(1)	2.391(2)	O(4) - C(6)	1.422(16)
Sb(1) - Cl(1A)	2.391(2)	C(1) - C(2)	1.413(22)
Sb(1) - Cl(2)	2.361(3)	C(3) - C(4)	1.473(22)
O(1) - C(1)	1.397(17)	C(5) - C(6)	1.391(21)
O(2) - C(2)	1.441(18)	Sb(1) - O(1)	3.025(11)
O(2) - C(3)	1.351(17)	Sb(1) - O(2)	2.989(10)
O(3) - C(4)	1.402(15)	Sb(1) - O(3)	3.401(10)
O(3) - C(5)	1.405(17)	Sb(1) - O(4)	3.290(12)

Bond angles

Cl(1) - Sb(1) - Cl(2)	90.1(1)	O(1) - C(1) - C(2)	108.5(1.0)
Cl(2) - Sb(1) - Cl(1A)	90.1(1)	C(1) - C(2) - O(2)	114.6(1.3)
Cl(1) - Sb(1) - Cl(1A)	90.3(1)	O(2) - C(3) - C(4)	111.2(1.2)
C(1) - O(1) - C(1A)	115.0(13)	C(3) - C(4) - O(3)	109.1(1.1)
C(2) - O(2) - C(3)	112.1(10)	O(3) - C(5) - C(6)	112.0(1.2)
C(4) - O(3) - C(5)	114.1(10)	C(5) - C(6) - O(4)	109.5(1.0)
C(6) - O(4) - C(6A)	110.5(12)		

Table A2.2.15 *Torsion angles (deg.) for SbCl₅(18-C-6)₂MeCN*

C(2) - C(1) - O(1) - C(1A)	-171.3
C(1) - C(2) - O(2) - C(3)	-91.0
O(1) - C(1) - C(2) - O(2)	-63.0
C(4) - C(3) - O(2) - C(2)	-178.9
C(3) - C(4) - O(3) - C(5)	172.4
O(2) - C(3) - C(4) - O(3)	-68.3
C(4) - O(3) - C(5) - C(6)	170.8
C(5) - C(6) - O(4) - C(6A)	-174.3
O(4) - C(6) - C(5) - O(3)	60.2
C(2A) - C(1A) - O(1) - C(1)	171.3
C(1A) - C(2A) - O(2A) - C(3A)	91.0
O(1) - C(1A) - C(2A) - O(2A)	63.0
C(4A) - C(3A) - O(2A) - C(2A)	178.9
C(5A) - O(3A) - C(4A) - C(3A)	-172.4
O(2A) - C(3A) - C(4A) - O(3A)	68.3
C(4A) - O(3A) - C(5A) - C(6A)	-170.8
C(5A) - C(6A) - O(4) - C(6)	174.3
O(4) - C(6A) - C(5A) - O(3A)	-60.2

Table A2.2.16 *Crystal data for* $\text{BiCl}_3 \cdot \text{C}_{10}\text{H}_{16}\text{O}_4$

Formula	$\text{BiCl}_3 \cdot \text{C}_{10}\text{H}_{16}\text{O}_4$
M_r	491.5
Crystal class	Monoclinic
Space group	$P2_1/c$
a (Å)	12.043(4)
b (Å)	7.834(3)
c (Å)	15.036(5)
β (deg.)	90.31(3)
V (Å ³)	1418.8(8)
Z	4
Systematic absences	$h0l, l \neq 2n; 0k0, k \neq 2n$
D_c (g cm ⁻³)	2.30
Crystal size (mm)	$0.26 \times 0.51 \times 0.15$
λ (Å)	0.71069
$\mu_{\text{Mo-K}\alpha}$ (mm ⁻¹)	12.96
T (K)	290
R	0.05 ($R_w = 0.062$)

Table A2.2.17 Bond lengths(Å) and bond angles(deg.) for $\text{BiCl}_2(12-C-4)$ **Bond Lengths**

Bi(1)-Cl(11)	2.499 (4)	Bi(1)-Cl(12)	2.510 (4)
Bi(1)-Cl(13)	2.549 (3)	Bi(1)-O(11)	2.683 (9)
Bi(1)-O(12)	2.742 (9)	Bi(1)-O(13)	2.729 (9)
Bi(1)-O(14)	2.652 (8)	O(11)-C(11)	1.409 (22)
O(11)-C(18)	1.446 (20)	O(12)-C(12)	1.404 (23)
O(12)-C(13)	1.405 (25)	O(13)-C(14)	1.429 (25)
O(13)-C(15)	1.374 (22)	O(14)-C(16)	1.383 (23)
O(14)-C(17)	1.451 (19)	C(11)-C(12)	1.364 (35)
C(13)-C(14)	1.412 (33)	C(15)-C(16)	1.438 (27)
C(17)-C(18)	1.394 (26)		

Bond Angles

Cl(11)-Bi(1)-Cl(12)	94.4 (1)	Cl(11)-Bi(1)-Cl(13)	92.4 (1)
Cl(12)-Bi(1)-Cl(13)	91.9 (1)	Cl(11)-Bi(1)-O(11)	102.1 (2)
Cl(12)-Bi(1)-O(11)	163.3(2)	Cl(13)-Bi(1)-O(11)	84.8(2)
Cl(11)-Bi(1)-O(12)	79.5(2)	Cl(12)-Bi(1)-O(12)	125.7(2)
Cl(13)-Bi(1)-O(12)	141.8(2)	O(11)-Bi(1)-O(12)	61.1(3)
Cl(11)-Bi(1)-O(13)	122.0(2)	Cl(12)-Bi(1)-O(13)	79.4(2)
Cl(13)-Bi(1)-O(13)	144.8(2)	O(11)-Bi(1)-O(13)	93.9(3)
O(12)-Bi(1)-O(13)	60.7(3)	Cl(11)-Bi(1)-O(14)	166.5(2)
Cl(12)-Bi(1)-O(14)	99.1(2)	Cl(13)-Bi(1)-O(14)	85.7(2)
O(11)-Bi(1)-O(14)	64.4(3)	O(12)-Bi(1)-O(14)	93.7(3)
O(13)-Bi(1)-O(14)	62.6(3)	Bi(1)-O(11)-C(11)	113.6(12)
Bi(1)-O(11)-C(18)	115.9(9)	C(11)-O(11)-C(18)	113.9(13)
Bi(1)-O(12)-C(12)	116.1(10)	Bi(1)-O(12)-C(13)	116.9(11)
C(12)-O(12)-C(13)	111.1(14)	Bi(1)-O(13)-C(14)	118.6(10)
Bi(1)-O(13)-C(15)	112.5(10)	C(14)-O(13)-C(15)	112.3(14)
Bi(1)-O(14)-C(16)	118.8(9)	Bi(1)-O(14)-C(17)	111.7(9)
C(16)-O(14)-C(17)	110.6(13)	O(11)-C(11)-C(12)	114.7(15)
O(12)-C(12)-C(11)	114.7(17)	O(12)-C(13)-C(14)	113.9(19)
O(13)-C(14)-C(13)	116.9(19)	O(13)-C(15)-C(16)	116.5(16)
O(14)-C(16)-C(15)	115.3(17)	O(14)-C(17)-C(18)	116.9(14)
O(11)-C(18)-C(17)	114.9(16)		

Table A2.2.18 *Torsion angles (deg.) for BICl₃(12-C-4)*

C(18)-O(11)-C(11)-C(12)	87.0
C(13)-O(12)-C(12)-C(11)	-162.5
O(11)-C(11)-C(12)-O(12)	50.0
C(12)-O(12)-C(13)-C(14)	95.7
C(15)-O(13)-C(14)-C(13)	-152.6
O(12)-C(13)-C(14)-O(13)	39.2
C(14)-O(13)-C(15)-C(16)	95.8
C(17)-O(14)-C(16)-C(15)	-152.6
O(13)-C(15)-C(16)-O(14)	43.1
C(16)-O(14)-C(17)-C(18)	89.7
C(11)-O(11)-C(18)-C(17)	-155.5
O(14)-C(17)-C(18)-O(11)	45.0

Table A2.2.19 *Crystal data for $\text{BiCl}_3(15\text{-C-5})$*

Formula	$\text{BiCl}_3 \cdot 10\text{H}_2\text{O}_2$
M_r	535.609
Crystal class	Orthorhombic
Space group	$P 2_1 2_1 2_1$
a (Å)	7.692(2)
b (Å)	13.285(3)
c (Å)	15.939(4)
V (Å ³)	1628
Z	4
Systematic absences	$h00, h \neq 2n; 0k0, k \neq 2n; 00l, l \neq 2n$
D_c (g cm ⁻³)	2.19
Crystal size (mm)	$0.23 \times 0.11 \times 0.25$
μ (Mo-K α) (mm ⁻¹)	11.30
Transmission range	0.22-0.44
Final R	0.043

Table A2.2.20 Bond lengths (Å) and Bond angles (deg.) for
BiCl₃(15-C-5)

Bond Lengths

Bi-Cl(1)	2.527	Bi-Cl(2)	2.536
Bi-Cl(3)	2.515	Bi-O(1)	2.778
Bi-O(2)	2.811	Bi-O(3)	2.916
Bi-O(4)	2.830	Bi-O(5)	2.832
O(1)-C(1)	1.431	O(1)-C(10)	1.452
O(2)-C(2)	1.483	O(2)-C(3)	1.391
O(3)-C(4)	1.397	O(3)-C(5)	1.414
O(4)-C(6)	1.425	O(4)-C(7)	1.479
O(5)-C(8)	1.398	O(5)-C(9)	1.381
C(1)-C(2)	1.481	C(3)-C(4)	1.468
C(5)-C(6)	1.536	C(7)-C(8)	1.452
C(9)-C(10)	1.451		

Bond angles

Cl(1)-Bi-Cl(2)	88.0	Cl(3)-Bi-O(1)	162.6
Cl(1)-Bi-Cl(3)	92.3	Cl(3)-Bi-O(2)	105.1
Cl(2)-Bi-Cl(3)	89.6	Cl(3)-Bi-O(3)	76.7
Cl(1)-Bi-O(1)	97.3	Cl(3)-Bi-O(4)	81.1
Cl(1)-Bi-O(2)	156.2	Cl(3)-Bi-O(5)	138.4
Cl(1)-Bi-O(3)	143.4	O(1)-Bi-O(2)	61.9
Cl(1)-Bi-O(4)	85.1	O(1)-Bi-O(3)	103.1
Cl(1)-Bi-O(5)	81.0	O(1)-Bi-O(4)	114.0
Cl(2)-Bi-O(1)	76.4	O(1)-Bi-O(5)	57.9
Cl(2)-Bi-O(2)	76.3	O(2)-Bi-O(3)	58.5
Cl(2)-Bi-O(3)	126.1	O(2)-Bi-O(4)	113.2
Cl(2)-Bi-O(4)	168.2	O(2)-Bi-O(5)	95.7
Cl(2)-Bi-O(5)	130.7	O(3)-Bi-O(4)	59.0
O(4)-Bi-O(5)	57.5	O(3)-Bi-O(5)	84.6
O(1)-C(1)-C(2)	112.2	C(1)-C(2)-O(2)	106.8
O(2)-C(3)-C(4)	113.7	C(3)-C(4)-O(3)	109.3
O(3)-C(5)-C(6)	105.7	C(5)-C(6)-O(4)	114.4
O(4)-C(7)-C(8)	105.3	C(7)-C(8)-O(5)	109.2
O(5)-C(9)-C(10)	110.4	C(9)-C(10)-O(1)	107.0
C(10)-O(1)-C(1)	110.6	C(2)-O(2)-C(3)	111.6
C(4)-O(3)-C(5)	110.7	C(6)-O(4)-C(7)	111.7
C(8)-O(5)-C(9)	117.0		

Table A2.2.21 *Torsion angles (deg.) for $\text{MCl}_3(15\text{-C-5})$*

C(10)-O(1)-C(1)-C(2)	-83.7
C(3)-O(2)-C(2)-C(1)	178.9
O(1)-C(1)-C(2)-O(2)	-66.5
C(2)-O(2)-C(3)-C(4)	-85.9
C(5)-O(3)-C(4)-C(3)	-176.7
O(2)-C(3)-C(4)-O(3)	-59.2
C(4)-O(3)-C(5)-C(6)	-169.8
C(7)-O(4)-C(6)-C(5)	78.1
O(3)-C(5)-C(6)-O(4)	59.0
C(6)-O(4)-C(7)-C(8)	-162.5
C(9)-O(5)-C(8)-C(7)	161.2
O(4)-C(7)-C(8)-O(5)	63.5
C(8)-O(5)-C(9)-C(10)	-171.5
C(1)-O(1)-C(10)-C(9)	167.0
O(5)-C(9)-C(10)-O(1)	-60.5

Table A2.2.22 *Crystal data for* $[BiCl_2(18-C-6)]_2 [Bi_2Cl_{12}]$

Formula	$C_{24}H_{48}O_{12}Bi_3Cl_{12}$
M_r	1790.0
Crystal class	Triclinic
Space group	$P\bar{1}$
a (Å)	8.278(4)
b (Å)	10.966(6)
c (Å)	14.818(6)
α	109.25(4)°
β	98.12(4)°
γ	103.68(4)°
V (Å ³)	1198(1)
Z	1
Systematic absences	h0l, l \neq 2n; 0k0, k \neq 2n
D_c (g cm ⁻³)	2.48
Crystal size (mm)	0.25 \times 0.30 \times 0.27
λ (Å)	0.71069
μ (Mo-K α) (mm ⁻¹)	15.32
T (K)	290
Final R	0.064 ($R_w = 0.084$)

Table A2.2.23 Bond lengths (Å) for $[\text{BiCl}_2(18\text{-C-6})]_2 [\text{Bi}_2\text{Cl}_4]$

Bi(1)-Cl(1)	2.500(6)	Bi(1)-Cl(2)	2.787(6)
Bi(1)-Cl(3)	2.506(6)	Bi(1)-Cl(4)	2.701(6)
Bi(1)-Cl(2A)	2.966(6)	Bi(2)-Cl(5)	2.503(7)
Bi(2)-Cl(6)	2.500(6)	Bi(2)-O(1)	2.644(17)
Bi(2)-O(4)	2.651	Bi(2)-O(7)	2.543(16)
Bi(2)-O(10)	2.657(12)	Bi(2)-O(13)	2.647(18)
Bi(2)-O(16)	2.491	Cl(2)-Bi(1A)	2.966(6)
O(1)-C(2)	1.328(41)	O(1)-C(18)	1.432(36)
O(4)-C(3)	1.339(46)	O(4)-C(5)	1.394(30)
O(7)-C(6)	1.480(35)	O(7)-C(8)	1.432(26)
O(10)-C(9)	1.432(26)	O(10)-C(11)	1.428(29)
O(13)-C(12)	1.402(25)	O(13)-C(14)	1.416(31)
O(16)-C(15)	1.451(33)	O(16)-C(17)	1.454(32)
C(2)-C(3)	1.375(53)	C(5)-C(6)	1.452(37)
C(8)-C(9)	1.450(36)	C(11)-C(12)	1.456(35)
C(14)-C(15)	1.485(29)	C(17)-C(18)	1.387(46)

Table A2.2.24 *Bond angles (deg.) for*
 $[BiCl_2(18-C-6)]_2 [Bi_2Cl_4]$

Cl(1)-Bi(1)-Cl(2)	89.8(2)	Cl(1)-Bi(1)-Cl(3)	93.3(2)
Cl(2)-Bi(1)-Cl(3)	86.1(2)	Cl(1)-Bi(1)-Cl(4)	88.1(2)
Cl(2)-Bi(1)-Cl(4)	177.5(2)	Cl(3)-Bi(1)-Cl(4)	92.7(2)
Cl(1)-Bi(1)-Cl(2A)	87.7(2)	Cl(2)-Bi(1)-Cl(2A)	78.6(2)
Cl(3)-Bi(1)-Cl(2A)	164.7(2)	Cl(4)-Bi(1)-Cl(2A)	102.6(2)
Cl(5)-Bi(2)-Cl(6)	91.0(2)	Cl(5)-Bi(2)-O(1)	147.6(4)
Cl(6)-Bi(2)-O(1)	84.4(4)	Cl(5)-Bi(2)-O(4)	152.3(5)
Cl(6)-Bi(2)-O(4)	89.3(4)	O(1)-Bi(2)-O(4)	59.9(6)
Cl(5)-Bi(2)-O(7)	88.8(4)	Cl(6)-Bi(2)-O(7)	83.2(4)
O(1)-Bi(2)-O(7)	122.2(5)	O(4)-Bi(2)-O(7)	63.7(6)
Cl(5)-Bi(2)-O(10)	82.4(3)	Cl(6)-Bi(2)-O(10)	146.9(4)
O(1)-Bi(2)-O(10)	117.6(5)	O(4)-Bi(2)-O(10)	82.4(5)
O(7)-Bi(2)-O(10)	64.4(5)	Cl(5)-Bi(2)-O(13)	91.4(4)
Cl(6)-Bi(2)-O(13)	151.5(3)	O(1)-Bi(2)-O(13)	78.5(6)
O(4)-Bi(2)-O(13)	101.4(6)	O(7)-Bi(2)-O(13)	125.2(4)
O(10)-Bi(2)-O(13)	61.4(5)	Cl(5)-Bi(2)-O(16)	85.1(4)
Cl(6)-Bi(2)-O(16)	87.9(4)	O(1)-Bi(2)-O(16)	62.7(5)
O(4)-Bi(2)-O(16)	122.6(6)	O(7)-Bi(2)-O(16)	169.2(5)
O(10)-Bi(2)-O(16)	123.4(5)	O(13)-Bi(2)-O(16)	64.0(4)
Bi(1)-Cl(2)-Bi(1A)	101.4(2)	Bi(2)-O(1)-C(2)	119.5(19)
Bi(2)-O(1)-C(18)	118.7(17)	C(2)-O(1)-C(18)	120.2(28)
Bi(2)-O(4)-C(3)	120.7(19)	Bi(2)-O(4)-C(5)	120.0(16)
C(3)-O(4)-C(5)	119.3(24)	Bi(2)-O(7)-C(6)	112.3(14)
Bi(2)-O(7)-C(8)	114.6(15)	C(6)-O(7)-C(8)	116.1(16)
Bi(2)-O(10)-C(9)	115.5(12)	Bi(2)-O(10)-C(11)	116.3(11)
C(9)-O(10)-C(11)	115.4(14)	Bi(2)-O(13)-C(12)	118.2(15)
Bi(2)-O(13)-C(14)	118.8(12)	C(12)-O(13)-C(14)	117.5(21)
Bi(2)-O(16)-C(15)	115.0(11)	Bi(2)-O(16)-C(17)	115.3(17)
C(15)-O(16)-C(17)	117.1(22)	O(1)-C(2)-C(3)	119.2(39)
O(4)-C(3)-C(2)	117.3(33)	O(4)-C(5)-C(6)	108.0(18)
O(7)-C(6)-C(5)	114.6(23)	O(7)-C(8)-C(9)	114.1(21)
O(10)-C(9)-C(8)	107.9(15)	O(10)-C(11)-C(12)	108.2(16)
O(13)-C(12)-C(11)	110.9(22)	O(13)-C(14)-C(15)	108.4(22)
O(16)-C(15)-C(14)	113.1(20)	O(16)-C(17)-C(18)	114.9(20)
O(1)-C(18)-C(17)	109.9(32)		

Table A2.2.25 *Torsion angles (deg.) for [BiCl₂(18-C-6)]₂ [Bi₂Cl₄]*

C(18)-O(1)-C(2)-C(3)	-174.1
C(5)-O(4)-C(3)-C(2)	172.9
O(1)-C(2)-C(3)-O(4)	-9.3
C(3)-O(4)-C(5)-C(6)	-153.3
C(8)-O(7)-C(6)-C(5)	-83.5
O(4)-C(5)-C(6)-O(7)	-50.2
C(6)-O(7)-C(8)-C(9)	87.1
C(11)-O(10)-C(9)-C(8)	-177.9
O(7)-C(8)-C(9)-O(10)	55.6
C(9)-O(10)-C(11)-C(12)	-172.8
C(14)-O(13)-C(12)-C(11)	-166.8
O(10)-C(11)-C(12)-O(13)	-55.9
C(12)-O(13)-C(14)-C(15)	-129.9
C(17)-O(16)-C(15)-C(14)	-90.1
O(13)-C(14)-C(15)-O(16)	-47.6
C(15)-O(16)-C(17)-C(18)	90.7
C(2)-O(1)-C(18)-C(17)	176.4
O(16)-C(17)-C(18)-O(1)	43.4

REFERENCES

REFERENCES

- (1) A.J.Blake, E.A.V.Ebaworth and A.J.Welch, *Acta Crystallogr.*, 1984, C40, 413.
- (2) B.Beagley and T.G.Hewitt, *Trans.Faraday soc.*, 1968, 64, 2561.
- (3) W.W.Laurie and J.E.Wollrab, *J.Chem.Phys.*, 1969, 51, 1580.
- (4) G.R.Wiley, *Edu.Chem.*, 1985, 22, 178.
- (5) K.R.Millington, S.R.Wade, G.R.Wiley and M.G.B.Drew, *Inorg.Chim.Acta*, 1984, 89, 185.
- (6) M.Ravindran, G.R.Wiley and M.G.B.Drew, *Inorg.Chim.Acta*, 1990, 175, 99.
- (7) B.J.Brisdon, G.W.A.Fowles and B.P.Osbourne, *J.Chem.Soc.*, 1962, 1330.
- (8) F.A.Cotton and G.Wilkinson, "Advanced inorganic chemistry" (fifth ed., Wiley Interscience)
- (9) R.E.Collis, *PhD Thesis, University of Southampton*, 1970.
- (10) B.J.Russ and J.S.Wood, *J.Chem.Soc., Chem.Comm.*, 1966, 745.
- (11) P.T.Greene, B.J.Russ and J.S.Wood, *J.Chem.Soc.*, 1971, A, 3636.
- (12) P.T.Greene and P.L.Orioli, *J.Chem.Soc.*, 1969, A, 1621.
- (13) G.W.A.Fowles, P.T.Greene and J.S.Wood, *J.Chem.Soc., Chem.Comm.*, 1967, 971.
- (14) R.Karia, G.R.Wiley and M.G.B.Drew, *Acta Crystallogr.*, 1986, C42, 558.
- (15) J.Hughes and G.R.Wiley, *Inorg.Chim.Acta*, 1975, 12, 145.
- (16) R.G.Wilkins, "The study of kinetics and mechanisms of reactions of transition metal complexes" (Allyn and Baron, Boston, 1974).
- (17) J.Hughes and G.R.Wiley, *Inorg.Chim.Acta*, 1976, 20, 137.
- (18) K.G.Higgins, F.A.Parrett and H.A.Patel, *J.Inorg.Nucl.Chem.*, 1969, 31, 1209.
- (19) G.R.Wiley, *Inorg.Chim.Acta*, 1977, 21, 112.
- (20) S.R.Wade and G.R.Wiley, *J.Less Common Metals*, 1979, 68, 105.
- (21) G.W.A.Fowles and R.A.Hoodless, *J.Chem.Soc.*, 1963, 33.
- (22) R.Kiesel and E.P.Schram, *Inorg.Chem.*, 1973, 12, 1090.
- (23) M.W.Duckworth, G.W.A.Fowles and P.T.Greene, *J.Chem.Soc.*, 1967, A, 1592.
- (24) L.S.Jenkins and G.R.Wiley, *Inorg.Chim.Acta*, 1978, 29, L201.
- (25) T.A.Lane and J.T.Yoke, *Inorg.Chem.*, 1976, 15, 484.
- (26) G.W.A.Fowles, *Prog.Inorg.Chem.*, 1964, 6, 1.
- (27) S.R.Wade, *PhD Thesis, University of Warwick*, 1979.
- (28) B.Rajesh Karia, *M.Sc. Thesis, University of Warwick*, 1986.

- (29) J. Hughes and G.R. Willey, *Inorg. Chim. Acta*, 1977, 25, L81.
- (30) M. Ravindran and G.R. Willey, *Unpublished work*.
- (31) M.G.B. Drew and G.R. Willey, *J. Chem. Soc. Dalton Trans.*, 1984, 727.
- (32) M.G.B. Drew and G.R. Willey, *J. Inorg. Nucl. Chem.*, 1981, 43, 1683.
- (33) A.S. Secco and J. Trotter, *Acta Crystallogr.*, 1983, C39, 317.
- (34) M. Kubiak and J. Glowiak, *Acta Crystallogr.*, 1986, C42, 419.
- (35) K. Folting, J.C. Huffman, R.L. Bansemer and K.G. Caulton, *Inorg. Chem.*, 1984, 23, 3289.
- (36) V.C. Adam, U.A. Gregory and B.T. Kilbourn, *J. Chem. Soc., Chem. Commun.*, 1970, 1400.
- (37) E.C. Alyea, G.T. Fey and R.G. Goel, *J. Co-ord. Chem.*, 1976, 5, 143; F.A. Cotton, S.A. Duraj, W.J. Roth and C.D. Schmulbach, *Inorg. Chem.*, 1985, 24, 525.
- (38) W.W. Wendlandt and J.P. Smith, *Nature*, 1964, 201, 73.
- (39) R. Colton and J.H. Canterford, *"Halides of the first row transition metals"*, (Wiley Interscience, New York, 1969).
- (40) R.J. Kern, *J. Inorg. Nucl. Chem.*, 1963, 25, 5.
- (41) N. Hebedanz, F.H. Kohler and G. Muller, *Inorg. Chem.*, 1984, 23, 3043.
- (42) C.A. McAuliffe and M.H. Jones, *J. Chem. Soc., Chem. Commun.*, 1979, 737.
- (43) R.S. Nyholm, M.R. Truter and C.W. Bradford, *Nature*, 1970, 228, 648.
- (44) A. Hoseiny, A.G. Mackie, C.A. McAuliffe and K. Minten, *Inorg. Chim. Acta*, 1981, 49, 99.
- (45) D.G. Tuck, *Rev. Inorg. Chem.*, 1979, 1, 209.
- (46) R.E. Cramer, R.B. Maynard and J.A. Ibers, *J. Amer. Chem. Soc.*, 1981, 103, 76.
- (47) R.G. Dickinson, *J. Am. Chem. Soc.*, 1922, 44, 744.
- (48) C.H. MacGillavry, J.M. Bijvoet, *Z. Krist.*, 1936, 94, 249.
- (49) R.C. Evans, F.G. Mann, H.S. Peiser and D. Purdie, *J. Chem. Soc.*, 1940, 1209.
- (50) G.A. Carlson, J.P. McReynolds and F.H. Verhoek, *J. Am. Chem. Soc.*, 1945, 67, 1334.
- (51) R.C. Cass, G.E. Coates and R.C. Hayter, *J. Chem. Soc.*, 1955, 4007.
- (52) A.V. Ablov and T.I. Malinovskii, *Doklady Akad. Nauk S.S.S.R.*, 1958, 123, 677; *C.A.*, 1959, 53, 4854g.
- (53) G.J. Sutton, *Austr. J. Chem.*, 1959, 12, 637.
- (54) G.J. Sutton, *Austr. J. Chem.*, 1961, 14, 545.
- (55) J. Lewis, R.S. Nyholm and D.J. Phillips, *J. Chem. Soc.*, 1962, 2177.
- (56) G.E. Coates and D. Ridley, *J. Chem. Soc.*, 1964, 166.
- (57) I.S. Ahuja, D.H. Brown, R.H. Nuttall and D.W.A. Sharpe, *J. Inorg. Nucl. Chem.*, 1965, 27, 1105.

- (58) I.S.Ahuja, D.H.Brown, R.H.Nuttall and D.W.A.Sharpe, *J.Inorg.Nucl.Chem.*, 1965, 27, 1625.
- (59) R.A.Walton, *J.Chem.Soc.(A)*, 1966, 365.
- (60) J.R.Allan, D.H.Brown, R.H.Nuttall and D.W.A.Sharpe, *J.Chem.Soc.(A)*, 1966, 1031.
- (61) G.Dyer, D.C.Goodall, R.H.B.Mais, H.M.Powell and L.M.Venanzi, *J.Chem.Soc.(A)*, 1966, 1110.
- (62) G.B.Deacon and J.H.S.Green, *Chem.Comm.*, 1966, 629.
- (63) N.S.Gill and H.J.Kingdon, *Aust.J.Chem.*, 1966, 19, 2197.
- (64) G.O.Quicksall and T.G.Spiro, *Inorg.Chem.*, 1966, 5, 2232.
- (65) G.Morgan and F.H.Burstall, *J.Chem.Soc.*, 1938, 1672.
- (66) W.Rudorff and K.Brodersen, *Z.Anorg.Chem.*, 1952, 270, 145.
- (67) T.I.Malinovskii and Y.A.Simonov, *Doklady Akad.Nauk S.S.S.R.*, 1962, 147, 96, C.A., 1963, 58, 6273h.
- (68) M.Goldstein and E.F.Mooney, *J.Inorg.Nucl.Chem.*, 1965, 27, 1601.
- (69) A.F.Cameron, K.P.Forrest and G.Ferguson, *J.Chem.Soc.(A)*, 1971, 1286.
- (70) R.G.Goel and W.O.Ogini, *Inorg.Chem.*, 1977, 16, 1968.
- (71) (a) F.G.Mann, D.Purdie and A.F.Wells, *J.Chem.Soc.*, 1936, 1503;
(b) M.R.Churchill, F.J.Rotella, *Inorg.Chem.*, 1979, 18, 166.
- (72) (a) R.C.Dickenson, F.T.Helm, W.A.Baker Jr., T.D.Black and W.H.Watson Jr., *Inorg.Chem.*, 1977, 16, 1530;
(b) M.R.Churchill, B.G.DeBoer and S.J.Mendak, *Inorg.Chem.*, 1975, 14, 2496.
- (73) D.W.Smith, *Co-ord.Chem.Rev.*, 1976, 21, 93.
- (74) R.D.Willet and U.Geiser, *Croat.Chem.Acta*, 1984, 57, 737.
- (75) L.P.Battaglia, A.B.Corradi, U.Geiser, R.D.Willet, A.Motori, F.Sandrolini, L.Antolini, T.Manfredini, L.Menabue and G.C.Pellacani, *J.Chem.Soc., Dalton Trans.*, 1988, 265.
- (76) R.M.Clay, P.M.Rust and J.M.Rust, *J.Chem.Soc., Dalton Trans.*, 1973, 595 and references therein.
- (77) H.Remy and G.Laves, *Ber.*, 1933, 66, 571.
- (78) D.S.Barratt, G.A.Gott and C.A.McAuliffe, *J.Chem.Soc., Dalton Trans.*, 1988, 2065.
- (79) (a) R.E.Caputo, S.Roberts, R.D.Willet and B.C.Gerstein, *Inorg.Chem.*, 1976, 15, 820;
(b) J.Goodyear, E.M.Ali, H.H.Sutherland, *Acta Crystallogr.*, 1978, B34, 2617.
- (80) B.Beagley, C.A.McAuliffe, K.Minten and R.G.Pritchard, *J.Chem.Soc., Dalton Trans.*, 1983, 1999.
- (81) B.Morosin and E.J.Graeber, *Acta Crystallogr.*, 1967, 23, 766.
- (82) K.Tichy, J.Benes, R.Kind and H.Arend, *Acta Crystallogr.*, 1980, 36B, 1355.

- (83) C.J.J. Van Loon, D.J.W. Idjo, *Acta Crystallogr.*, 1975, 31B, 770.
- (84) J.J. Foster and N.S. Gill, *J. Chem. Soc. A*, 1968, 2625.
- (85) G. Chapius and F.J. Zuniga, *Acta Crystallogr.*, 1980, B36, 807.
- (86) N.A. Bell, T.D. Dee, M. Goldstein and I.W. Nowell, *Inorg. Chim. Acta.*, 1982, 65, L87.
- (87) H. Noth, E. Wiberg and L.P. Winter, *Z. Anorg. Allg. Chem.*, 1969, 370, 209.
- (88) M. Goldstein and R.J. Hughes, *Inorg. Chim. Acta.*, 1979, 37, 71.
- (89) M. Goldstein and R.J. Hughes, *Inorg. Chim. Acta.*, 1980, 40, 229.
- (90) R.J.H. Clark and T.M. Dunn, *J. Chem. Soc.*, 1963, 1198.
- (91) D.M. Adams, J. Chatt, J.M. Davidson and J. Gerratt, *J. Chem. Soc. (B)*, 1963, 2189.
- (92) A. Sabatini and L. Sacconi, *J. Amer. Chem. Soc.*, 1964, 86, 17.
- (93) K.E. Halvorson, C. Patterson and R.D. Willet, *Acta Crystallogr.*, 1990, B44, 508.
- (94) C.J. Pederson, *J. Amer. Chem. Soc.*, 1967, 89, 7017.
- (95) E. Hough, D.G. Nicholson and A.K. Vasudevan, *J. Chem. Soc., Dalton Trans.*, 1987, 427.
- (96) P.A. Cusack, B.N. Patel, P.J. Smith, D.W. Allen and I.W. Nowell, *J. Chem. Soc., Dalton Trans.*, 1984, 1239.
- (97) C.J. Pederson, *J. Org. Chem.*, 1971, 36, 1690.
- (98) M.R. Truter, *Structure and Bonding*, 1973, Vol. 16, Springer-Verlag, Berlin.
- (99) J.J. Christensen, J. Delbert, D.J. Eatough and R.M. Izatt, *Chem. Rev.*, 1974, 74, 351.
- (100) B.E. Jepson, R. Dewitt, *J. Inorg. Nucl. Chem.*, 1976, 38, 1175.
- (101) D.C. Tosteson, *Fed. Proc.*, 1968, 27, 1269.
- (102) O. Ryba and J. Petránek, *J. Electroanal. Chem. Interf. Electrochem.*, 1973, 44, 423.
- (103) C.J. Pederson, *Org. Syn.*, 1972, 52, 66.
- (104) J.J. Christensen, J.S. Bradshaw, S.A. Nielsen, J.D. Lamb and R.M. Izatt, *Chem. Rev.*, 1985, 85, 271.
- (105) S.M. Ohlberg, *J. Amer. Chem. Soc.*, 1959, 81, 811.
- (106) J.D. Lamb, R.M. Izatt, S.W. Swain, J.J. Christensen, *J. Amer. Chem. Soc.*, 1980, 102, 475.
- (107) R.M. Izatt, D.P. Nelson, J.H. Rytting, B.L. Haymore, J.J. Christensen, *J. Amer. Chem. Soc.*, 1971, 93, 1619.
- (108) G.W. Gokel, D.M. Goli, C. Minganti, L. Echegoyen, *J. Amer. Chem. Soc.*, 1983, 105, 6786.
- (109) C.J. Pederson, *J. Amer. Chem. Soc.*, 1967, 89, 2495.
- (110) C.J. Pederson, *J. Amer. Chem. Soc.*, 1970, 92, 386.
- (111) N.K. Dalley, R.M. Izatt, J.J. Christensen, *"Synthetic multidentate macrocyclic compounds"*, Eds., Academic press, New York,

1978

- (112) H.K. Frensdorff, *J. Amer. Chem. Soc.*, 1971, 93, 600.
- (113) M.A. Bush, M.R. Truter, *J. Chem. Soc., Chem. Commun.*, 1970, 1439; and M.A. Bush, M.R. Truter, *J. Chem. Soc., (B)*, 1970, 1440.
- (114) R.M. Izatt, R.E. Terry, D.P. Nelson, Y. Chan, D.J. Eatough, J.S. Bradshaw, L.D. Hansen, J.J. Christensen, *J. Amer. Chem. Soc.*, 1976, 98, 7626.
- (115) J.D. Lamb, *PhD Thesis, Brigham Young University, Provo, Utah* (1978).
- (116) P.U. Fruh und W. Simon *Protides of the biological fluids*, 20th colloquium (H. Peeters, ed.) Pergamon Press, New York (1973).
- (117) R.M. Izatt, R.E. Terry, B.L. Haymore, L.D. Hansen, N.K. Dalley, A.G. Avondet and J.J. Christensen, *J. Amer. Chem. Soc.*, 1976, 98, 7620.
- (118) N. Matsura, K. Umemoto, Y. Takeda, A. Saeki, *Bull. Chem. Soc. Jpn.*, 1976, 49, 1246.
- (119) E. Shchori, J. Jagur-Grodzinski, *Israel J. Chem.*, 1973, 11, 243.
- (120) E. Shchori, J. Jagur-Grodzinski, M. Shporer, *J. Amer. Chem. Soc.*, 1973, 95, 3842.
- (121) D.E. Kime, J.K. Norymberski, *J. C.S. Perkin I*, 1977, 1048.
- (122) F. De Jong, M.G. Siegel and D.J. Cram, *J. Chem. Soc., Chem. Commun.*, 1975, 551.
- (123) D.K. Cabiness and D.W. Margerum, *J. Amer. Chem. Soc.*, 1969, 91, 6540.
- (124) M. Kodama, E. Kimura, *Bull. Chem. Soc. Jpn.*, 1976, 49, 2465.
- (125) B.L. Haymore, J.D. Lamb, R.M. Izatt, J.J. Christensen, *Inorg. Chem.*, 1982, 21, 159.
- (126) R.G. Pearson, *J. Amer. Chem. Soc.*, 1963, 85, 3533.
- (127) D.J. Cram, R.C. Helgeson, L.R. Snusa, J.M. Timko, M. Newcomb, P. Moreau, F. De Jong, G.W. Gokel, D.H. Hoffman, L.A. Domeier, S.C. Peacock, K. Madan and L. Kaplan, *Pure Appl. Chem.*, 1975, 43, 327.
- (128) R.M. Izatt, R.E. Terry, L.D. Hansen, A.G. Avondet, J.S. Bradshaw, N.K. Dalley, T.E. Jensen, B.L. Haymore and J.J. Christensen, *Inorg. Chim. Acta*, 1978, 30, 1.
- (129) A.V. Bajaj and N.S. Poonia, *Co-ordin. Chem. Rev.*, 1988, 87, 55.
- (130) F.P. Van Remoortere and F.P. Boer, *Inorg. Chem.*, 1974, 13, 2071.
- (131) F.P. Boer, M.A. Newman, F.P. Van Remoortere and E.C. Steiner, *Inorg. Chem.*, 1974, 13, 2826.
- (132) E. Mason and H.A. Eick, *Acta Crystallogr.*, 1982, 38B, 1821.
- (133) J. Hasek, D. Hlavata and K. Huml, *Acta Crystallogr.*, 1980, 36B, 1782.
- (134) J. Hasek, K. Huml and D. Hlavata, *Acta Crystallogr.*, 1979, 35B, 330.
- (135) P. Seiler, M. Dobler and J.D. Dunitz, *Acta Crystallogr.*, 1974, 30B, 2744.
- (136) M.A. Bush and M.R. Truter, *J. Chem. Soc. Perkin Trans. 2*, 1972, 341.
- (137) P. Groth, *Acta Chem. Scand.*, 1981, 35A, 463.
- (138) F.A. Von Iter, F. Vogtle, G. Weber and G.M. Sheldrick, *Z. Naturforsch., B*, 1983, 38, 262.

- (139) R. Hilgenfeld and W. Saenger, *Angew. Chem., Int. Ed. Engl.*, 1981, 20, 1045.
- (140) D.L. Hughes, C.L. Mortimer and M.R. Truter, *Acta Crystallogr.*, 1978, 34B, 43.
- (141) N.S. Poonia, M.R. Truter, *J. Chem. Soc., Dalton Trans.*, 1973, 2062.
- (142) J.D. Owen and M.R. Truter, *J. Chem. Soc., Dalton Trans.*, 1979, 1831.
- (143) M. Dobler and R.P. Phizackerley, *Acta Crystallogr.*, 1974, 30B, 2746.
- (144) M. Dobler and R.P. Phizackerley, *Acta Crystallogr.*, 1974, 30B, 2748.
- (145) K. Venkatasubramanian, K. Joshi, N.S. Poonia, W.R. Montfort, S.R. Ernst and M.L. Hackert, *J. Incl. Phenom.*, 1985, 3, 453.
- (146) F.P. Van Remoortere, F.P. Boer and E.C. Steiner, *Acta Crystallogr.*, 1975, 31B, 1420.
- (147) C.R. Paige and M.F. Richardson, *Can. J. Chem.*, 1984, 62, 332.
- (148) M.G.B. Drew and D.G. Nicholson, *J. Chem. Soc., Dalton Trans.*, 1986, 1543.
- (149) M.G.B. Drew, P.P.K. Claire and G.R. Willey, *J. Chem. Soc. Dalton Trans.*, 1988, 215.
- (150) A. Elbaayouny, H.J. Brugge, K. Von Deuten, M. Dickel, A. Knochel, K.U. Koch, J. Kopf, D. Melzer and G. Rudolph, *J. Amer. Chem. Soc.*, 1983, 105, 6573.
- (151) J.E.D. Davies and D.A. Long, *J. Chem. Soc. (A)*, 1968, 1757.
- (152) J.E.D. Davies and D.A. Long, *J. Chem. Soc. (A)*, 1968, 1761.
- (153) P.P.K. Claire, *PhD Thesis*, 1988.
- (154) J. Kisenyi, *PhD Thesis*, 1984.
- (155) R. Enjalbert and J. Galy, *Acad. Sci. Ser. C*, 1978, 287, 259.
- (156) A. Lipka, *Acta Crystallogr.*, 1979, B35, 3020.
- (157) S.C. Nyburg, G.A. Ozin and J.T. Szymanski, *Acta Crystallogr.*, 1971, 27B, 2298.
- (158) (a) K.N. Trueblood, C.B. Knobler, D.S. Lawrence and R.V. Stevens, *J. Amer. Chem. Soc.*, 1982, 104, 1355;
 (b) H.M. Colquhoun, D.F. Lewis, J.F. Stoddart and J.D. Williams, *J. Chem. Soc. Dalton Trans.*, 1983, 607;
 (c) H.M. Colquhoun, G. Jones, J.M. Mand, J.F. Stoddart and D.J. Williams, *J. Chem. Soc., Dalton Trans.*, 1984, 63;
 (d) Y.Y. Wei, B. Tinant, J.-P. Declercq, M. Van Moerssche and J. Dale, *Acta Crystallogr.*, 1988, 44C, 77 and references therein.
- (159) A. Hazill, *Acta Crystallogr.*, 1988, 44C, 88.
- (160) A. Herschaft and J.D. Corbett, *Inorg. Chem.*, 1963, 2, 979.
- (161) L.P. Battaglia, A. Bonamartini Corradi, M. Nardelli and M.E. Vidoni Tani, *J. Chem. Soc., Dalton Trans.*, 1978, 583.
- (162) (a) R.D. Rogers, P.D. Richards and E.J. Voss, *J. Incl. Phenom.*, 1988, 6, 65;
 (b) R.L. Garrell, J.C. Smyth, F.R. Fronczek and R.D. Gaudour, *J. Incl. Phenom.*, 1988, 6, 73.
- (163) G.W. Gokel, D.J. Cram, C.L. Liotta, H.P. Harris and F.L. Cook, *J. Org. Chem.*, 1974, 39, 2445.

- (164) N.R. Streltsova, V.K. Bel'skii, B.M. Bullychev, P.A. Storozhenko and L.V. Ivakina, *Koord Khimiya*, 1987, 13, 1101.
- (165)(a) D.J. Cram, R.C. Helgeson, K. Koga, E.P. Kyba, K. Madan, L.R. Sousa, M.G. Siegel, P. Moreau, G.W. Gokel, J.M. Timko, C.D.Y. Sogah, *J. Org. Chem.*, 1978, 43, 2758.
(b) E. Webber, F. Vogtle, *Angew. Chem., Int. Ed. Engl.*, 1980, 92, 1067.
- (166)(a) F. De Jong, D.N. Reinhoudt, C.J. Smit, *Tetrahedron Lett.*, 1976, 1371.
(b) K.E. Koenig, R.C. Helgeson, D.J. Cram, *J. Amer. Chem. Soc.*, 1976, 98, 4018.
- (167)(a) K. Takayama, N. Nambu, T. Nagai, *Chem. Pharm. Bull.*, 1979, 27, 215.
(b) A. Knochel, J. Kopf, J. Oehler, G. Rudolph, *J. Chem. Soc., Chem. Commun.*, 1978, 595.
- (168)(a) F. Vogtle, W.M. Muller, E. Webber, *Chem. Ber.*, 1980, 113, 1130.
(b) F. Vogtle, W.M. Muller, *Naturwissenschaften*, 1980, 67, 255.
- (169) N.N. Greenwood and A. Earnshaw, *Chemistry of the Elements*, 1984, 652, Pergamon Press.
- (170)(a) R. Kaufmann, A. Knochel, J. Kopf, J. Oehler, G. Rudolph, *Chem. Ber.*, 1977, 110, 2449.
(b) A. El Basyony, J. Klimes, A. Knochel, J. Oehler, G. Rudolph, *Z. Naturforsch. B: Anorg. Chem., Org. Chem.*, 1976, 31B, 1192.
- (171)(a) J.M. Timko, D.J. Cram, *J. Amer. Chem. Soc.*, 1974, 96, 7159.
(b) J.M. Timko, S.S. Moore, D.M. Walba, P.C. Hiberty, D.J. Cram, *J. Amer. Chem. Soc.*, 1977, 99, 4207. (c) I. Goldberg, *Acta Crystallogr.*, 1975, 31B, 754.
- (172) A. Van Zan, F. De Jong, D.N. Reinhoudt, G.J. Torney, Y. Onwezen, *Recl. Trav. Chim. Pays-Bas*, 1981, 100, 453.
- (173) M.G.B. Drew, D.G. Nicholson I. Sylte and A.K. Vasudevan, *Inorg. Chim. Acta*, 1990, 171, 11.
- (174) H. Moureu, G. Wettruff, M. Maget, *Pro. Indian Acad. Sci.*, 1938, 8A, 356.
- (175) M.R. Snow, M.H.B. Stiddard, *Chem. Commun.*, 1965, 580.
- (176)(a) J. Holmes and R. Pettit, *J. Org. Chem.*, 1963, 28, 1695;
(b) P. Day, *Inorg. Chem.*, 1963, 2, 452;
(c) K. Lewis and L.S. Singer, *J. Chem. Phys.*, 1965, 43, 2712;
(d) O.W. Howarth and G.K. Fraenkel, *J. Amer. Chem. Soc.*, 1966, 88, 4514;
(e) G.W. Cowell, A. Ledwith, A.C. White and H.J. Woods, *J. Chem. Soc. B*, 1970, 227;
- (177) P.P.K. Claire, G.R. Willey and M.G.B. Drew, *J. Chem. Soc., Chem. Commun.*, 1987, 1100.
- (178) P.N. Billinger, P.P.K. Claire, H. Collins and G.R. Willey, *Inorg. Chim. Acta*, 1988, 149, 63.
- (179) J.K.P. Aryante, M.L.H. Groen, *J. Chem. Soc.*, 1963, 2976.
- (180) G.S. Heo and R.A. Bartach, *J. Org. Chem.*, 1982, 47, 3557.
- (181) H.M. Newmann, *J. Amer. Chem. Soc.*, 1954, 76, 2611.

- (182) R.M. Izatt, B.L. Haymore and J.J. Christensen, *J.Chem.Soc., Chem.Comm.*, 1972, 1308.
- (183) J.-P. Behr, P.Dumas and D.Moras, *J.Amer.Chem.Soc.*, 1982, 104, 4540.
- (184) C.B. Shoemaker, L.V. McAfee, D.P. Shoemaker and C.W. Dekock, *Acta Crystallogr.*, 1986, C42, 1310.
- (185) M.Wang, B.Wang, P.J. Zheng, W.Wang and J.Lin, *Acta Crystallogr.*, 1988, C44, 1913.
- (186) J.L. Atwood, S.G. Bott, A.W. Coleman, K.D. Robinson, S.B. Whelstone and C.M. Means, *J.Amer.Chem.Soc.*, 1987, 109, 8100.
- (187) J.L. Atwood, S.G. Bott, C.M. Means, A.W. Coleman, H. Zhang and M.T. May, *Inorg. Chem.*, 1990, 29, 467.
- (188) P.J. Zheng, M.Wang, B.Y. Wang, J.H. Wu, W.J. Wang and J.Lin, *Huaxue Xuebao*, 1988, 46, 837; *C.A.*, 1989, 110, 67297k.
- (189) R. Chenevert, D. Chamberland, M. Simard and F. Brisse, *Can. J. Chem.*, 1989, 67, 32.
- (190) R. Chenevert, D. Chamberland, M. Simard and F. Brisse, *Can. J. Chem.*, 1990, 68, 797.
- (191) G. Ranghino, S. Romano, J.M. Lehn and G. Wipff, *J.Amer.Chem.Soc.*, 1985, 107, 7873.
- (192) H. Matsuura, K. Fukuhara, K. Ikeda and M. Tachikake, *J.Chem.Soc., Chem.Comm.*, 1989, 1814.
- (193) (a) R.P. Sharma and P. Kebarle, *J.Amer.Chem.Soc.*, 1984, 106, 3913.
(b) M. Burgard and J. MacCordick, *Inorg. Nucl. Chem. Lett.*, 1970, 6, 599.
- (194) (a) D.C. Bradley, *Chem. Rev.*, 1989, 89, 1317;
(b) L.A. Ryabova, *Curr. Top. Mater. Sci.*, 1981, 7, 587;
(c) B.J.J. Zelinski and D.R. Uhlmann, *J. Phys. Chem. Sol.*, 1984, 45, 1069.
- (195) C.J. Brinker, D.E. Clark, D.R. Ulrich, *Better ceramics through chemistry II; Eds Mater. Res. Soc. Symp. Proc.*, 1986, 73 and references therein.
- (196) L.G. Hubert-Pfalzgraf, *New J. Chem.*, 1987, 11, 663.
- (197) (a) J.G. Bednorz, K.A. Muller, M. Takashige, *Science (Washington D.C.)*, 1987, 236, 73;
(b) M.B. Maple, *Ed. Bull. Mater. Res. Soc.*, 1989, 14, 20-71 and references therein;
(c) H.S. Horowitz, S.J. McLain, A.W. Sleight, J.D. Druliner, P.L. Gai, M.J. Vankaveelaar, J.L. Wagner, B.D. Biggs, S.J. Poon, *Science*, 1989, 243, 66-69.
- (198) J.R. Dilworth, J. Hanich, M. Krestel, J. Beck and J. Strahle, *J. Organomet. Chem.*, 1986, 315, C9.
- (199) W.J. Evans, J.M. Olofson, J.W. Ziller, *Inorg. Chem.*, 1989, 28, 4309.

- (200)(a) P.B.Hitchcock, M.F.Lappert, A.Singh, *J.Chem.Soc., Chem.Commun.*, 1983, 1499.
(b) P.B.Hitchcock, M.F.Lappert, R.G.Smith, *Inorg.Chim.Acta*, 1987, 139, 184.
- (201)W.J.Evans, J.H.Hain Jr. and J.W.Ziller, *J.Chem.Soc., Chem.Commun.*, 1989, 1628.
- (202)P.K.Grasselle and J.D.Burrington, *Adv.Catal.*, 1981, 30, 133. (Examples include the bismuth molybdate catalysts used in the SOHIO process),
- (203)R.Dagani, *Chem.Engng.News*, 1988, 66, 24.
- (204)D.C.Bradley, R.C.Mehrotra, D.P.Gaur, *Metal Alkoxides*, 1978, Academic Press, New York.
- (205)D.C.Bradley, R.C.Mehrotra and W.Wardlaw, *Prog.Inorg.Chem.*, 1960, 2, 303.
- (206)D.C.Bradley, R.K.Multani and W.Wardlaw, *J.Chem.Soc.*, 1958, 4153.
- (207)I.P.Rothwell, *Polyhedron*, 1985, 4, 177.
- (208)(a) S.L.Latesky, A.K.McMullen, I.P.Rothwell and J.C.Huffman, *J.Amer.Chem.Soc.*, 1985, 107, 5981.
(b) L.R.Chamberlain, I.P.Rothwell and J.C.Huffman, *J.Amer.Chem.Soc.*, 1986, 108, 1502.
(c) L.Chamberlain and I.P.Rothwell, *J.Amer.Chem.Soc.*, 1983, 105, 1665.
- (209)S.Spange and G.Henblein, *Z.Anorg.Allg.Chem.*, 1989, 571, 181.
- (210)M.A.Khan, A.Osman and D.K.Tuck, *Acta Crystallogr.*, 1986, C42, 1399.
- (211)L.Chamberlain, J.Keddington, I.P.Rothwell and J.C.Huffman, *Organometallics*, 1982, 1, 1538.
- (212)(a) T.V.Howell and L.M.Venanzi, *J.Chem.Soc.(A)*, 1967, 1007.
(b) M.H.B.Stiddard and R.E.Townsend, *J.Chem.Soc.(A)*, 1969, 2355.